


REVIEW

# Progress in TENG technology—A journey from energy harvesting to nanoenergy and nanosystem

Jianxiong Zhu<sup>1,2,3</sup> | Minglu Zhu<sup>1,2,3</sup> | Qiongfeng Shi<sup>1,2,3</sup> | Feng Wen<sup>1,2,3</sup> |  
Long Liu<sup>1,2,3</sup> | Bowei Dong<sup>1,2,3</sup> | Ahmed Haroun<sup>1,2,3</sup> | Yanqin Yang<sup>1,2,3</sup> |  
Philippe Vachon<sup>1,2,3</sup> | Xinge Guo<sup>1,2,3</sup> | Tianyi He<sup>1,2,3</sup> | Chengkuo Lee<sup>1,2,3,4</sup> 

<sup>1</sup>Department of Electrical and Computer Engineering, National University of Singapore, Singapore, Singapore

<sup>2</sup>Center for Intelligent Sensors and MEMS (CISM), National University of Singapore, Singapore, Singapore

<sup>3</sup>NUS Suzhou Research Institute (NUSRI), Suzhou, China

<sup>4</sup>NUS Graduate School for Integrative Science and Engineering (NGS), National University of Singapore, Singapore, Singapore

## Correspondence

Chengkuo Lee, Department of Electrical and Computer Engineering, National University of Singapore, Singapore.  
Email: elelc@nus.edu.sg

## Funding information

A\*STAR-NCBR, Grant/Award Number: R-263-000-C91-305; HIFES Seed Funding, Grant/Award Number: R-263-501-012-133; National Key Research and Development Program of China, Grant/Award Numbers: 2019YFB2004800, R-2020-S-002; RIE Advanced Manufacturing and Engineering (AME) programmatic grant, Grant/Award Number: A18A4b0055

## Abstract

Triboelectric nanogenerator (TENG) technology is a promising research field for energy harvesting and nanoenergy and nanosystem (NENS) in the aspect of mechanical, electrical, optical, acoustic, fluidic, and so on. This review systematically reports the progress of TENG technology, in terms of energy-boosting, emerging materials, self-powered sensors, NENS, and its further integration with other potential technologies. Starting from TENG mechanisms including the ways of charge generation and energy-boosting, we introduce the applications from energy harvesters to various kinds of self-powered sensors, that is, physical sensors, chemical/gas sensors. After that, further applications in NENS are discussed, such as blue energy, human-machine interfaces (HMIs), neural interfaces/implanted devices, and optical interface/wearable photonics. Moving to new research directions beyond TENG, we depict hybrid energy harvesting technologies, dielectric-elastomer-enhancement, self-healing, shape-adaptive capability, and self-sustained NENS and/or internet of things (IoT). Finally, the outlooks and conclusions about future development trends of TENG technologies are discussed toward multifunctional and intelligent systems.

## KEYWORDS

energy harvesting, nanoenergy and nanosystem, self-powered sensor, triboelectric nanogenerator, wearable sensor

## 1 | INTRODUCTION

Energy generation is a global interest of research which dramatically influences the quality of our daily life and

the industrialization development of modern society.<sup>1–10</sup> In dealing with the global energy shortage and current environmental pollution, searching for sustainable power sources with reduced carbon emissions and renewable energy technologies are urgent for green economics and healthy development of human civilization.<sup>11–21</sup> Moreover, as the world is marching into the era of the internet

Jianxiong Zhu, Minglu Zhu, and Qiongfeng Shi contributed equally to this work.

This is an open access article under the terms of the Creative Commons Attribution License, which permits use, distribution and reproduction in any medium, provided the original work is properly cited.

© 2020 The Authors. *EcoMat* published by The Hong Kong Polytechnic University and John Wiley & Sons Australia, Ltd.

of things (IoT) and the fifth-generation wireless networks (5G), various self-powered electronics are considered as the building blocks for the foundation of the coming industrial revolution toward a smart world.<sup>22–25</sup> This wide distribution of self-powered electronics cover spheres of application ranging from industrial electronics to personal electronics, wearable electronics to implantable electronics, and macrosystem to a sustainable system in every corner of our life. With the development trends of the electronic devices in miniaturization, lightweight, and portability, a sustainable power supplying solution is needed to meet the requirement of the upcoming intelligent world, where the traditional batteries are facing a challenge due to their limited lifetime, environmental impact, and periodical replacement.<sup>26,27</sup> In order to overcome such drawbacks, the best solution is to design devices that can pull energy from their surroundings. As a matter of fact, mechanical energy is one of the most widespread and abundant energies in the environment, making mechanical-to-electrical energy transduction a promising technique for powering small electronics.<sup>26–34</sup> Many mechanisms for energy harvesting have already been developed including piezoelectric effect, electrostatic effect, and electromagnetic (EM) induction, and so on. However, those technologies normally necessitate complicated structures and operate under high-frequency stimuli, with low transducing efficiency and low voltage output in the low-frequency domain, which dramatically constrains their potential applications in the intelligent world.<sup>2,6,35–42</sup>

To overcome those disadvantages, the triboelectric nanogenerator (TENG) was first invented by Zhong Lin Wang in 2012, and has attracted worldwide research interests and underwent significant developments, becoming a promising technology in energy harvesting and especially in nanoenergy and nanosystem (NENS).<sup>12–14,22,23,43–65</sup> The working mechanism of TENG comes from the coupling of the triboelectrification effect and the electrostatic induction effect. When two dissimilar triboelectric materials come in contact and separation from one another, electrons will flow back and forth through the external circuit to keep balance because of the instantaneous voltage difference.<sup>31,66–72</sup> Normally, the working mechanism of TENG can be divided into four fundamental modes: the vertical contact-separation mode, the in-plane sliding mode, the single-electrode mode, and the free-standing mode. To increase the efficiency of energy harvesting from TENG, plenty of researches have been carried out along the direction of the nano and micro surface structuration for augmented charge generation.<sup>4,73–79</sup> With the benefit of charge generation and transfer, the various self-powered sensors with their unique functions were well-developed, such as the physical sensors, the chemical/gas sensors,

and the fluid sensors.<sup>14,22,23,55,80,81</sup> Beyond its excellent energy harvesting capability and wide collection of self-powered sensors it enables, TENG can also be easily integrated into NENS to detect or interact with its surrounding environment, such as blue energy sensor nodes, wearable sensors/human-machine interfaces (HMIs), neural interfaces/implanted devices, and optical interfaces/wearable photonics.<sup>66–72,77</sup> Furthermore, by integrating with other potential technologies for a sustainable system, TENG hence unlocks a vast pool of applications targeting properties like more power output, self-healing, and synergy with IoT in the intelligent world.<sup>74,75</sup>

In this article, we systematically report the progress of TENG technology along its path from energy harvesting, self-powered sensing to NENS. With the various advantages of the TENG technology to convert mechanical energy into electricity and potential applications in the intelligent system, a roadmap is summarized for the technology development, research directions, and the commercialization of TENG. Starting from the introduction of the TENG mechanisms including the ways of charge generation and energy-boosting from composite materials, mechanical structure design, and external circuit-assisted (bennet doubler, diode, and switches), we then present the universal adaptability of TENG to all kinds of physical and chemical sensing scenarios with self-powered strategy. After that, we further introduce its diversified applications in NENS, such as blue energy, wearable electronics/HMI, neural interfaces/implanted devices, and optical interfaces/wearable photonics. With the aid of TENG technology in NENS mentioned-above, the resultant smart system with advanced self-powered sensor nodes enables a broad range of impressive applications in many scenarios, such as sports training simulation, medical rehabilitation, entertainment, and machine learning-assisted approaches for convenience of human life. Moving forward to the new research directions beyond TENG technology, with the rapid development of the information industry and 5G, the self-sustained NENS would be dramatically benefited from the hybrid energy harvesting technologies (ie, EM and/or piezoelectric integration), dielectric-elastomer-enhancement, self-healing, shape adaptive capability, and IoT sensor nodes. In the last section of this review, perspectives about the future development trends of the TENG technologies are discussed, that is, toward multifunctional and sustainable intelligent systems.

## 2 | ROADMAP OF TENG TECHNOLOGY

Since the starting point from the year of 2012 about the triboelectric mechanism in terms of the contact and

separation mode, TENG technology has been developed extensively from the energy harvesting to the sustainable and intelligent NENS. The energy harvesting using TENG technology is sufficient to drive many electronics and to make self-powered electronics networks viable as shown in Figure 1. The first phase of the roadmap of TENG technology is about the in-depth understanding of the mechanisms for energy-boosting and achievable form of a voltage (alternative current, AC, and direct current, DC).<sup>81–94</sup> Beyond taking advantage of the micro/nano surface structures, the pre-charging process, the external circuit units (diode, switch, or charge pump), and the design of the mechanical structure (surface pattern and operation programming) would be the novel research direction for efficiency improvement. For example, a coupling of the triboelectrification and dielectric polarization from the ferroelectric material was reported in 2017 with an energy density of  $430 \mu\text{C}/\text{m}^2$ .<sup>83</sup> Very shortly, the approach of a supplement channel using a diode with  $\sim 10$  times more voltage output and the solution using an external-charge pump for high and stable output were reported in 2018, respectively.<sup>82</sup> As for the achievable form of voltage for directly powering electronic units, the coupling the triboelectrification effect and electrostatic breakdown was proposed in 2019.<sup>94</sup>

With the generated power from mechanical sources using TENG technology, a large quantity of self-powered physical sensors has been developed, such as the

pressure/force sensor, the tactile sensor, the strain/bending sensor, the acceleration and rotation sensors for the applications in tactile, sensory robotics, HMI, and healthcare monitoring. For example, researchers reported a tactile sensory matrix for various human-machine interactions<sup>71</sup> and a TENG-based gyroscope ball for monitoring the healthcare biomechanical parameter in various human motions in 2016.<sup>58</sup> On the aspect of the fluidic, a flexible microfluidic pressure sensor using both the triboelectrification and the capacitive mechanism for more complex human motion monitoring was discussed in 2017.<sup>95</sup> To achieve minimalist and flexible electronic devices, a bio-inspired spider-net-coding design forming a single-electrode interface was first reported in 2019.<sup>96</sup> Except the above-mentioned physical sensing, since early 2018, the chemical/gas sensors<sup>97</sup> using TENG technology were gradually developed to match with digital robotics/man. With the benefit of those technologies in energy harvesting, the second phase of the roadmap of TENG technology enables self-powering capabilities inside sensors to sustainable NENS. To get rid of the use of the battery, the enormous number of self-powered sensors (physical sensors and chemical/gas sensors) got benefits from TENG technologies in the era of 5G, also TENG technology provided a feasible solution for minimal power consumption of sensors in operation. Meanwhile, beyond the energy harvesting and self-powered sensing, NENS integration with the aid of the TENG technology is

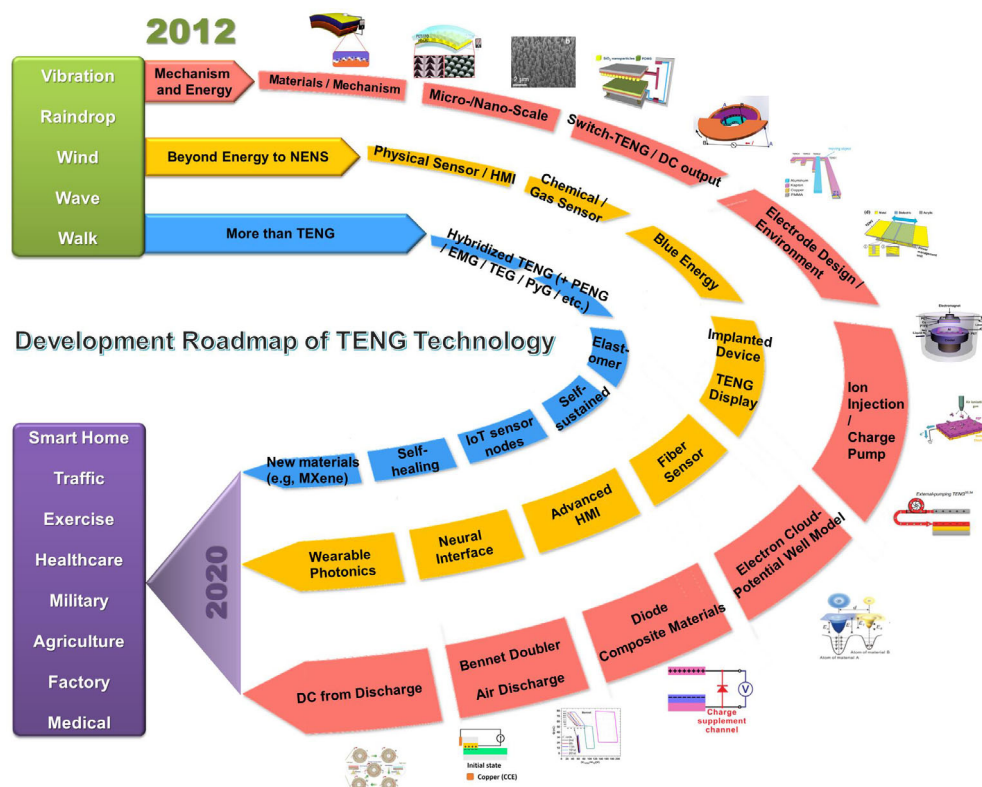


**FIGURE 1** The TENG technology evolution milestones—a journey from energy harvesting to nanoenergy and nanosystems (NENS)

attracting more and more attention to solve the smart to sustainable applications, such as the applications in blue energy, wearable HMI, neural interface/implanted device, and optical interface/photronics. For example, a biodegradable TENG was developed for in vivo energy harvesting as a sustainable power source in 2016.<sup>98</sup> Later in 2018, a jellyfish-inspired TENG with the waterproof and shape-adaptive property was reported for blue energy harvesting.<sup>99</sup> Here, the blue energy is mainly in the forms of wave energy, tidal energy, thermal energy, and osmotic energy, which was first proposed in 2016 with the duck-shaped TENG<sup>100</sup> and further a tube-structured TENG<sup>101</sup> using a liquid-solid interface in 2018. In 2016, the implantable device was reported to provide potentials for self-sustainable neuromodulation, sensing, therapy, muscle stimulation, and powering electronics.<sup>102</sup> As to the sustainable wearable HMIs, human-machine interaction is reported regarding in cyberspace or controlling of advanced robots in 2017.<sup>103</sup> Meanwhile, the TENG technology also has augmented a wide range of optical functions including light emission, photodetection, and optical modulation for the realization of applications including self-powered luminescence, smart display, wireless communication, personal privacy protection, motion monitoring, the self-powered optical wireless transmission (in 2019),<sup>104</sup> and even further nanophotonic modulation by integrating TENG with AlN nanophotonics (in 2020).<sup>105</sup>

As a promising technique for energy harvesting from the ambient environment, TENG has shown great advantages as a power supply for IoT in simple structure and with unique advantages (high efficiency, high energy density, cost-effectiveness, and good reliability). Beyond TENG technology, along with the third phase of the roadmap of TENG technology, the combination of EM and piezoelectric technologies with TENG for hybrid energy harvesting is later summarized, respectively. Moreover, the dielectric elastomer can also be employed to enhance the performance of TENG, which provides the flexibility and stretchability, that is, multilayer elastomeric-enhanced-TENG (in 2017)<sup>106</sup> and fully stretchable TENG (in 2019).<sup>107</sup> Another new research direction is to endow TENGs with new functionalities by exploring novel materials including shape memory, self-healing, and shape adaptive. With the enhancement of energy harvesting and unique properties from other materials, the NENS would be a feasible solution to obtain ambient energy sources and to act as multi-functional sensors. Energy supply toward distributed IoT sensor nodes is a critical challenge. In 2018, wireless TENGs with the ability for wireless power delivery are developed, which extends TENGs' potential in unprecedented noncontact and wireless applications.<sup>108</sup> As a vast

promising energy harvesting technology of TENG, integration with this technology shows superior advantages of both simple and diverse configurations, remarkable flexibility, high output performance, no material limitation, cost-effectiveness, and good scalability.

### 3 | FROM ENERGY TO SELF-POWERED SENSORS

With the development of new mechanisms for energy-boosting and achievable form of a voltage (AC and DC) in TENG technology, the approaches for the stable and expectation charges could be discussed, such as the composite materials, the external circuit units (diode, switch, or charge pump), and the design of the mechanical structure (surface pattern and operation programming).<sup>82-94,109,110</sup> The TENG technology as power sources would dramatically drive the development trends of the era of the coming 5G and IoT. To help the readers to understand the development of the self-powered sensors in TENG technology, the multi-functional sensors (physical sensors, chemical/gas sensors, advanced designed multi-sensors) are discussed along with the energy harvesting as follows.

#### 3.1 | Mechanisms in energy-boosting

The triboelectric effect has been first proposed years ago.<sup>84-86</sup> This phenomenon refers to the surface charge transfer between two dissimilar materials for balancing the electrochemical potential when they are brought into contact, due to the distinct electronegativity. To be more specific, the electrons can be transferred from the attached-electrode of the relatively positive material to the electrode close to the relatively negative material as the variation of their effective work functions. Additionally, these materials with strong triboelectric effects usually have low conductivity, and the electrode films are then attached with those materials for making TENG in operation, as the opposite charges can be induced on the electrodes via electrostatic induction. In general, the group of Zhong Lin Wang has concluded four typical operation modes as shown in Figure 2A. The first is the vertical contact-separation mode, in which the physical contact and separation of two materials cause the potential drop, and the external connection allows the electrons to flow and balance the potential difference. Second, the lateral sliding mode can be described as two materials that have relative parallel sliding motion against each other, resulting in the triboelectric charges and the polarization of the variation against the contact



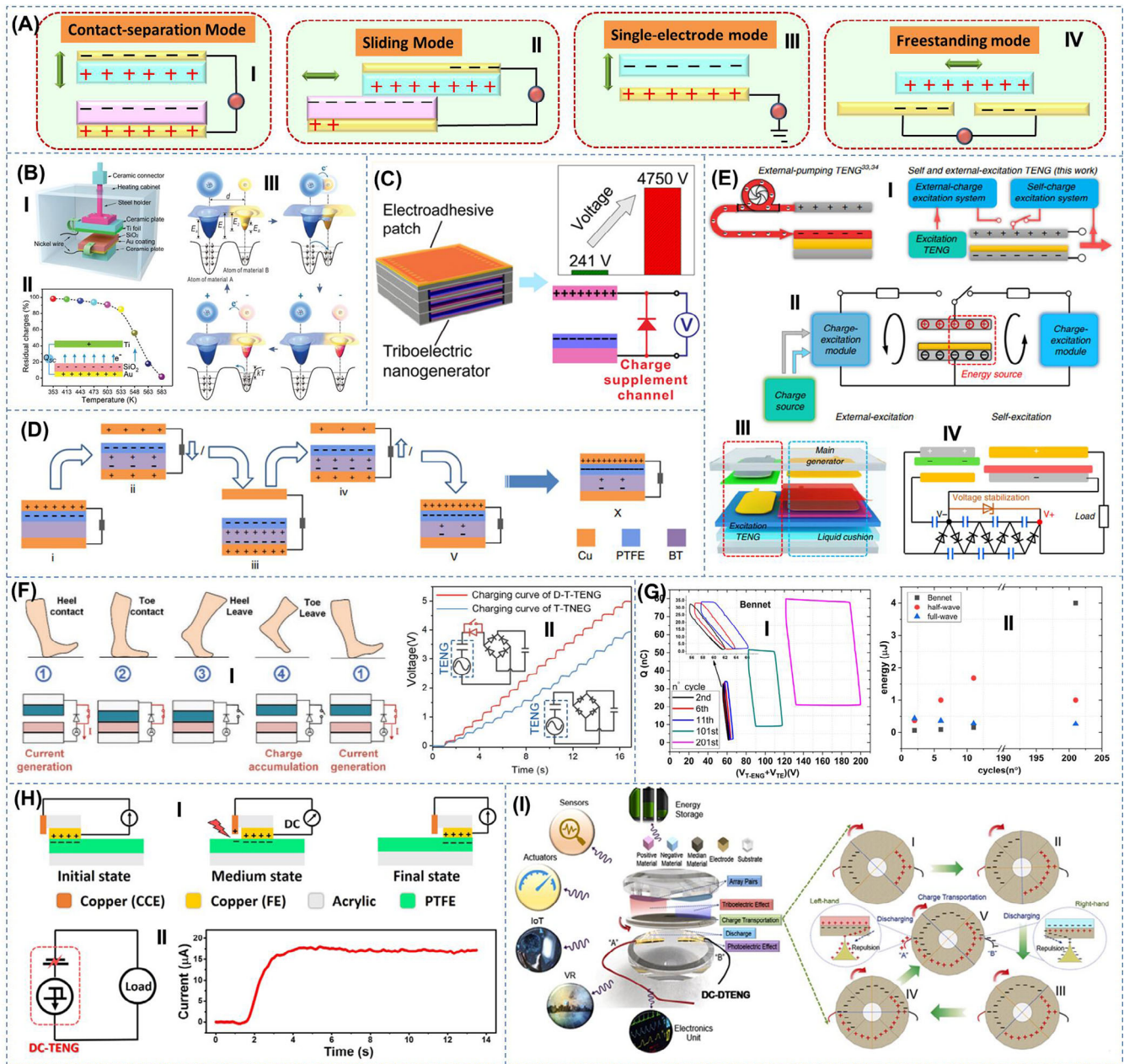


**FIGURE 2** Mechanisms in materials/structure/circuit based energy-boosting. A, Four basic modes of TENG. B, Contact and separation of electrons transfer using an electron cloud potential well model. Reproduced with permission. Copyright 2018, Wiley-VCH.<sup>87</sup> C, Giant voltage enhancement via the charge supplement channel. Reproduced with permission. Copyright 2018, American Chemical Society.<sup>82</sup> D, Working mechanism using composite material, the dielectric polarization ferroelectric material. Reproduced with permission. Copyright 2017, Nature.<sup>83</sup> E, The “charge pump” and self-charge excitation in TENG for improving the output density. Reproduced with permission. Copyright 2019, Nature.<sup>88</sup> F, Working mechanism using a combination of diode and switch in TENG for effectively harvesting human walking energy. Reproduced with permission. Copyright 2019, Wiley-VCH.<sup>90</sup> G, Comparison of the charge-voltage curve in the cycle of three conditioning circuits (Bennet’s doubler, half-wave rectifier, and full-wave rectifier). Reproduced with permission. Copyright 2018, Elsevier.<sup>93</sup> H, Working principle for DC output by triboelectrification and electrostatic breakdown. Reproduced with permission. Copyright 2019, American Association for the Advancement of Science.<sup>94</sup> I, Working process for DC output from charge generation, charges transportation, and charges releasing by repulsive force. Reproduced with permission. Copyright 2020, Elsevier<sup>110</sup>

area. The third one is single electrode mode, except the free moving side, there is only one electrode connected to the corresponding triboelectric material, and the

electrode is connected to the ground to ensure the potential change. Finally, the freestanding mode can be defined as the symmetric electrodes on the back of one

triboelectric material that can lead to the electron flow when another material is moving across the surface and leads to imbalanced charge distribution. All of these four operation modes guarantee the feasibility of TENGs to be applied to diversified scenarios for practical usage, ranging from energy harvesting to physical and chemical sensors. With the aid of electrostatic induction, electrons relating to the surface of materials would flow from one electrode to the other electrode through the external load to obtain a new balance of the potential.<sup>10-15</sup> To better explain the charge generation and the charge transfer in the contact interface of TENG, as shown in Figure 2B, an electron cloud potential well model was reported to describe the TENG theory as a function of temperature (Figure 2B-II).<sup>87</sup> The triboelectric electrons from the instantaneous contact and separation would have flowed from high potential to low potential as shown in Figure 2B-III. To increase the efficiency of energy harvesting, a supplement channel using a diode in TENG was demonstrated with  $\sim 10$  times more voltage output (from  $\sim 230$  V to  $\sim 4750$  V) than that without any external electrical element as shown in Figure 2C.<sup>82</sup> The supplement channel enables the highest voltage out due to a mechanism of replenishing in TENG. Except for the external circuit in assisting energy harvesting, from the aspect of the composite material (piezoelectric material), Figure 2D reported a charge density of  $1003 \mu\text{C}/\text{m}^2$  by the coupling effect of the triboelectrification and dielectric polarization from the ferroelectric material of  $\text{BaTiO}_3$  (BTO) nanoparticles.<sup>83</sup> It was assumed that the dielectric polarization from the ferroelectric material is acted as an internal “charge pump” for much higher energy output in TENG. Along this direction on the “charge pump,” another possible solution is that an external “charge pump” would be an ideal strategy (called a self-charge excitation) for high and stable output of  $1.25 \text{ mC}/\text{m}^2$  as shown in Figure 2E.<sup>88,89</sup> It noted that the function of the external “charge pump” is similar to the charge accumulation, which provides maximum energy output in a short time. Similar to the theory of “charge pump”, the combination of the diode and switch in the electrical circuit system is another potential solution for applicable energy output. As shown in Figure 2F, a self-enhancing conditioning circuit was reported for exponential amplification of the output electrical energy.<sup>78,90-92</sup> The switch “on” and “off” are controlled by the foot motions when a human walks. With the aid of the conditioning circuit, the more complicated electrical system (with a combination of more diodes and switches in time sequence) for energy-boosting can be achieved as shown in Figure 2G.<sup>93</sup> The comparisons of the different electrical circuits (called the half-wave rectifiers, the full-wave rectifiers, and Bennet’s doubler) were discussed in

Figure 2G-II, which demonstrated the more power output from the Bennet doubler than the other mechanisms (the half-wave rectifiers or the full-wave rectifiers).

Most of the existing electric devices and IoT sensor nodes are in operation with the DC power source. Thus, the external electrical circuit is needed to aid the output voltage from conventional TENG (AC form).<sup>94,109</sup> To improve the efficiency of TENG in DC form, as shown in Figure 2H, a DC output for the next-generation TENG was reported by the coupling of the triboelectrification effect and electrostatic breakdown with a charge density of  $430 \mu\text{C}/\text{m}^2$ .<sup>94</sup> The DC output from TENG shows good performance and can be directly applied to the electrical device. In the same period, the dual-TENG configuration was developed as shown in Figure 2I, which takes the advantage of two TENGs’ interactions (AC + AC) for a DC output.<sup>110</sup> Here, the charges would be in unidirectional flow through charge transportation (by tribo-polarity reversal material among the ultra-negative and ultra-positive materials). Due to the charge transport and repulsive discharge, a much higher DC output voltage was obtained through the air breakdown discharge. Furthermore, the capability of the dual-interaction TENGs is well demonstrated by all kinds of wireless networks and continuous motion control for real-time VR applications.

### 3.2 | Self-powered physical sensors

Since TENGs can directly convert various forms of mechanical/physical stimuli into electrical outputs based on the four self-generated operation modes, the sensory information contained in the output signals can be adopted as the ideal indicator to reflect the external physical parameters. Along the past few years, a large quantity of self-powered physical sensors have been developed by using diversified TENG configurations, including pressure/force, tactile, strain, bending, acceleration, and rotation sensors, and so on.<sup>111-119</sup> Here, several typical kinds of TENG-based self-powered physical sensors are summarized and discussed. Detection of pressure/force which is one of the most common stimuli to trigger the operation of TENGs is of great significance to enable the applications in tactile sensing, sensory robotics, HMI, and healthcare monitoring.<sup>120-128</sup> As illustrated in Figure 3A, a self-powered pressure sensor was constructed with a weaving structure for noninvasive measurement of blood pressure and pulse wave.<sup>129</sup> When external pressure is applied, the charged weaving structure is compressed toward the bottom dielectric layer and electrode, leading to voltage generation by the variation of electrical potential difference. Measurements show that the pressure sensor exhibits a high sensitivity of  $45.7 \text{ mV}/\text{Pa}$ , a rapid



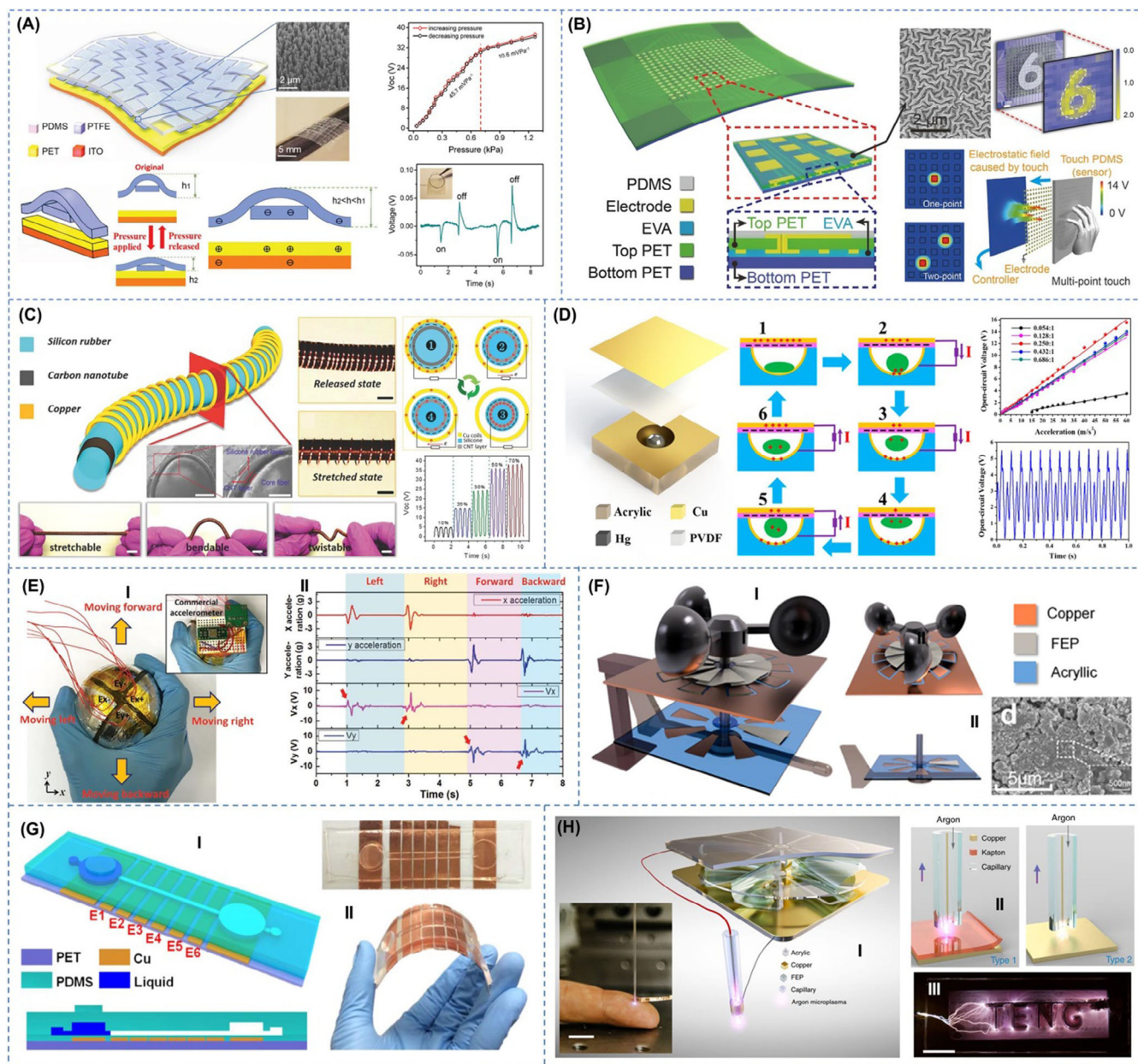


**FIGURE 3** Self-powered physical sensors. A, Triboelectric pressure sensor with a weaving structure for noninvasive blood pressure measurement. Reproduced with permission. Copyright 2018, Wiley-VCH.<sup>129</sup> B, High-resolution triboelectric tactile sensory matrix. Reproduced with permission. Copyright 2016, Wiley-VCH.<sup>130</sup> C, Stretchable fiber-shaped TENG for self-powered strain sensing. Reproduced with permission. Copyright 2016, Wiley-VCH.<sup>131</sup> D, Triboelectric acceleration sensor with the encapsulated liquid metal droplet. Reproduced with permission. Copyright 2017, American Chemical Society.<sup>132</sup> E, TENG-based gyroscope ball for monitoring left, right, forward, and backward motions. Reproduced with permission. Copyright 2017, Wiley-VCH.<sup>58</sup> F, Structural design of TENG-based wind sensor with a pie-shaped rotator and a stator. Reproduced with permission. Copyright 2019, Wiley-VCH.<sup>133</sup> G, The microfluidic pressure sensor and the outputs in response to the applied force. Reproduced with permission. Copyright 2016, Elsevier.<sup>95</sup> H, Schematic and photos of triboelectric plasma driven by freestanding TENG. Reproduced with permission. Copyright 2018, Nature<sup>134</sup>

response time of  $<5$  ms, and excellent stability with performance maintained over 40 000 motion cycles. Then a pulse sensing system is developed to precisely monitor the pulse status from different body parts of humans, such as fingertips, wrist, ear, and ankle. Based on the large database of 100 people, the blood pressure results

measured by the pressure sensor show only a small discrepancy of 0.87% to 3.65% compared to those measured by a commercial device. Thus, the developed self-powered pressure sensor demonstrates promising potentials in human health monitoring toward higher convenience and self-sustainability. On the other hand, the

tactile sensory matrix formed by the integration of multi-sensors can achieve real-time stimulus mapping for various human-machine interactions.<sup>135-140</sup> As shown in Figure 3B, a self-powered triboelectric tactile sensory matrix was developed to realize high-resolution tactile mapping by pressure-sensitive pixels.<sup>130</sup> When an object contacts or moves on the top polydimethylsiloxane (PDMS) surface, electrical signals are generated on the corresponding pixels according to the charge transfer between the sensing electrodes and the ground. Through multi-channel data acquisition, a  $16 \times 16$  sensory matrix is able to achieve both single-point and multi-point tactile mapping in a real-time manner, with a resolution of 5 dpi and pressure sensitivity of  $0.06 \text{ kPa}^{-1}$ . To reduce the device complexity and shorten the measuring time for larger matrices, a cross-type electrode layout (ie, row and volume electrodes) other than individual electrodes can be adopted, which greatly decrease the electrode number from  $m \times n$  to  $m + n$  and largely enables the real-time tactile mapping. Another type of common self-powered physical sensors, that is, strain sensors, are normally developed by elastomer-based stretchable TENGs.<sup>11,141-143</sup> Figure 3C presented a stretchable fiber-shaped TENG for power generation and self-powered strain sensing.<sup>131</sup> With the fabricated elastic fiber structure and the stretchable electrodes, the fiber-shaped TENG can withstand a high stretching strain up to 70%. It is demonstrated that the sensor output increases with the stretching strains (from 10%, 20%, 30%, 50%, to 70%), where higher sensitivity is achieved in the lower strain range (<50%). The developed fiber-shaped TENG can be used for power generation and self-powered strain sensing in the application of stretchable wearable electronics. In terms of vibration measurement, acceleration sensors are indispensable components to extract the interesting vibration features.<sup>144-149</sup> To achieve high sensitivity and self-powered sensing capability, a TENG-based acceleration sensor was proposed in Figure 3D, in which an encapsulated liquid metal droplet (mercury) acts as the movable mass.<sup>132</sup> On the top surface, polyvinylidene fluoride (PVDF) thin film with nanofiber-networked structure is utilized as the negative triboelectric layer to improve the contact area and the output performance. As a result, an open-circuit voltage ( $V_{oc}$ ) of 15.5 V and a short-circuit current ( $I_{sc}$ ) of 300 nA can be reached at an acceleration level of  $60 \text{ m/s}^2$ . Besides, the acceleration sensor shows a large sensing range from 0 to  $60 \text{ m/s}^2$ , as well as a high sensitivity of  $0.26 \text{ Vs}^2/\text{m}$ , which can be applied for acceleration measurement of various human motions and mechanical equipment.

Beyond the single-functional self-powered physical sensor, TENG technology can also be applied as multi-functional sensors.<sup>58,130,150-154</sup> As shown in Figure 3E, a

3D symmetric TENG-based gyroscope ball with dual capability of energy harvesting and self-powered sensing was reported for healthcare biomechanical parameters monitoring about the motion, acceleration, and rotation.<sup>58</sup> The TENG-based gyroscope ball can reach up to a sensitivity of 6.08, 5.87, and  $3.62 \text{ V/g}$ , which demonstrates good performance in hand motion recognition and human activity. Except for the TENG-based gyroscope, Figure 3F reported the ability to detect the simultaneously wind speed and direction based on an anemometer TENG.<sup>133</sup>  $V_{oc}$  of 88 V and  $I_{sc}$  of  $6.3 \mu\text{A}$  can be reached with the optimization of sensitivity, resolution, and wide measurement scale. After that, on the area of the liquid-solid interface, a flexible microfluidic pressure sensor based on triboelectrification and the capacitive mechanism was reported for more complex human motion monitoring applications as shown in Figure 3G.<sup>95</sup> The dynamic pressure can be identified by the TENG without external power supply. Meanwhile, the capacitive mechanism is used for the detection of both dynamic pressure and static pressure. Moreover, the other interesting topic is about the plasma physical sensor as shown in Figure 3H.<sup>134</sup> The microplasma by integrating TENGs is developed by mechanical stimuli, where TENG was used to provide the power for the plasma source. The triboelectric microplasma offers a promising, facile, portable, and safe supplement compared to traditional plasma sources, which enriches the diversity of plasma applications based on the TENG technology.

### 3.3 | Advanced physical sensors with particular electrode design/single electrode

To achieve certain functionalities, advanced electrode designs can be incorporated into the conventional TENGs, resulting in various TENG configurations with specifically designed electrodes.<sup>95,155-161</sup> As depicted in Figure 4A, to quantitatively differentiate the forward and the backward finger bending motion, a bending sensor was designed by integrating traditional grating electrodes with two plane electrodes.<sup>162</sup> For a certain bending direction, the charge flow induced by the big plane electrodes is unidirectional, while the charge flow induced by the grating electrodes shows an alternative feature. Through the combination, the overall output signals have a unique polarity for one bending direction, where the number of alternative peaks indicates the actual bending angle. That is, a forward finger bending will generate positive output signals, while a backward finger bending will generate negative output signals. In this way, both the bending direction and the bending angle can be determined by this advanced electrode design. It is demonstrated that an



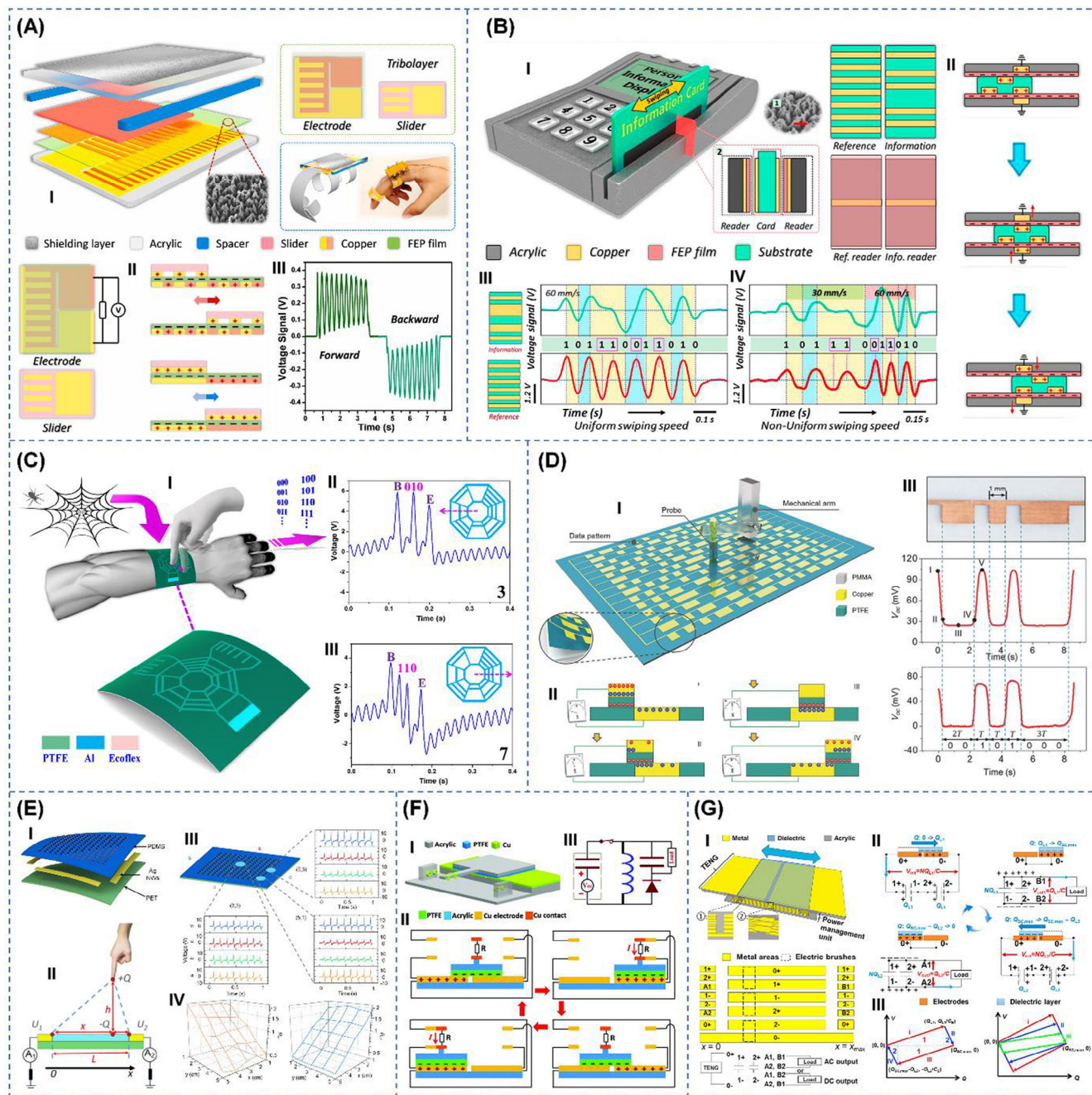


**FIGURE 4** Self-powered physical sensors with advanced electrode designs. A, Finger bending sensor by integrating traditional grating electrodes with two plane electrodes to detect both bending directions and angles. Reproduced with permission. Copyright 2018, Elsevier.<sup>162</sup> B, Barcode system with an information electrode and a reference electrode for speed-independent sensing. Reproduced with permission. Copyright 2017, Elsevier.<sup>163</sup> C, Minimalist single-electrode interface with bio-inspired spider-net-coding design. Reproduced with permission. Copyright 2019, Wiley-VCH.<sup>96</sup> D, Self-powered data storage system by the parallel-connected metal patterns on a PTFE substrate. Reproduced with permission. Copyright 2018, Wiley-VCH.<sup>164</sup> E, Analogue smart skin with only four edge electrodes for tactile sensing. Reproduced with permission. Copyright 2016, American Chemical Society.<sup>165</sup> F, Unidirectional switch-based TENG with both direct-current output and maximized energy transfer. Reproduced with permission. Copyright 2018, Wiley-VCH.<sup>109</sup> G, Auto-power-management electrode design by the operation-driven switch connections between serial capacitors and parallel capacitors to achieve higher charging efficiency. Reproduced with permission. Copyright 2016, Elsevier<sup>166</sup>

angle sensing resolution of  $3.8^\circ$  can be achieved, showing great potentials in practical self-powered bending monitoring and human-machine interfacing. Previously, a

barcode system is normally developed based on the variation of output signal magnitude associated with the encrypted information, which is highly dependent on the

swiping speed and thus with low stability. Hence a barcode system with an additional reference electrode other than just the information electrode was developed to get rid of the swiping speed effect, as shown in Figure 4B.<sup>163</sup> When swiping the reference electrode (ie, periodic metal patterns) on one side and the information electrode (ie, purposely arranged metal patterns) on the other side together, the encrypted information can be detected by comparing the information outputs with respect to the reference outputs. A positive peak means a binary bit of “1”, whereas a negative means a binary bit of “0”. Then in between, if there are also peaks in the reference output, then the same number of bits should be added into the information output, according to the former binary bit. With the reference electrode, the encrypted information can still be successfully identified even under random swiping speed, indicating its good reliability to be applied in self-powered barcode systems for personalized identification and information security.

To realize multi-directional sensing and control with minimalist design, a single-electrode interface based on bio-inspired spider-net-coding (BISNC) configuration was proposed in Figure 4C.<sup>96</sup> First, all the grating electrodes are connected together as a single-electrode output, while for each direction, the width or position of the grating electrode is encoded with binary information for differentiation. Hence, according to the generated output signal patterns, the encoded information as well as the sliding direction can be detected. Moreover, the detection mechanism is only based on the relative output peak magnitudes or the peak positions in the time domain, thus exhibiting high stability and robustness in practical usage scenarios regardless of the ambient humidity and sliding speed/force. This wearable and minimalist interface can provide great advantages over the traditional pixel-based interfaces, such as facile device structure, layout design, electrode connection, signal readout, data acquisition, and processing. Based on the binary coding concept, parallel-connected metal patterns could also be used for self-powered data storage, as illustrated in Figure 4D.<sup>164</sup> The stored data is incorporated into the parallel-connected metal patterns on a polytetrafluoroethylene (PTFE) film. When the scanning probe slides on the patterned surface, contact electrification and electrostatic induction between them will produce an alternative quasi-square voltage according to the contacting area (ie, metal or PTFE). The resultant crest and trough of the voltage signal can be coded with binary bits of “1” and “0”, respectively. Meanwhile, the time interval of the crest and trough indicates the number of the same bits for constant scanning speed. According to the demonstrated data and numerical calculation, a maximum data storage density of 38.2 Gbit/in<sup>2</sup> is theoretically predicted,

which can pave a new path to high-density data storage with widespread applications.

For the conventional tactile sensors, they are commonly developed based on integrated pixel array, which shows significant complexity in layout, connection, and signal processing, especially when a higher resolution is required. Unlike the conventional pixel-based sensor arrays, an analog smart skin was developed with only four edge electrodes, as presented in Figure 4E.<sup>165</sup> The analog smart skin is able to detect single-point contact locations based on the contact electrification at the contact area and the planar electrostatic induction to the four edge electrodes. The location detection is realized using the voltage ratios of the two pairs of opposite electrodes, which define the horizontal and vertical position of the contact point, respectively. Benefited by this analog localizing method, the resolution of two dimensional (2D) location detection is as small as 1.9 mm, showing that a high-resolution detection can be achieved with only sensing electrodes. Along with the TENG advancement, the switch can be introduced into the operation cycles of TENG to achieve maximum energy transfer. Furthermore, novel electrode design could even enable unidirectional switch, realizing both direct-current output and maximized energy transfer simultaneously (Figure 4F).<sup>109</sup> Due to the characteristics of the switch, the maximized energy transfer can always be reached regardless of the connected load resistance, that is, wide impedance matching. Then a passive power management circuit is designed to boost the charging efficiency of this TENG, with an actual measured efficiency for capacitor charging of 48.0%. In practical demonstrations, an electronic watch and a quantum-dot light-emitting diode (LED) can be successfully driven by the unidirectional switch-based TENG and the passive circuit. Likewise, to address the low charging efficiency of TENGs due to its high voltage but low current characteristics, another advanced electrode design was proposed in Figure 4G.<sup>166</sup> The auto-power-management design is based on operations-driven switch connections between serial capacitors and parallel capacitors at different stages of operation. That is, there are  $N$  capacitors connected in series during the charging-capacitor stage and gives the total voltage  $N$  times higher than the voltage of each capacitor. Afterward, the automatic switches will make those  $N$  capacitors connected in parallel during the powering-electronics stage, so that the total voltage is changed to be the same as a single capacitor. Hence, the output voltage of TENG can be lowered for each capacitor, whereas the output current can be enhanced during the powering stage. As a comparison, the charging rate for a supercapacitor can be increased by five times with the auto-power-management



electrode design, which greatly enhances the charging capability of TENGs.

### 3.4 | Self-powered chemical/gas sensors

Other than the various physical sensors, different types of self-powered chemical/gas sensors have also been developed based on the TENG technology, playing important roles in the applications of human health, environmental and industrial monitoring. The chemical/gas sensors with TENG technology own the advantages of small size, zero-power consumption, and compatibility, which results in

good matches with the development of 5G technologies in all kinds of extreme environments and complicated systems. As shown in Figure 5A, a triboelectric sensor was demonstrated by using PDMS with pyramids and Pd nanoparticle coated ZnO nanorods to detect the  $H_2$  leakage for potential industrial applications. Exposure to the  $H_2$  atmosphere, the proposed device provides the output voltage with a value of 1.1 V at 10 000 ppm, showing a great response (373%) and acceptable response time (100 seconds) at this concentration. These early findings suggest TENG as an effective approach for environmental monitoring.<sup>167</sup> Apart from a metal oxide, the conductive polymer holds remarkable promises for gas sensing due

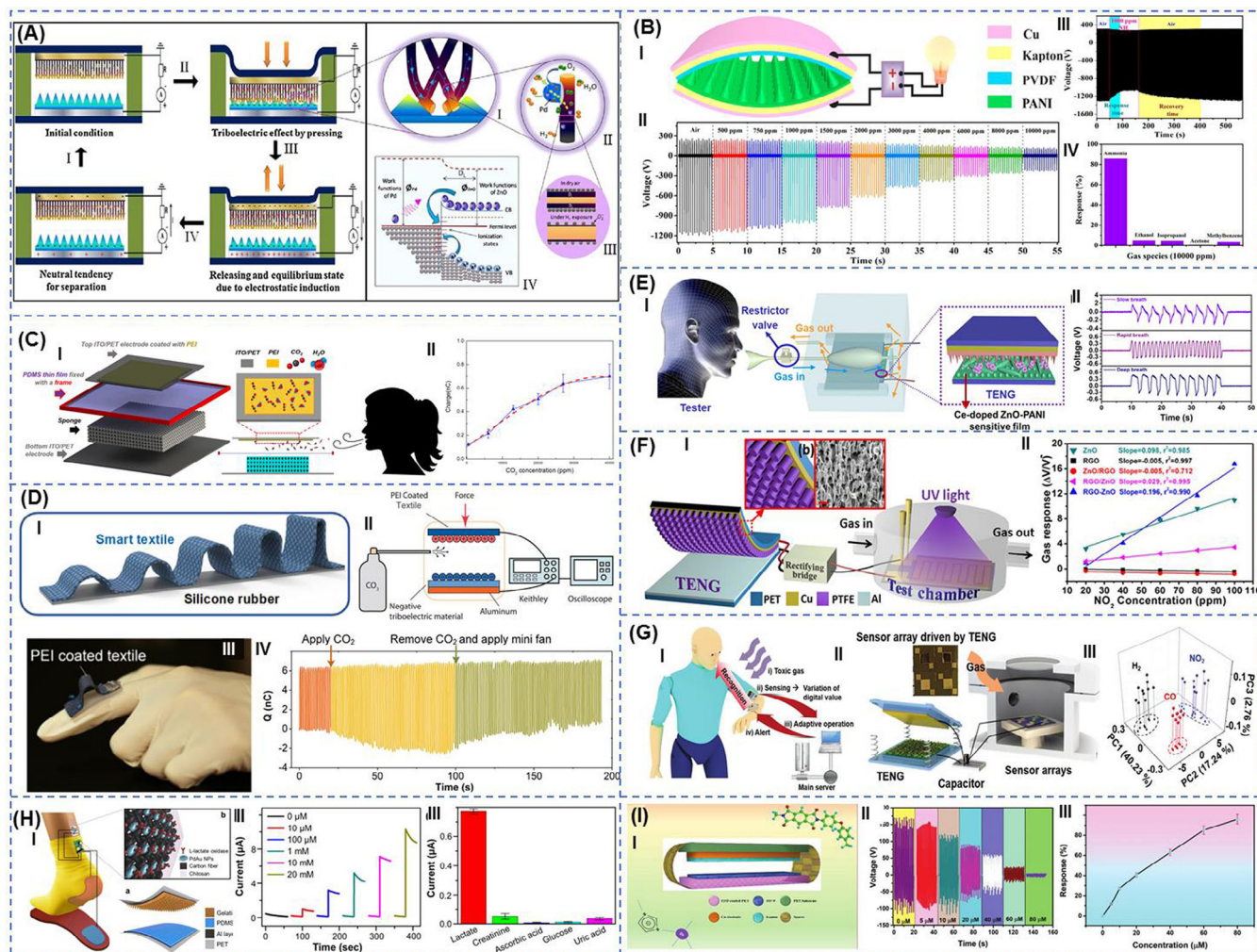


**FIGURE 5** Wearable self-powered gas and chemical sensors. A, Self-powered triboelectric  $H_2$  sensor based on PDMS/ZnO layers. Reproduced with Permission. Copyright 2016, Elsevier.<sup>167</sup> B, PANI-based TENG for  $NH_3$  sensing. Reproduced with Permission. Copyright 2018, Elsevier.<sup>97</sup> C, Ce-PANI-based TENG for  $NH_3$  tracking in human respiration. Reproduced with Permission. Copyright 2019, Elsevier.<sup>168</sup> D, Arch-shaped triboelectric textile sensor for  $CO_2$  sensing. Reproduced with Permission. Copyright 2019, Elsevier.<sup>169</sup> E, Water-air TENG for  $CO_2$  sensing. Reproduced with Permission. Copyright 2017, American Chemistry Society.<sup>170</sup> F, TENG has driven a self-powered  $NO_2$  sensor. Reproduced with Permission. Copyright 2018, Elsevier.<sup>171</sup> G, Multifunctional gas sensing array driven by TENG. Reproduced with Permission. Copyright 2019, Wiley-VCH.<sup>172</sup> H, TENG-driven electrochemical sensor for lactate detection. Reproduced with Permission. Copyright 2017, Elsevier.<sup>173</sup> I, Antibiotic detection based on triboelectric effect. Reproduced with Permission. Copyright 2019, Wiley-VCH<sup>174</sup>

to abundant active sites and tunable electrical property.<sup>175</sup> Accordingly, Cui et al reported self-powered poly-aniline (PANI)  $\text{NH}_3$  sensor based on the triboelectric effect as provided in Figure 5B, in which PANI serves as not only the electrification layer but also the active element for  $\text{NH}_3$  screening. Large  $I_{\text{sc}}$  of 45.7  $\mu\text{A}$  and  $V_{\text{oc}}$  of 1186 V in the air offers the opportunity toward sensitive  $\text{NH}_3$  sensing due to obviously reduced outputs. With good selectivity to  $\text{NH}_3$ , the room-temperature sensor experiences a high sensitivity of 0.21 V/ppm and a desirable limit of detection of 500 ppm.<sup>97</sup>

In addition to applications in environmental monitoring, respiration, as an important vital parameter, is another possible process that needs to integrate gas sensors. As shown in Figure 5C, Wang et al demonstrated a Ce-doped ZnO-PANI nanocomposite film to track the  $\text{NH}_3$  level in human respiration based on TENG. The self-powered  $\text{NH}_3$  sensor exhibits an obvious reduction with increased concentration from 0.1 to 25 ppm. Remarkably, a good performance (ie, low limit of detection) is observed when exposed to a trace-level  $\text{NH}_3$  atmosphere ranging from 0.1 to 1 ppm, showing a promising future for practical usage.<sup>168</sup> Besides, owing to an urgent need on fully wearable electronics, materials with intrinsic softness such as textiles have drawn attention in recent years.<sup>176</sup> The work from Lee's group described an arch-shaped  $\text{CO}_2$  sensor by leveraging triboelectric mechanism and polyethyleneimine (PEI) decorated fabric. The sensitivity of the device from 500 ppm to 9000 ppm is calculated to be  $2.69 \times 10^{-4}$  nC/ppm when the active textile contacts with PTFE (Figure 5D). Looking forward, this smart textile sensor enables incorporation into real garments for healthcare applications.<sup>169</sup> However, it is generally known that triboelectric output is susceptible to ambient variation, especially for humidity and force. Thus, as demonstrated in Figure 5E, Wang et al developed a suspended water-air triboelectric  $\text{CO}_2$  sensing platform with the capability of two major interferences elimination (ie, humidity and force). Two single-variable processes that are humidity-dependent and force-dependent contact-separation electrification can be separately determined under different  $\text{CO}_2$  concentrations. Such a novel design inspires the humidity-susceptible triboelectric sensors toward stable ones.<sup>170</sup>

In general, there are two approaches to achieve a self-power gas sensing system. One is employing TENG as a self-powered sensor, another is involving TENG as a power source to maintain the operation of other types of gas sensors. As depicted in Figure 5F, a TENG-driven chemoresistive sensor was developed for room temperature  $\text{NO}_2$  detection under UV illumination (365 nm), where the capacitance of the interdigital electrodes (IDEs) experienced a proportional decrease with

increased  $\text{NO}_2$  concentration.<sup>171</sup> Furthermore, as shown in Figure 5G, Lee et al demonstrated a multifunctional gas sensor array powered by polyimide-based polymer (6 FDA-APS) TENG that possesses the most negative electrostatic potential to provide high charge density (860  $\mu\text{cm}^{-2}$ ). The self-powered multiplexed gas sensing array enables the identification of  $\text{H}_2$ ,  $\text{CO}$ , and  $\text{NO}_2$  via principal component analysis of distinct current signal profiles. In practical application, the self-powered sensing system is integrated into an electronic watch, where specific gas is corresponding to light-emitting diodes (LEDs) with different light colors.<sup>172</sup>

Except for gas molecule recognition, TENG could afford the capability for other chemical monitoring. For example, as shown in Figure 5H, Lin's group introduced a micropatterned PDMS based TENG for a self-powered electrochemical sensor, that could detect the lactate concentration in human sweat. Compared with the dominant effort on self-powered physical physiological signal monitoring, a deep understanding of chemical information in human biofluids holds remarkable potential for more penetrating health assessment.<sup>173</sup> Similarly, Khandelwal et al included metal-organic framework (MOF) into the TENG system as one of the electrification layers to build a novel material based self-powered tetracycline sensor (Figure 5I). Through the interaction between MOF and benzene ring of tetracycline, the as-prepared TENG device shows a maximum response of 96.4% with calculated sensitivity of 3.12 V/ $\mu\text{m}$ .<sup>174</sup> Aforementioned works are summarized in Table 1 for a clear comparison.

## 4 | TOWARD NENS

Beyond the energy harvesting and the self-powered sensing by individual TENG, NENS in the concept of integrated systems are rapidly emerging in various research areas for their promising future in diversified applications, that is, blue energy, wearable electronics/HMI, neural interface/implanted device, and optical interfaces/photonics, and so on.<sup>177-184</sup> This section summarizes various aspects of the research applications using TENG technology in terms of materials, transducing mechanisms, and applications in an intelligent system.

### 4.1 | Blue energy

The blue energy, naming energy from the ocean area, now attracts massive attention due to its advantages of less dependence on weather, seasonality, and day-night rhythm.<sup>185</sup> Refer to the macro scale of over 70% of the



**TABLE 1** The summary of triboelectric gas sensors

Target analyte	Material	Sensing range	Sensitivity	Limit of detection	Response time (s)	Recovery time (s)	References
H <sub>2</sub>	PDMS/Pd/ZnO	10-10 000 ppm	0.35%. ppm <sup>-1</sup>	10 ppm	100 (5000 ppm)	N.A.	[167]
NH <sub>3</sub>	PVDF/PANI	500-10 000 ppm	0.028%. ppm <sup>-1</sup>	500 ppm	40 (1000 ppm)	225 (1000 ppm)	[97]
CO <sub>2</sub>	PDMS/PEI	1000-6000 ppm	4.8 × 10 <sup>-4</sup> nC. ppm <sup>-1</sup>	1000 ppm	<5	2	[168]
CO <sub>2</sub>	PTFE/PEI	1000-14 000 ppm	2 × 10 <sup>-4</sup> nC. ppm <sup>-1</sup>	1000 ppm	N.A.	N.A.	[169]
NH <sub>3</sub>	PDMS/PANI/ Ce-doped ZnO	0.1-25 ppm	13.66%. ppm <sup>-1</sup>	0.1 ppm	109 (1 ppm)	233 (1 ppm)	[170]
NO <sub>2</sub>	ZnO-RGO	20-100 ppm	0.196%. ppm <sup>-1</sup>	N.A.	566 (100 ppm)	547 (100 ppm)	[171]
H <sub>2</sub> /CO/NO <sub>2</sub>	6FDA-APS PI/Ag-SnO <sub>2</sub>	5-100 ppm	N.A.	N.A.	600 (25 ppm)	550 (25 ppm)	[172]
Lactate	PDMS/Gelatin/PdAu coated Carbon fiber	10 <sup>-5</sup> -10 <sup>-2</sup> M	0.650 mA. M <sup>-1</sup>	10 <sup>-5</sup> M	N.A.	N.A.	[173]
Antibiotic	MOF of ZIF-8/Kapton	0-80 μM	1.25%. μM <sup>-1</sup>	N.A.	N.A.	N.A.	[174]

Earth's surface covered by ocean, the blue energy presents a promising potential to solve the energy crisis of traditional fossil fuels. The blue energy is mainly in the forms of wave energy, tidal energy, thermal energy, and osmotic energy. Among these forms of energy, the wave energy around the global coastline has reached more than 2 TW according to the estimation.<sup>186</sup> Most existing researches limited the principles around piezoelectric, electromagnetic, and capacitive for sensing and energy harvesting applications. However, TENG based technology shows its tremendous advantages (high-voltage output and simple structure) and potential application opportunities for green energy harvesting and various functional sensing. Former types of research have proved that TENGs potential in harvesting mechanical energy, thus various kinds of TENGs are also proposed as blue energy harvesters.<sup>187-189</sup> Current blue energy harvester based on TENG can be roughly divided into two types: encapsulated devices relying on solid-solid contact,<sup>99,190</sup> and direct liquid-solid contact.<sup>191,192</sup> The encapsulated devices minimize the adverse impacts from humidity environment but introduce the complexity of fabrication and maintenance.<sup>193-198</sup> The devices based on liquid-solid contact TENG are normally thin-film typed devices which can be attached on well-designed structure, but their performances are limited by the materials' electrification with water, surface roughness, and ambient conditions.<sup>101,199-202</sup>

An overview of TENG in harvesting blue energy is illustrated in Figure 6. Different types of devices have been progressed to efficiently harvesting blue energy. As shown in Figure 6A, Liu et al proposed a torus-structured TENG (TS-TENG) which encloses an inner nylon ball inside a torus shell.<sup>203</sup> The ball can be rolling inside when TS-TENG is triggered by water waves, and generate electricity with six pieces of trapezoid fluorinated ethylene

propylene (FEP) electrodes equipped on each semi-torus shells. Owing to this circumferential symmetry of the torus shell, the TS-TENG can harvest random wave energy from all directions. With an agitation's frequency of 2 Hz and an oscillation angle of 5°, the TS-TENG is expected to give a maximum peak power density of 0.21 W/m<sup>2</sup>. Moreover, 16 units have been organized into arrays of 4 × 4 with parallel connection, successfully powering various electronics such as a thermometer or a commercial wireless transmitter. Compared with a former single rolling ball, a fully encapsulated duck-shaped TENG with a number of small Nylon balls has been reported by Ahmed et al in Figure 6B.<sup>100</sup> According to COMSOL simulation of electric potential distribution, the maximum charge quantity increases by reducing the ball diameter and increasing the electrode width. Moreover, multilayered duck-shaped TENG has been fabricated to utilize the space of the encapsulated package. When three of these devices are linked with a stiff shaft, the output power reaches to 1.366 W/m<sup>2</sup> in tests of water waves. A commercial wireless temperature sensor (eZ430-RF2500T, Texas Instruments) is successfully powered with a 1 mF capacitor as a storage unit for conversed electricity from water waves. Spherical structure is more commonly used to package TENG device.<sup>208-210</sup> Yang et al. proposed a self-assembly network based on spherical TENG units for blue energy harvesting as shown in Figure 6C.<sup>204</sup> Benefit with assembly magnetic joints, scattered spherical TENG units can spontaneously assemble together agitated by water waves. Thus, the network is capable of self-healing up after a rupture occurs in extreme conditions like storms. FEP pellets and 3D electrodes are applied in a single unit. In the test of 4 × 9 arrays assembled with 2 × 9 TENG units and 2 × 9 model balls, a peak power of 34.6 mW and average power of 9.89 mW for the network can be achieved with a matched

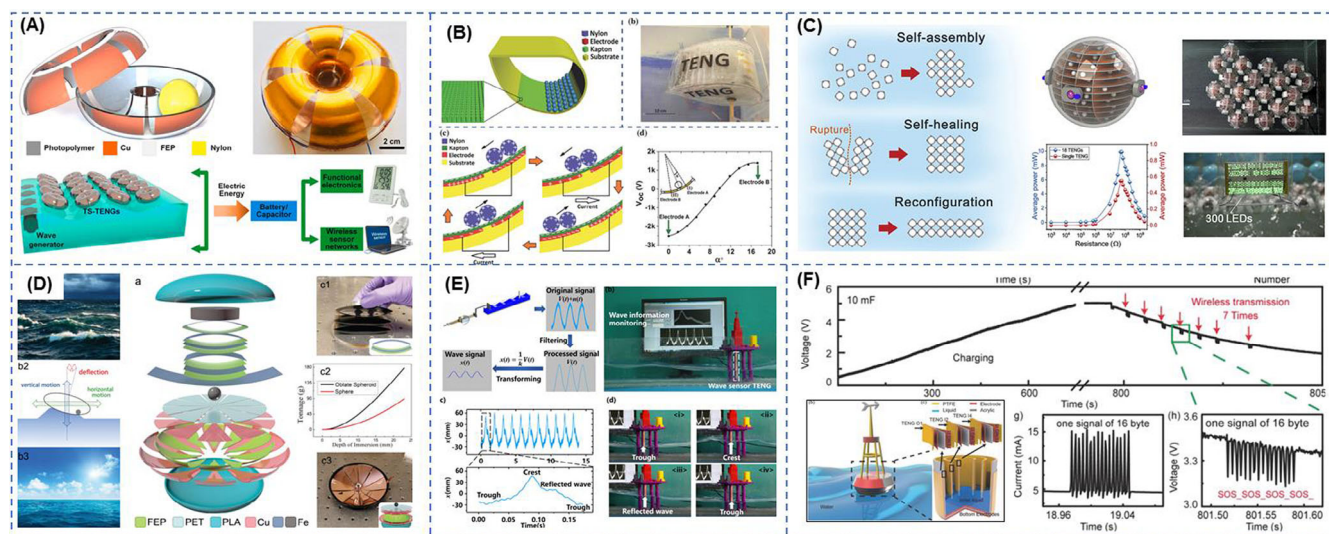


**FIGURE 6** TENG for blue energy applications. A, A torus structured TENG with a movable solid nylon ball. Reproduced with permission. Copyright 2019, Elsevier.<sup>203</sup> B, A duck-shaped TENG with multiple movable nylon balls. Reproduced with permission. Copyright 2016, Wiley-VCH.<sup>100</sup> C, A ball-shell structured TENG network using magnets on the connection points. Reproduced with permission. Copyright 2019, Elsevier.<sup>204</sup> D, An oblate spheroidal blue energy harvester based on multiple TENG operation modes. Reproduced with permission. Copyright 2019, Wiley-VCH.<sup>205</sup> E, A tube structured TENG based on liquid-solid interface contact electrification. Reproduced with permission. Copyright 2019, Elsevier.<sup>206</sup> F, A buoy structured TENG based on liquid-solid interface contact electrification. Reproduced with permission. Copyright 2018, Wiley-VCH<sup>207</sup>

impedance around 50 MΩ, with the average power density of 2.05 W/m<sup>3</sup> for per spherical TENG unit. A wireless transmitter is operated with a capacitor of 236.6 μF charged to about 3.5 V by this network. Oblate spheroidal TENG (OS-TENG) has been further reported for all-weather blue energy harvesting by Liu et al exhibited in Figure 6D.<sup>205</sup> Through calculation, the iron shot applied in OS-TENG goes farther than that in sphere shell under the same slant angle. Moreover, 42% of sphere shell volume can be saved in OS-TENG, which means less material consumption, easier mass manufacture, and greater applicability for large-scale TENG arrays. The network of OS-TENG can maintain stability without an external frame and presents the potential of harvesting substantial power energy from the ocean in all-weather.

The operation of TENG based on liquid-solid contact is closely related to the variable water environment. As shown in Figure 6E, Xu et al proposed a highly sensitive wave sensor focused on smart marine equipment.<sup>206</sup> The wave sensor is made of a copper electrode covered by a poly-tetra-fluoroethylene film with a microstructural surface. The output voltage increases linearly with wave height with a sensitivity of 23.5 mV/mm for the electrode width of 10 mm, implying that the wave sensor could sense the wave height in the millimeter range. When it is equipped on 3D printed marine platform's leg in a water wave tank, the wave sensor is successfully monitoring wave around a simulated offshore platform in real-time. Besides as sensors, TENG based on liquid-solid contact

also can be applied as a blue energy harvester. Li et al reported a buoy structured TENG containing three cylinders with different diameters,<sup>207</sup> and both liquid inside and outside can help TENG generate electricity in movements like up and down, shaking, or rotation. As shown in Figure 6F, this buoyed TENG has been applied to prevent metal corrosion and establish a self-powered wireless SOS system.

## 4.2 | Wearable sensors/HMI

Currently, the dominant HMIs still belong to touchpad, keyboard, mouse, and joystick. Although the voice and vision control is showing the rapid expansion in recent years, the privacy issue and the precision of controlling are frequently concerned. Hence, the wearable HMIs possess their necessities in realizing the advanced manipulation with the digital world. Meanwhile, in addition to the TENG based pure physical sensor, the optimization can be implemented to design the wearable TENG HMI, with great conformability, lower cost, and more functions.<sup>211–218</sup>

A stretchable transparent TENG tactile sensor was proposed by Wang et al for tracking the motion trajectory as shown in Figure 7A. The fabricated device consists of the PDMS electrification layer, two layers of Ag nanofiber-based electrodes made by electrospinning, cross-bar shape matrix, and a response time of 70 ms.



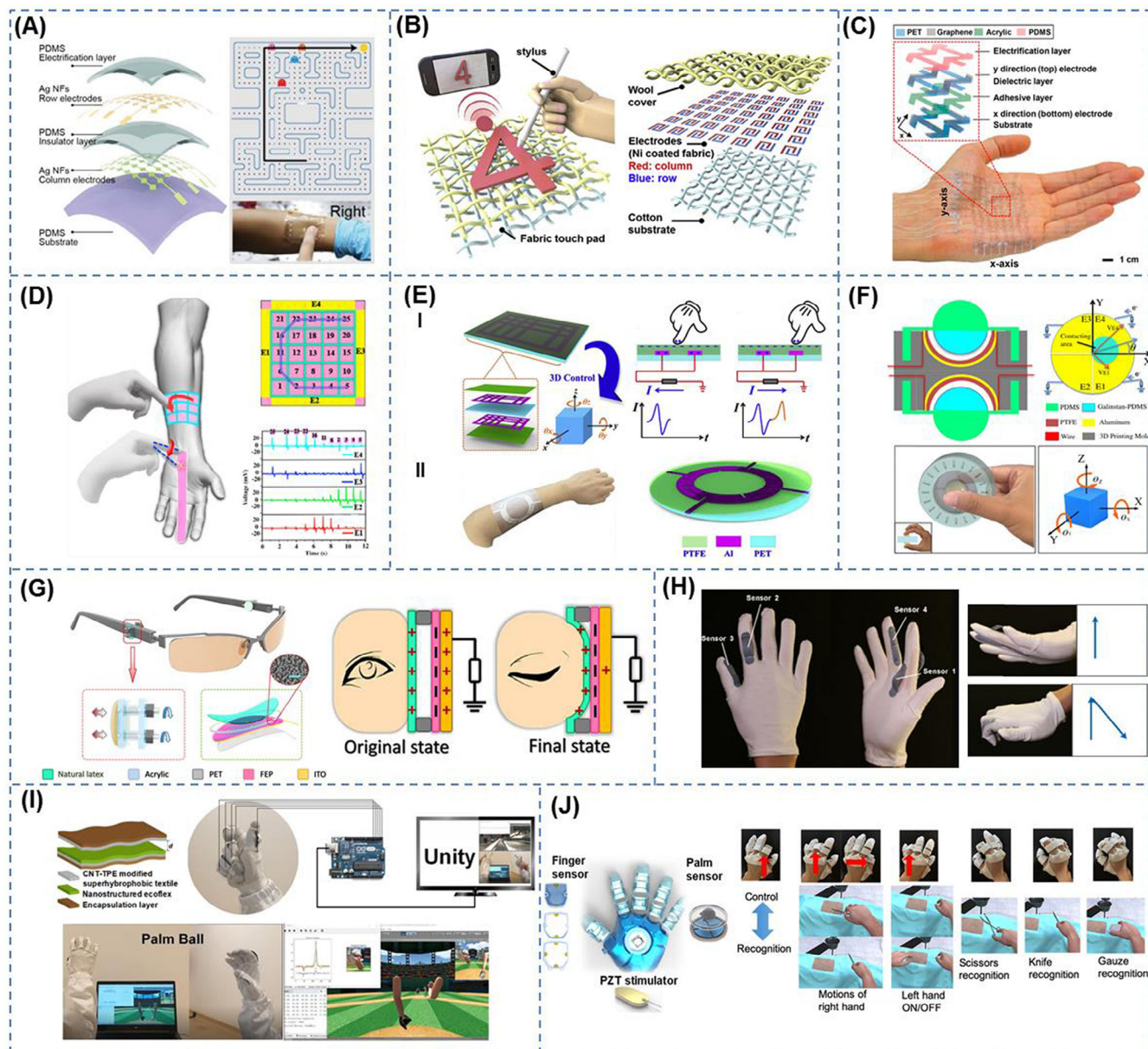


**FIGURE 7** Wearable TENG for HMI applications. A, Stretchable transparent triboelectric tactile sensor with metalized nanofibers. Reproduced with permission. Copyright 2018, Wiley-VCH.<sup>219</sup> B, Wearable touchpad using a crossline array of fabric TENG. Reproduced with permission. Copyright 2019, Elsevier.<sup>220</sup> C, Graphene-based stretchable/wearable self-powered touch sensor. Reproduced with permission. Copyright 2019, Elsevier.<sup>221</sup> D, Triboelectric flexible patch as 3D motion control interface. Reproduced with permission. Copyright 2018, American Chemical Society.<sup>158</sup> E, Triboelectric single-electrode-output control interface using a patterned grid electrode, and HMI using a ring-shaped triboelectric patch. Reproduced with permission. Copyright 2019, Elsevier.<sup>103,222</sup> F, TENG 3D-control sensor. Reproduced with permission. Copyright 2018, Elsevier.<sup>223</sup> G, Eye motion-triggered communication system using TENG. Reproduced with permission. Copyright 2017, American Association for the Advancement of Science.<sup>224</sup> H, Fabric glove-based intuitive interface. Reproduced with permission. Copyright 2018, Elsevier.<sup>225</sup> I, Machine learning glove using conductive superhydrophobic textile for gesture recognition. Reproduced with permission. Copyright 2020, Wiley-VCH.<sup>226</sup> J, Haptic-feedback smart glove for virtual/augmented reality applications. Reproduced with permission. Copyright 2020, American Association for the Advancement of Science<sup>24</sup>

The acquired data from an  $8 \times 8$  tactile array demonstrated the detection of finger operation instruction when playing Pac-Man. As a skin patch, it shows a stable signal output at 100% strain.<sup>219</sup> Moreover, by utilizing cloth as the largest platform on the human body, the wearable

HMIs with textile-based TENGs are also reported. Jeon et al have developed a wearable fabric touchpad as shown in Figure 7B. The nickel-coated fabrics were used to make the rows and columns of a crossline array. Each column or row of electrodes contains seven  $\eta$ -shaped unit

cells act as a pixel, and a  $7 \times 7$  array was formed. With a PTFE stylus and the wool cover, the writing path could be recorded by row and column electrodes.<sup>220</sup> An ultrathin stretchable TENG mesh was developed by fabricating a stack of polyethylene terephthalate (PET), bilayer graphene, and PDMS using the transfer technique, with a thickness of 18  $\mu\text{m}$ . The S-shaped design could afford a strain of 13.7% and 8.8% along x and y direction respectively as shown in Figure 7C.<sup>221</sup> However, these wearable sensing arrays usually applied crossbar type electrodes which would increase the difficulty of data processing. The analog approach is then necessary.<sup>165</sup> Chen et al have developed a silicon-based TENG touch patch with only four electrodes for the multipixel array, while still maintained the capability of trajectory tracing as shown in Figure 7D. Two electrodes formed an electrode pair which was placed at the patch. The finger touch induced triboelectric signal in the middle pixels could then be detected and processed as a voltage ratio from the electrode pair, and the grating structure ensured the automatic contact-separation motion during sliding.<sup>158</sup> Besides, a series of minimalist electrode-based wearable HMIs using PTFE thin film and Al electrode (Figure 7E) were reported by Shi et al. By specific design of electrode pattern, that is, asymmetric mesh, ring shape, the finger sliding along different directions would generate different peaks, which represented the corresponding control commands.<sup>103,222</sup> On the other hand, a 3D control sensor made by liquid metal mixed within the PDMS sphere was presented as shown in Figure 7F. The underneath electrodes were designed into four quadrants, to respond to the shear force caused by pushing the PDMS sphere, so that the 3D rotation and translation control can be achieved.<sup>223</sup> For assisting those disabled or elderly, some special methods of operation are crucial.<sup>154</sup> Pu et al. has presented the glasses mounted TENG made by natural latex membrane, FEP, and ITO electrode (Figure 7G). The proposed device could detect the eye blink induced deformation and programmed the blinking pattern into the control command, to assist the disabled patient to operate the appliance.<sup>224</sup> Similarly, by applying the membrane structure, a triboelectric cochlea device for an intelligent auditory system was developed. With the holes on the membrane, the acoustic wave induces the deformation and vibration, which could generate the triboelectric electric signal output under varied input frequency. The inner boundary design of the membrane enabled the tunable frequency response to achieve the optimized solution of hearing aid.<sup>152</sup>

Human hand as an important tool to achieve human-machine interaction is in charge of various dexterous motions in cyberspace or controlling of advanced robots.<sup>162,227,228</sup> He et al have developed a facile designed

TENG glove based on poly (3,4-ethylene dioxythiophene) polystyrene sulfonate (PEDOT: PSS) coated cotton fabric as shown in Figure 7H. By applying the arch-shaped strip on each joint of a finger, the conductive PEDOT: PSS coating could generate the triboelectric output with the silicone coating on the glove, and hence, to indicate the bending motion of each finger for realizing HMI.<sup>225</sup> Additionally, with the aid of the machine learning technique, a TENG glove made by superhydrophobic CNT-TPE coating was reported by Wen et al as shown in Figure 7I.<sup>226</sup> The proposed glove not only enhanced the durability of the textile-based TENG sensor under high humidity but also demonstrated the gesture recognition capability. Moving forward, Zhu et al reported a smart glove consists of TENG based finger bending sensor and a palm sliding sensor, as well as a piezoelectric haptic stimulator (Figure 7J). The hemisphere shaped soft finger sensor enabled the detection of both up-down bending and left-right swinging. And the palm sliding sensor was in charge of sensing the interaction with the external object. By applying machine learning and haptic feedback, the integrated glove demonstrated the advanced interaction in baseball and surgical training, with intuitive control and accurate object recognition.<sup>24</sup> Generally, TENG based wearable sensors expose the great potential of being the next generation of self-powered HMIs for the detection of multi-dimensional physical activities.<sup>229</sup> Meanwhile, there are also several obstacles that need to be considered, such as sensitivity, environmental influences, and so on.

### 4.3 | Neural interfaces/implanted devices

Recent breakthroughs about the implantable device using TENG have provided great potentials for self-sustainable neuromodulation, muscle stimulation, sensing therapy, and powering other medical devices, which reduces the heavy reliance on battery and prolongs the lifetime of these devices. As shown in Figure 8A,G. Yao et al presented a vagus nerve stimulation system based on a flexible TENG. In response to the stomach movement, the self-generated signal stimulates the nerve that administers the food intake and hence affects the obesity possibility. This strategy successfully reduces the rate of food intake and eventually achieves 38% of weight reduction.<sup>230</sup> Apart from the direct utilization of TENG as a neural interface, unremitting efforts on indirect nerve stimulation in which the generated current is applied to the neural electrode, establish another branch of implantable TENG for neuromodulation. Accordingly, a flexible neural clip interface integrated with TENG is provided in Figure 8B. The zigzag multilayer TENG is connected with



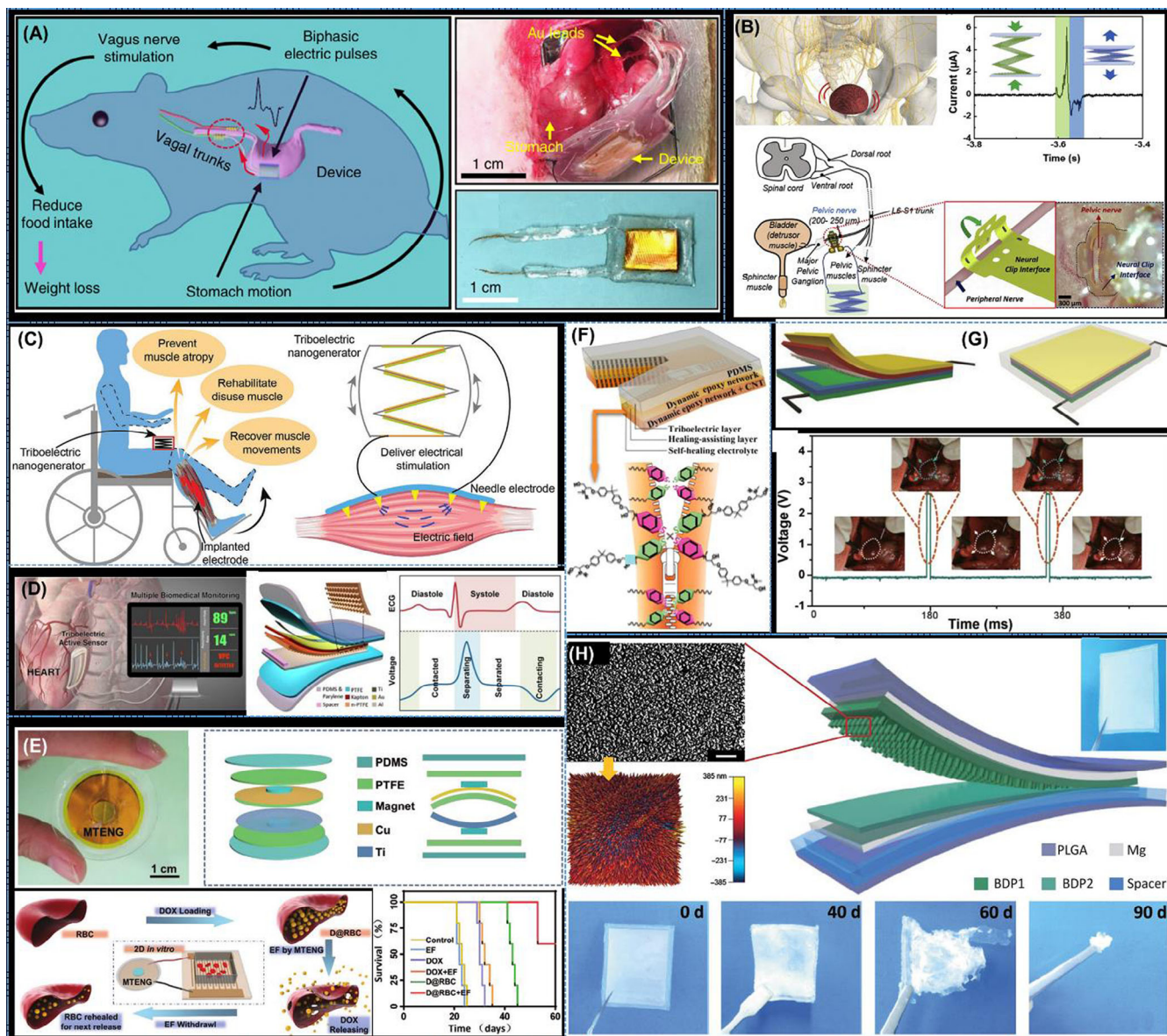


**FIGURE 8** TENG for neural interfaces and implantable devices. A, Weight control via an implanted self-powered TENG device for vagus nerve stimulation. Reproduced with Permission. Copyright 2018, Nature Publisher.<sup>230</sup> B, Implantation of triboelectric neuromodulation integrated with flexible neural clip for bladder nerve stimulation. Reproduced with Permission. Copyright 2019, Elsevier.<sup>231</sup> C, Low-current direct stimulation for muscle function loss treatment using TENG. Reproduced with Permission. Copyright 2019, Wiley-VCH.<sup>66</sup> D, Triboelectric active sensor for real-time cardiac monitoring. Reproduced with Permission. Copyright 2016, American Chemistry Society.<sup>102</sup> E, Cancer therapy by an implantable magnet TENG. Reproduced with Permission. Copyright 2019, Wiley-VCH.<sup>232</sup> F, Near-infrared irradiation-induced self-healing TENG for potential implantable electronics. Reproduced with Permission. Copyright 2019, Elsevier.<sup>233</sup> G, in vivo powering of the pacemaker by respiration-driven implanted TENG. Reproduced with Permission. Copyright 2014, Wiley-VCH.<sup>234</sup> H, Biodegradable TENG as an implantable power source. Reproduced with Permission. Copyright 2016, American Association for the Advancement of Science<sup>98</sup>

the neural electrode that is implanted onto the peripheral nerve for the adjuvant stimulation of inactive bladder.<sup>231</sup> The mechano-neuromodulation is further developed by the same group, leading to the extended applications in limb function rehabilitation<sup>235</sup> and motoneuron excitability investigation.<sup>236</sup> Additionally, a similar mechano-muscle stimulation using a self-powered TENG system is described

in Figure 8C. The stacked-layered TENG is connected with a multiple-channel epimysia electrode, where the electric current flows through the needle electrodes to stimulate the muscle for loss function recovery. With further study, it is found that systematic mapping can be achieved to overcome the low efficiency of muscle stimulation due to the low current of TENG.<sup>66</sup>

As the representative of implantable TENG for sensing shown in Figure 8D, Lee's group demonstrated a triboelectric active sensor that is implanted on the surface of an adult swine to record the heart and respiratory rate, where the triboelectric pair is composed of Al and nanostructured PTFE with the biocompatible PDMS encapsulation. The implantable triboelectric sensor maintains its functionality during 72 hours of continuous operation, indicating the perspective for long-term use.<sup>102</sup> Meanwhile, leveraging TENG into an implantable drug delivery system makes the way to self-sustainable therapeutic systems. Thus, magnet TENG driven in vivo drug delivery system for cancer therapy is presented in Figure 8E, in which the specially designed structure eliminates the commonly used spacer via magnet integration. Stimulated by electric outputs, a drug-loaded red blood cell membrane provides a well-controlled drug release, inhibiting the growth of cancer cells and accelerating the cell apoptosis.<sup>232</sup> Although the robustness of implantable devices is considered at the beginning of design, the damage is inevitable in the process of implantation and usage, inducing painful surgical replacement. Therefore, the self-healable TENG is vitally important to reduce the extra medical cost and pain of patients. Guan et al. proposed a self-healing TENG induced by near-infrared irradiation (NIR) for potential implantable electronics as shown in Figure 8F. The zipper-like self-healing process of disulfide metathesis can be expressed as that the carbon nanotube in epoxy efficiently absorbs the heat from near-infrared and transfers it to the epoxy layer, enabling self-healable capability provided by dynamic disulfide bonds.<sup>233</sup> Last but not least, implantable TENG was also usually adopted to scavenge biomechanical energy and sustain the operation of electronics. As shown in Figure 8G, the breath-driven implantable TENG is directly used to power a pacemaker that stimulates the rat heart regulated by the TENG. It was the early work that demonstrates TENG based in vivo biomechanical-energy harvesting in 2014.<sup>234</sup> Moving forward, the same group designs a biodegradable TENG as an implantable power source, which provides bright future for matured transient medical device development (Figure 8H). The biodegradable polymers and absorbable metals are employed to fabricate the device that shows the  $V_{oc}$  of  $\sim 40$  V and  $I_{sc}$  of  $\sim 1$   $\mu$ A. In the application scenario, the biodegradable TENG is used to power the grating electrodes, promoting the growth of nerve cells.<sup>98</sup>

#### 4.4 | Optical interface/wearable photonics

While the development of TENG has advanced various electronic applications, it has also brought indispensable

advantages to optical applications. The optical platform complements the electronic platform by providing intuitive display functions, offering a sensing platform that is invulnerable to EM interference, and enabling high-speed wireless transmission of information. The TENG technology, since its invention, has augmented a wide range of optical functions including light emission, photodetection, and optical modulation for the realization of applications including self-powered luminescence, smart display, wireless communication, personal privacy protection, and motion monitoring.

The simplest way of using TENG for light emission is to directly use TENGs output current to power LEDs. The TENG produces two pulse-like currents upon mechanical contact and separation. The peak current amplitude is enough to turn on a series of LEDs. In 2012 right after the invention of TENG, a series of 50 LEDs was lightened up by a simple TENG with PTFE and PET as the two triboelectric layers.<sup>237</sup> The maximum instantaneous output power was recorded as 4.125 mW by finger tapping. An interesting design call "TENG tree" was reported in 2018 (Figure 9A).<sup>238</sup> The TENG trees are composed of leaves and stems that are fabricated using the almost identical TENG platform with Al and Kapton as the triboelectric layers. Four supercells (a leaf-TENG and a stem-TENG) are connected in parallel to boost the output current. Due to the free-standing triboelectric layer, this design is suitable for wind energy harvesting in particular. At a wind speed of 11 m/s, 145 LEDs could be lightened up with high illumination intensity. In principle, the number of lightened LEDs can be scaled up by connecting more TENGs in parallel, with the help of a power management system to synchronize the current output. Another way for TENG-enabled light emission is to utilize the triboelectrification-induced electroluminescence.<sup>244-246</sup> As shown in Figure 9B-I, when an object slides on the triboelectric layer, an abrupt electric potential can be built across the ZnS: Cu particles in the PMMA matrix, leading to the green light emission of the phosphor.<sup>74</sup> Based on this mechanism, an image acquisition system is developed that mimics a writing pad (Figure 9B-II). The continuous trajectory of the word "light" and its corresponding Chinese character is successfully recorded (Figure 9B-III). To enhance the luminescence intensity, a similar device with micro-sized contact was developed.<sup>247</sup> The electric field at the micro-pillar edges is higher due to the abrupt change of electric potential at material interfaces. The resultant luminescence intensity is enhanced by two folds compared with a plain-surface counterpart. And each micro-sized pixel could act as a luminescence pixel. A method of optimizing the luminescence resolution was proposed in 2019.<sup>248</sup> An Ag nanowires layer was included whose function is to



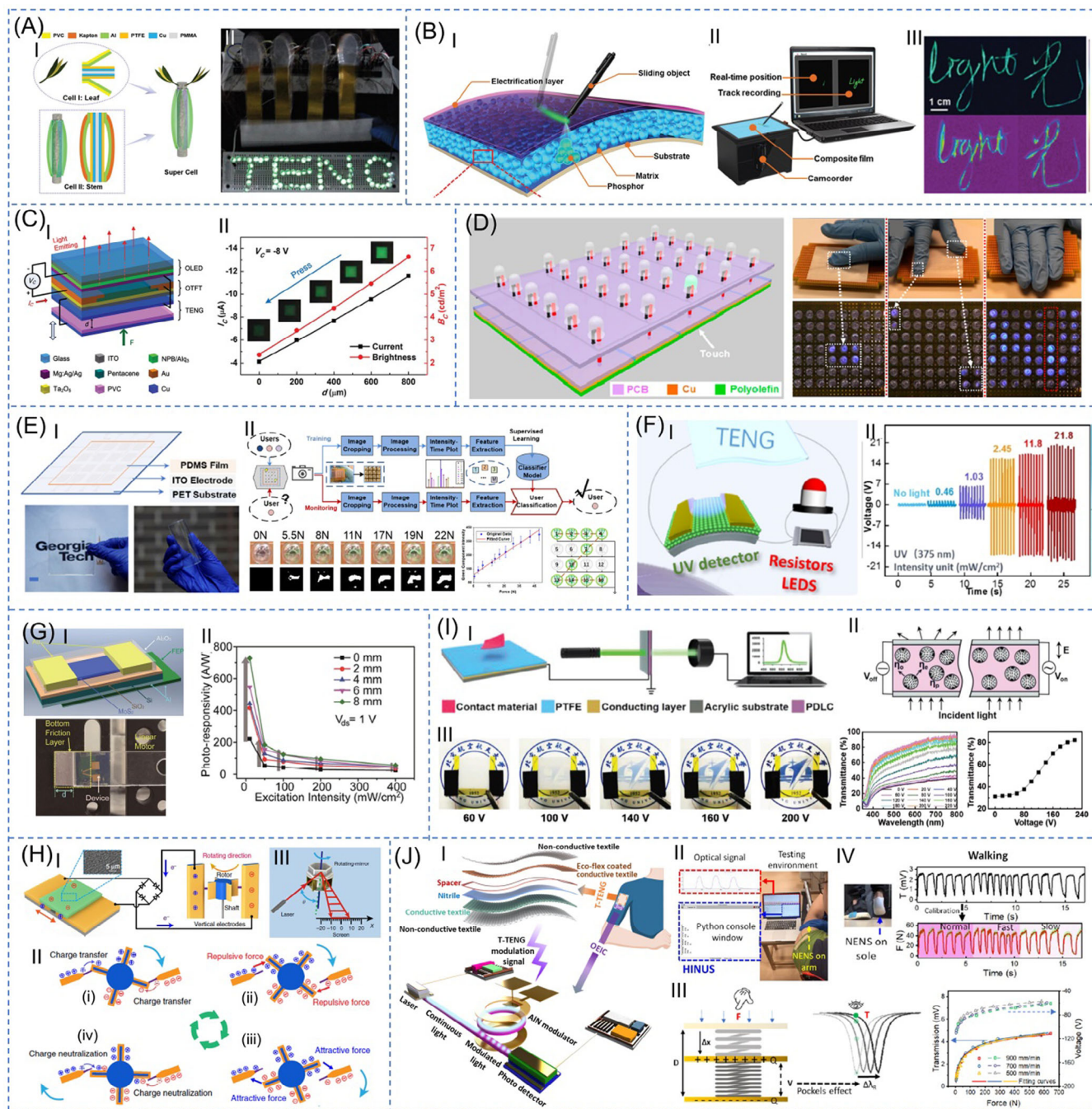


**FIGURE 9** TENG for optical applications. A, LEDs driven by TENGs output current. Copyright 2018, Wiley-VCH.<sup>238</sup> B, Triboelectrification induced electroluminescence. Reproduced with permission. Copyright 2016, Wiley-VCH.<sup>74</sup> C, TENG for OTFT controlled OLED. Reproduced with permission. Copyright 2015, Wiley-VCH.<sup>239</sup> D, TENG tactile sensing array with visualization function. Reproduced with permission. Copyright 2014, American Chemical Society.<sup>240</sup> E, TENG enabled self-powered optical wireless transmission. Reproduced with permission. Copyright 2018, Royal Society of Chemistry.<sup>15</sup> F, Self-powered UV light detection system with alarm LED. Reproduced with permission. Copyright 2020, American Chemical Society.<sup>241</sup> G, TENG for MoS<sub>2</sub> phototransistor. Reproduced with permission. Copyright 2015, Wiley-VCH.<sup>242</sup> H, Self-powered optical scanner by coupling a micromotor with TENG. Reproduced with permission. Copyright 2019, Springer.<sup>105</sup> I, Optical modulation by TENG-driven liquid crystal alignment. Reproduced with permission. Copyright 2019, Wiley-VCH.<sup>104</sup> J, Nanophotonic modulation by integrating TENG with AlN nanophotonics. Reproduced with permission. Copyright 2020, Wiley-VCH.<sup>243</sup>

guide the direction of electric fields and confine it within the profile boundary by leveraging the electric static shielding effect. The luminescence intensity was

enhanced by 90% while a lateral spatial resolution of 500  $\mu\text{m}$  was achieved. In the same year, a textile-based triboelectrification-induced electroluminescence system

was reported toward wearable applications.<sup>249</sup> The third method of TENG for light emission is leveraging the TENG voltage output as the gate voltage for organic thin-film transistor (OTFT) that monitors an organic light-emitting device (OLED). Figure 9C-I presents the system schematics.<sup>239</sup> The electrostatically induced TENG voltage serves as the OTFTs gate voltage and changes its channel characteristics. As the distance between two triboelectric layers increases, the larger gate voltage turns on the channel (Figure 9C-II). The corresponding larger source-drain current produces stronger light emission. In terms of practical applications, self-powered instantaneous tactile imaging was realized by using an electret film-enhanced TENG matrix. When pressing pixels in the matrix, the pressed areas generate triboelectric charges, and the consequent electrostatically induced current that lights up the embedded LEDs. The intensity of LEDs reveals the tactile information as shown in Figure 9D.<sup>240</sup> The luminescence also serves for wireless optical communication.<sup>250,251</sup> One characteristic system uses a camera to capture the image of the lightened LED (Figure 9E). The TENG device is transparent and simply composed of a PDMS triboelectric layer, an ITO electrode, and a PET substrate. The detected light intensity reflects the applied force on TENG. Complemented by the machine learning assisted image recognition, the system is able to perform identity recognition defined by finger sweeping patterns on a  $4 \times 4$  TENG-driven LED arrays. More recently, a self-powered low detection limit and high sensitivity wind speed sensor was demonstrated based on triboelectrification-induced electroluminescence.<sup>252</sup> Another characteristic system was proposed by connecting the TENG in parallel with a capacitor-inductor oscillating circuit and a laser diode (LD).<sup>15</sup> The amplitude and frequency of the wirelessly transmitted signal depend on different interaction force and the embedded identity capacitor respectively. To generate a strong wireless signal, a high TENG current is required. A microswitch is embedded in the system to regulate the discharging time. All the triboelectrically generated charges flow instantaneously when the switch is turned on, leading to a peak power of hundreds of mW. As a result, the transmitted signal can travel more than 3 m in the ambient. TENG has also benefited photodetection applications.<sup>253</sup> As shown in Figure 9F, with the help of TENG, self-powered photodetection for ultraviolet (UV) light exposure alarm has been realized.<sup>241</sup> In this work, the TENG was connected in series with a UV detector and a resistor type LED (Figure 9F-I). The TENG output current depends on the impedance match between TENG and the UV detector. Upon UV illumination, the impedance of the UV detector changes and leads to the variation in TENGs output which further determines the brightness of the

LED for visual assessment of UV exposure (Figure 9F-II). Similar to the application of TENG for OTFT-controlled OLED, TENG has also been applied to phototransistors. Figure 9G-I shows the device configuration where the charge generated by the contact of Al and FEP induces a voltage on the back-gate silicon to modulate the  $\text{SiO}_2$  dielectric layer.<sup>242,254</sup> Via the successful control of back-gate, the photo responsivity of the  $\text{MoS}_2$  phototransistor can be enhanced by around 4-fold to reach 700 A/W at low excitation power (Figure 9G-II). Beyond light emission and photodetection, optical modulation is equally important for light manipulation. In 2019, a self-powered optical scanner achieved by coupling a micromotor and a TENG was proposed.<sup>243</sup> The generated electrons from TENG are applied to two fixed electrodes via a rectifying circuit as shown in Figure 9H-I. The micromotor with four electrodes is placed between the two fixed electrodes. Upon contact, the electrons from the fixed electrodes are transferred to the micromotor electrodes (Figure 9H-II). Due to the repulsive force, the micromotor rotates clockwise. The clockwise motion is continued by the attractive force as the motor further rotates. Finally, the next rotation cycle starts after the charge neutralization. When the TENG slides a range of 5 cm at 0.1 Hz, the micromotor starts to rotate and reach over 1000 r/min at 0.8 Hz. The operation efficiency can reach a high value of 41%. Furthermore, as shown in Figure 9H-III, barcode recognition is demonstrated by using the TENG-driven micromotor for an optical scanner.<sup>105</sup> Self-powered optical modulation was also realized by coupling a TENG and a dielectric elastomer. As shown in Figure 9I-I, the system is simply composed of a TENG made of PTFE in the single-electrode configuration, and a polymer dispersed liquid crystal.<sup>255</sup> Due to the triboelectrically generated voltage induced alignment change in the liquid crystal, the transmittance of the liquid crystal changes from 85% to 5%, this is enough for privacy protection (Figure 9I-II, III). Besides polymer dispersed liquid crystal, self-powered elastomer-based tunable displays are also realized by TENG.<sup>104,256</sup> The voltage output from TENG induces rippling of the elastomer that varies its transparency. Recently, TENG has been successfully applied for nanophotonic modulation. Conventionally, nanophotonics adopt silicon photonic modulators that require high current for modulation, making them incompatible with TENGs high voltage but low current feature. As shown in Figure 9J-I, in the proposed system, aluminum nitride (AlN) photonics replace silicon photonics. Due to the second-order nonlinearity in AlN, the modulation efficiency of the ring resonator modulator is boosted by the high voltage from TENG. Since the top and bottom electrodes sandwich the ring resonator, the capacitive nature of this photonic device



does not degrade TENGs high voltage output. Self-powered photonic modulation was demonstrated for Morse code communication (Figure 9J-II). On the other hand, the nanophotonic modulator enables the open-circuit working condition of the TENG so that stable and real-time sensing can be realized using TENG. An analytical model was proposed to find a one-to-one correspondence between the force applied on TENG and the resultant transmission from the photonic modulator (Figure 9J-III). This characteristic was utilized for human motion monitoring (Figure 9J-IV).<sup>243</sup>

## 5 | MORE THAN TENG FOR SUSTAINABLE SYSTEMS

Moving forward to the new research directions more than TENG technology, this section summarizes the hybrid energy harvesting technologies, such as integration with EM generator (EMG) and/or piezoelectric nanogenerator (PENG), dielectric-elastomer-enhancement, self-healing, shape adaptive capability, self-sustained NENS, and/or IoT sensor nodes, and so on, toward the realization of sustainable systems.

### 5.1 | Hybrid generation by TENG and EMG

As a promising technique for energy scavenging from the ambient environment, TENG has shown great advantages while serving as a power supply for wireless sensor networks (WSN) and IoT with simple structure, relatively high efficiency of power density, cost-efficiency, and good reliability.<sup>96,108,130,257</sup> However, the energy supplied only by TENG is still not enough due to insufficient sustainable power output and also low output current caused by the intrinsic characteristics of TENG.<sup>169,258,259</sup> Therefore, to increase the output power density and utilize various ambient energy sources more effectively, the integration of other energy scavenging mechanisms with triboelectric has been widely explored in the past few years, including piezoelectric, thermoelectric, solar cell, and EM.<sup>116,260-262</sup> Compared with other kinds of energy generators, EMGs would have an advantage of compensation for the drawback (low power density in high frequency) in TENG, which is the low output current, with their large induction current and high-power generation.<sup>263-265</sup> Figure 10 shows several typical examples for the hybridized triboelectric-electromagnetic energy generators.<sup>266-270</sup>

The energy generator shown in Figure 10A is aiming at scavenging the ambient energy from airflow, which contains two EMG units and two TENG units.<sup>266</sup> The

Kapton film with the magnet in an acrylic tube is able to contact the upper side and bottom side of the acrylic tube with the driven of wind as shown in Figure 10A-II. Thanks to the transformer to balance the impedance of TENG and EMG, the final overall current can reach nearly 4 mA and enable the charge of a 3300  $\mu$ F capacitor up to 2 V in 50 seconds. To further increase the conversion efficiency of airflow, Figure 10B proposed a hybridized triboelectric-electromagnetic energy generator with a rotating-sleeve-based structure with improved efficiency to 36.4%.<sup>267</sup> Apart from the wind energy, the application of the generator with a similar structure can also be extended to another wide-spread renewable and clean energy source, called the ocean energy from the water wave. However, as encountered at sea, variable environmental conditions pose a new challenge for energy generation devices like TENG to avoid degradation of the output. For example, condition like high humidity is well known to counter the triboelectrification effect.<sup>271</sup> Hence, perfect encapsulation with the consideration of the mechanical transmission is essential for this hybridized triboelectric and EM energy generator applied in a harsh environment with large humidity or even underwater. One of the solutions is provided in Figure 10C, of which the moving part of the TENG is driven through the non-contact magnetic force.<sup>268</sup> This enables complete isolation of the TENG part from the environment and ensures the robustness. With the transformers and rectifiers to balance the impedance and also the synchronous design of TENG and EMG to keep them operating in phase, their output now can be directly added together, and great charging performance is achieved as shown in Figure 10C-III. Besides using the sliding mode of TENG, Figure 10D shows a cubic structure designed for the water wave with the utilization of freestanding contact mode of TENG aiming at more effective energy transmission.<sup>269</sup> Except for wind energy and ocean energy, a non-resonant hybridized generator based on elastic impact in Figure 10E was proposed to harvest mechanical vibration energy sources in the ambient environment.<sup>270</sup> With the non-resonant structure, the output power can become more stable and less influenced by the limitations of real-world vibration, such as random and large frequency variation range.

### 5.2 | Hybrid generation by TENG and PENG

The well-known triboelectric series built through the years are essential tools for designing a TENG.<sup>272,273</sup> However, the nature of the series itself shows one main drawback of TENG, namely the finite values of surface

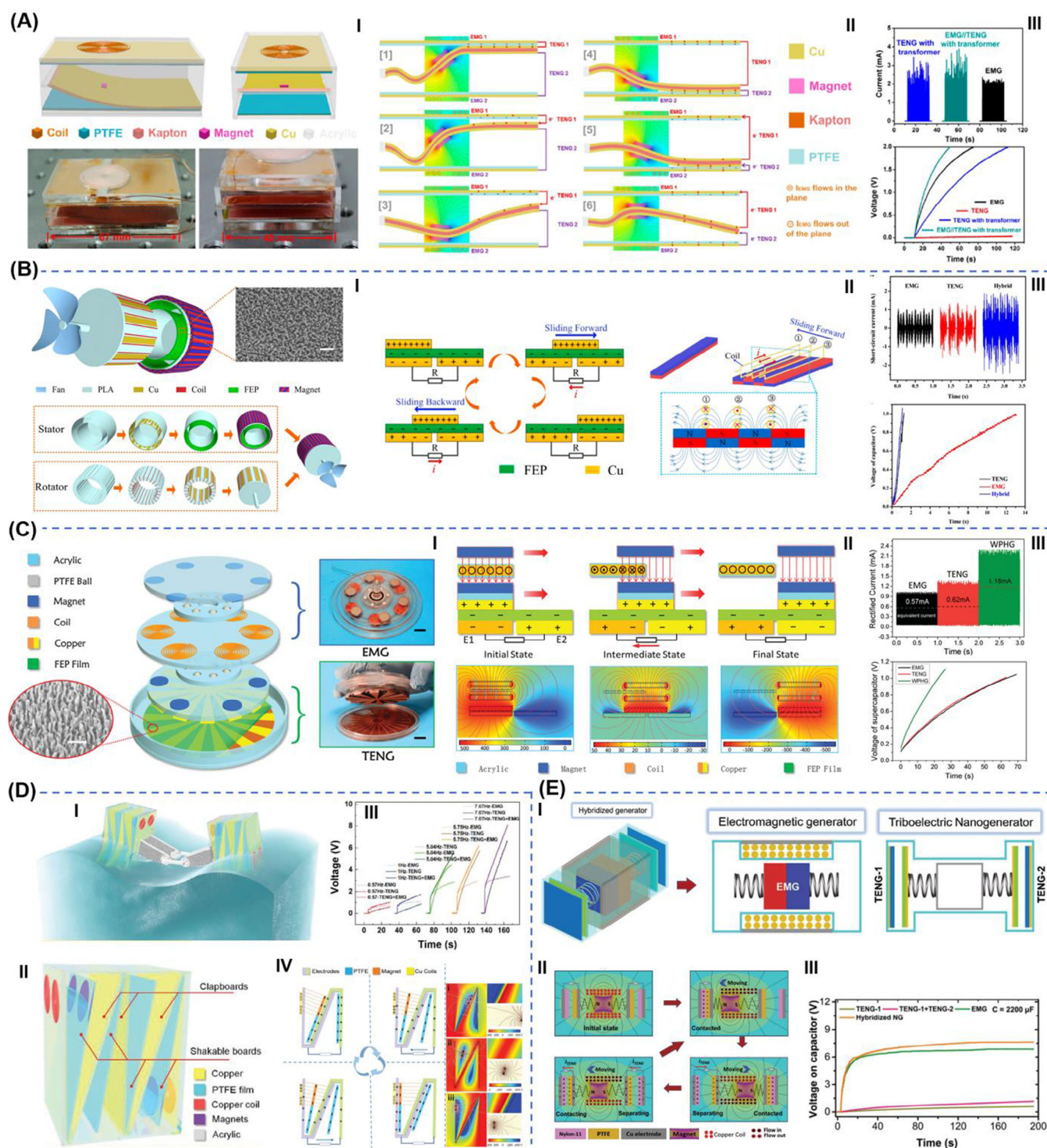


**FIGURE 10** Hybrid generators by TENG and EMG. A, Schematic of a hybridized TENG&EMG generator aiming at wind energy, the working principles, and charging curves for a 3300  $\mu\text{F}$  capacitor. Reproduced with permission. Copyright 2015, American Chemical Society.<sup>266</sup> B, Schematic of a hybridized TENG&EMG generator with a rotating structure, the working principles, and charging curves for a 470  $\mu\text{F}$  capacitor. Reproduced with permission. Copyright 2017, American Chemical Society.<sup>267</sup> C, Schematic of a hybridized TENG&EMG generator for blue energy, working principles, and charging curves for a 20 mF capacitor. Reproduced with permission. Copyright 2016, Wiley-VCH.<sup>268</sup> D, Illustration of the device on a water wave from the hybridized TENG&EMG generator and charging curves for a 10  $\mu\text{F}$  capacitor. Reproduced with permission. Copyright 2019, Wiley-VCH.<sup>269</sup> E, Schematic of a non-resonant hybridized TENG&EMG generator and charging curves for a 1000  $\mu\text{F}$  capacitor. Reproduced with permission. Copyright 2020, Wiley-VCH<sup>270</sup>



charges available in a material. This intrinsic limiting factor forced researchers into countless directions to push back the limit of power generation using triboelectricity. Coupling electromagnetic-based generators with triboelectric ones, as seen in section 5.1, is a smart way to enhance the efficiency of nanogenerators in terms of the ratio between the energy harvested and the energy available. Such coupling relies principally on enhancing the

mechanical behavior of the harvesting device to complement the part of the motion that is not covered by the TENG. This mechanism-oriented method has also been seen with piezoelectric-based generators through approaches such as wind energy harvesters in rotation (Figure 11G), and flying ribbon motion, footwear-integrated, and wearable energy harvesters, broadband vibration harvesters, and friction-like motion harvesters.<sup>278–286</sup>

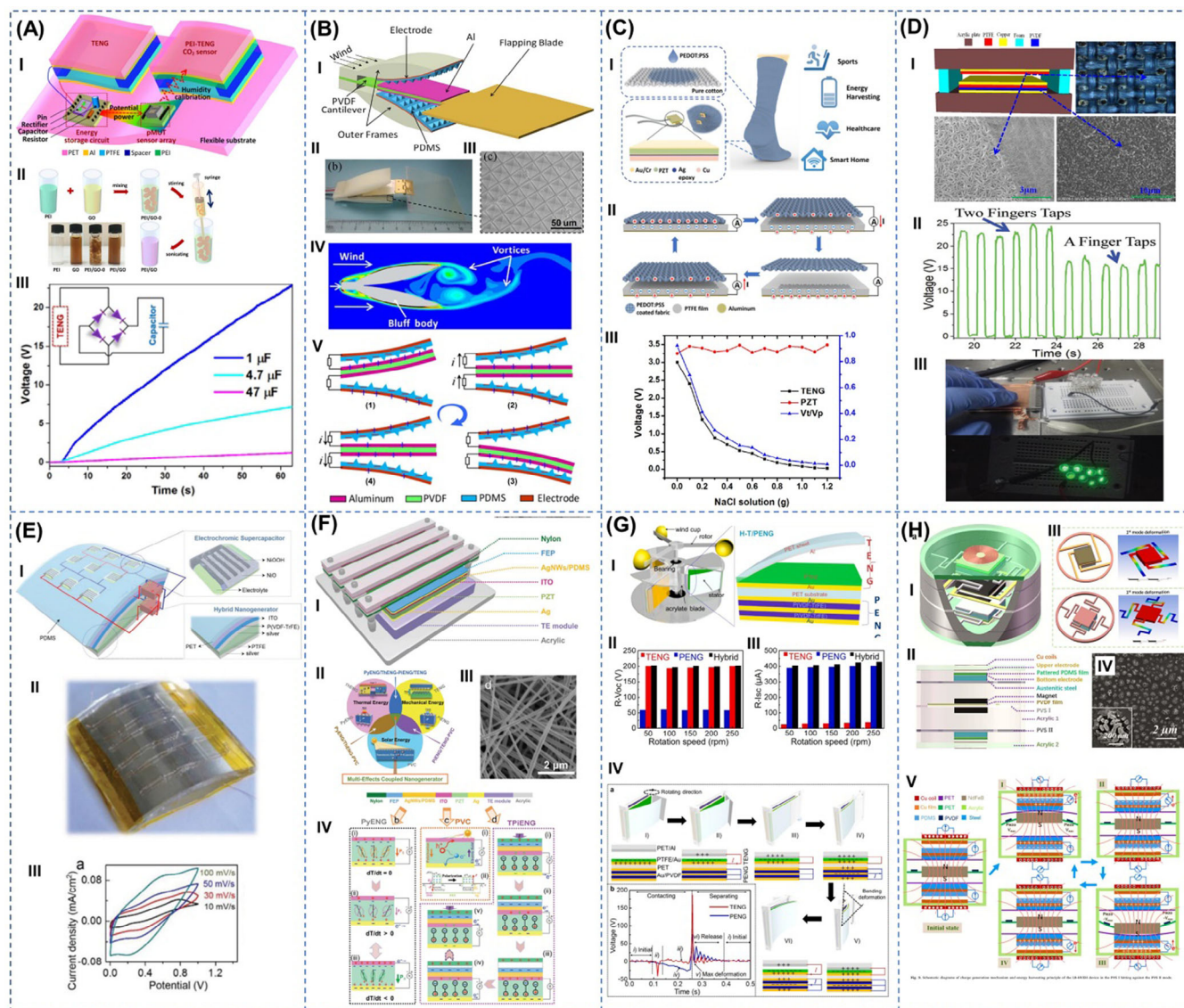


**FIGURE 11** TENG and PENG hybrid energy harvesting. A, Self-powered multifunctional monitoring system using hybrid integrated triboelectric nanogenerators and piezoelectric microsensors. Reproduced with permission. Copyright 2019, Elsevier.<sup>70</sup> B, Hybrid PE-TENG flapping-blade wind energy harvester. Reproduced with permission. Copyright 2016, IEEE.<sup>274</sup> C, Self-powered and self-functional piezoelectric and triboelectric hybrid wearable sock. Reproduced with permission. Copyright 2019, American Chemical Society.<sup>127</sup> D, A hybrid PE-TENG with PVDF nanoparticles and PTFE film for mechanical energy harvesting. Reproduced with permission. Copyright 2017 WILEY-VCH.<sup>275</sup> E, Hybrid PE-TENG self-charging electrochromic supercapacitor package. Reproduced with permission. Copyright 2018, Wiley-VCH.<sup>276</sup> F, A one-structure-based PE-PyE-TE-PVC coupled nanogenerator for simultaneous energy harvesting. Reproduced with permission. Copyright 2016 Wiley-VCH.<sup>277</sup> G, Hybrid PE-TENG for highly efficient and stable rotation energy harvesting. Reproduced with permission. Copyright 2019, Elsevier.<sup>278</sup> H, Low-frequency PE-EM-TENG hybrid broadband vibration energy harvester. Reproduced with permission. Copyright 2017, Elsevier.<sup>279</sup>



Yet, it is the augmented electrostatic induction method from the integration of polarized piezoelectric material into the TENG that has garnered the most interest in recent years. This method is based on the synergetic coupling between the electric field and charges separation of the PENG and TENG, as shown by Yang et al using aluminum and zinc oxide nanorod.<sup>287</sup> One paper even demonstrated that leveraging this phenomenon, the triboelectric series can even be neglected since the same material, under inverse polarization, can generate remarkable output signals from PE-TENG hybrid harvester.<sup>288</sup> However, to get the maximum out of this electrostatic coupling in PE-TENG, researchers have been hard at work to find the optimal material combination for the task. Polyvinylidene fluoride (PVDF), being a polymer with piezoelectric properties, is the most popular material for hybrid PE-TENGs since it allows for flexibility, which is a desirable property for applications such as wearable sensors and energy harvesters. PE-TENG motion sensors using PVDF fibers as only the piezoelectric layer or as both the piezoelectric layer and triboelectric contact surface have been reported, along with vibration sensors and nanogenerators made with polarized PVDF film and PVDF nanoparticles.<sup>275,289-293</sup> One eloquent example of the polyvalence of PVDF is displayed in Figure 11B. A flapping-blade wind energy harvester with TENG integrated wing-like outer frame oscillates up and down, following the vortices created by the wind perturbations. The high amplitude motion actuates the PE-TENG hybrid system for high-output wind energy generation.<sup>274</sup> Another polymer with similar properties of PVDF is poly(vinylidene fluoride-co-trifluoroethylene) (P(VDF-TrFE)), from which various wearable nanogenerators have been realized.<sup>294-296</sup> In Figure 11E, one particular device based on P(VDF-TrFE) integrates electrochromic supercapacitors alongside the nanogenerator, hence leveraging high output power density and high energy storage, both propitious for sustainable self-powered systems.<sup>276</sup> For other applications, flexibility is not always a requirement, and rigid piezoelectric ceramics such as lead zirconate titanate (PZT) are used as a layer into PE-TENG for enhanced output and measurement capacity. Figure 11C depicts a wearable smart sensors system compound of PZT pads attached to a PEDOT: PSS-coated fabric TENG. The assembled PE-TENG monitors a wide variety of environmental and physiological factors such as humidity, temperature, and pressure variation during on foot motion.<sup>127</sup> Such ambulatory pattern monitoring capabilities were also investigated using PE-TENG,<sup>297-299</sup> allowing for data collection for gait analysis and health monitoring based on PE-TENG sensors. Combining flexible polymers with rigid piezoelectric ceramics has been extensively investigated in the last years to push further back the intrinsic energy harvesting limit

set by the material physics behind TENG, leading to the creation of a multitude of composite polymers with greatly improved characteristics. Using BTO nanoparticles embedded in a polymer matrix layer to act as a triboelectric contact and polarized piezoelectric layer has been reported for P(VDF-TrFE) and PDMS composite.<sup>300,301</sup> The later, BTO + PDMS has even been microstructured and combined with multiwalled carbon nanotube (MWCNT) for augmented surface area.<sup>298,302</sup> Triboelectric contact and a piezoelectric layer made of barium zinc-oxide titanate (BZTO) nanoparticles variations and optimized in concentration forming a composite with PDMS and PVDF have also shown great performances.<sup>303-305</sup> Furthermore, flexible ZnSnO<sub>3</sub> nanocubes in PDMS with optimized mixing concentration for triboelectric contact and the piezoelectric layer<sup>306</sup>; along ZnO nanorods, nanowires and nanoflakes in PDMS and LiZnO nanowires inside PVDF matrix with MWCNT,<sup>297,307-309</sup> for triboelectric contact and the piezoelectric layer have been investigated.<sup>310</sup>

Besides polymer composites with enhanced triboelectric and piezoelectric properties, another family of materials has garnered much interest for its great mechanical properties. Fabric-based triboelectric contact and piezoelectric layer are fast developing and several working designs have been unveiled. In Figure 11D, PVDF nanoparticles and woven PTFE fiber film have been assembled into a flexible PE-TENG core. Improved contact surface due to the nature of the woven fabric and polarized nanoparticle film can indeed provide good energy harvesting capabilities while still maintaining crucial mechanical properties.<sup>275</sup> The PEDOT: PSS-coated smart sock with embedded PZT chips presented in Figure 11C also shows a good balance between triboelectric and piezoelectric materials on textiles for health care monitoring and rehabilitation. It achieved great wearing comfort and shape conformality to not only provide detection of foot motions, but also achieve the sweat sensing via sensor fusion concept, that is, use PZT as a reference sensor to measure the degradation of triboelectric output under increasing sweat level.<sup>127</sup> Similarly, He et al presented a device,<sup>311</sup> where the full PE-TENG itself follows an inter-woven fabric-like design that can be put into contact with the wearer's skin or clothes. Experiments demonstrate that the device is able to attach to different body parts and generate a valuable biomechanical energy output. Furthermore, an all-fiber hybrid PE-TENG wearable has also been presented by Guo et al, pushing even further the development of fully wearable PE-TENG based systems for motion detection and health monitoring in the upcoming IoT era.<sup>290</sup>

It is undeniable that material synthesis and development for optimizing PE-TENG currently benefit from a strong momentum. Nonetheless, other directions in the

PE-TENG research have also made great progress. Integrated PE-TENG devices used as sensors and energy harvesting in different applications have also recently emerged. A self-powered flexible multifunctional system based on TENG energy harvesters and TENG gas sensors coupled with piezoelectric micromachined ultrasonic transducer has been developed.<sup>70</sup> This system monitors ambient parameters such as temperature, relative humidity, and gas concentration. Simultaneous detection of parameters has been achieved with good overall stability and great selectivity in terms of CO<sub>2</sub> sensing (Figure 11A). With academia and industry's growing interest in IoT devices and flexible electronics, the integration of TENG for energy harvesting and sensing into a configurable flexible self-powered multifunctional sensing system is assured to stay a primary topic of research. Going even further than PE-TENG, some teams have presented TENG systems taking advantage of multiple other sources of energy such as temperature variation via pyroelectric nanogenerators (PyENG) and even photovoltaic cells (PVC), as seen in Figure 11F.<sup>277,312</sup> Other designs rely on EM to enhance the efficiency of vibrational energy harvesting by combining PE-EM-TENG in one system,<sup>279</sup> illustrated in Figure 11H. In the era of the IoT, where integrated self-sustained wireless sensor nodes are getting closer and closer to reality, this kind of engineering approach based on multi-effect coupled generators to improve the efficiency is indeed an important direction not only for TENG but for all nanogenerators in general.

### 5.3 | Dielectric-elastomer-enhanced TENG

Dielectric elastomers can be employed to enhance the performance of TENG in different ways. They can provide flexibility and stretchability to triboelectric layers which can improve the output performance through increasing the tribo-surface charge. In addition, adequate stretchability is essential for the application of TENG with the next generation of soft and stretchable electronics.

Dielectric elastomers are introduced into TENGs to improve their output performance in many works. For example, Li et al.<sup>313</sup> proposed a fully stretchable triboelectric nanogenerator (FS-TENG). It is made up of a porous-PDMS friction layer with an anti-nickel foam structure and a flexible electrospun electrode (Figure 12A). Flexible TENGs are usually constructed by flexible friction layer materials such as PDMS, polyurethane (PU), and silicon rubber.<sup>317</sup> However, porous PDMS in this work increases the surface-to-volume ratio and surface roughness, which

enhances the output performance. In addition, the integration with the electrospun electrode makes the TENG fully stretchable. The electrical output and mechanical flexibility of FS-TENG are significantly improved with an optimal output voltage of 92 V and electrical output reduction by only 21.2% with up to 50% stretch ratio. Nayak et al in 2019 also presented a TENG made from a mouldable soft porous material (Figure 12B).<sup>314</sup> The pores in the material act as tiny TENGs. The porous material is made of a composite of a liquid metal alloy (LMA), Ecoflex 0030, and NaCl particles that are used as a water-scalable sacrificial template to create pores in the elastomer. An optimum composite of (LMA: NaCl: Ecoflex = 3:5: 10) shows  $I_{sc}$  of ~466 nA and  $V_{oc}$  of ~78 V for a sample of 5 cm × 5 cm × 1 cm subjected to 5 mm compression relaxation cycles. The output current is nearly 20% higher than previously reported triboelectric foams based on PDMS and PZT/CNT of the equivalent area. Wang et al. in 2016 proposed a triboelectric layer that is formed by embedding aligned carbon nanotubes (CNTs) on the PDMS surface (Figure 12C).<sup>315</sup> The CNT-PDMS layer acts as an effective triboelectric layer to donate electrons. It does not only increase electron generation for high output performance but also shows notable stretchability. For example, the CNT-PDMS layer with 40 μm CNT shows a TENG output voltage of 150 V and a current density of 60 mA/m<sup>2</sup>, which undergoes a 250% and 300% enhancement compared to the TENG using directly doped-PDMS/multiwall carbon nanotubes, respectively. Highly stretchable and healable energy generators are essential for the development of soft electronics. Parida et al in 2019 developed a new extremely deformable and healable TENG.<sup>107</sup> Significant works have been done before for highly stretchable and healable TENGs. The stretchability was limited to ~1000%. Most of these generators are based on commercial elastomers like PDMS, silicon rubber, and VHB. However, Parida et al proposed a composite which is highly conductive, extremely stretchable, and healable based on thermoplastic elastomer with liquid metal particles, and silver flakes (Figure 12D). The elastomer is used as a matrix for the conductor and a triboelectric layer with a stretchability of 2500%, and it is made of polyurethane acrylate (PUA). The challenge to achieve such high stretchable and mechanical durable TENG is the interface compatibility between the triboelectric layer and the conductor. However, they address this problem by developing TENG with high stretchable and healable PUA elastomer which acts as a triboelectric layer and, also as a polymer matrix for the conductor consisting of liquid metal and silver flakes. The high stretchability and healability of the developed PUA can be ascribed to the supramolecular hydrogen-bonding interactions with a

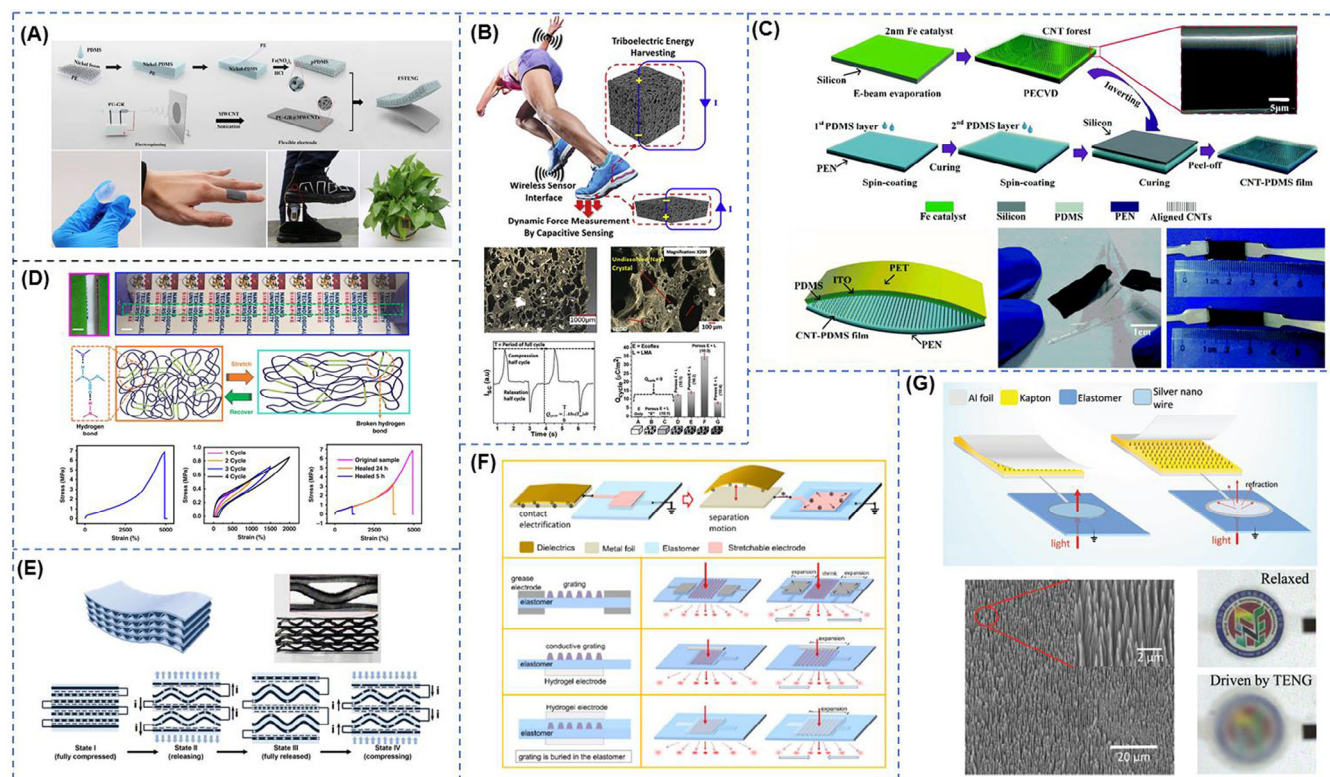


**FIGURE 12** Dielectric-elastomer-enhanced TENG. A, Fully stretchable triboelectric nanogenerator (FS-TENG) composed of an electrospun electrode and a porous PDMS friction layer with anti-nickel foam structure. Reproduced with permission. Copyright 2019, Elsevier.<sup>313</sup> B, Liquid-metal-elastomer foam-based TENG for energy harvesting and force sensing. Reproduced with permission. Copyright 2019, Elsevier.<sup>314</sup> C, Stretchable and high-performance TENG using aligned carbon nanotubes. Reproduced with permission. Copyright 2016, The Royal Society of Chemistry.<sup>315</sup> D, Stretchable and self-healing conductor-TENG based on the thermoplastic elastomer. Reproduced with permission. Copyright 2019, Nature.<sup>107</sup> E, Multilayer elastomeric-enhanced-TENG. Reproduced with permission. Copyright 2017, Wiley-VCH.<sup>106</sup> F, Self-powering and control of elastomeric optical grating using TENG. Reproduced with permission. Copyright 2017, Elsevier.<sup>316</sup> G, Triboelectric tunable smart optical modulator (SOM) based on TENG-DEA. Reproduced with permission. Copyright 2017, Wiley-VCH<sup>255</sup>

large number of weak hydrogen bonds, which repeatedly break and reform during mechanical damage. Elastomers are used to improve the output performance of TENG by structure modification. Li et al in 2017 presented an innovative multilayer elastomeric TENG and corresponding self-charging power system (Figure 12E).<sup>106</sup> Due to the materials and structure innovation of the proposed TENG, it performs an outstanding electric output with the maximum volume charge density of  $\sim 0.055 \text{ C/m}^3$ . The improvement by this TENG comes from the high flexibility and stretchability of the elastomer, which can improve the effective contact area between two triboelectric layers and consequently surface charge generation. The structure of the proposed TENG consists of two main parts, a plane dielectric-conductive-dielectric part lays over a conductive-dielectric-conductive as shown in Figure 12E. The thickness of the conductive layer is  $\sim 0.3 \text{ mm}$ , and the dielectric layer is  $\sim 1 \text{ mm}$  for each part. In this manner, the whole space taken by the

multilayer TENG can be divided into several layers of small arch-shaped space. Each small arch is one unit. When the units are stacked together closely without any spare space, the whole space can be efficiently utilized for high charge density and corresponding to electric current density. This design has another advantage. Since the plane and wavy parts can be lengthened for effective contact and separation, the structure would be also effective for harvesting stretching mechanical energy. Structure parameters of this TENG are also optimized in this work based on both experimental and simulation results for high volume tribocharge density.

On the other side, TENGs are used to power/control dielectric elastomer actuators (DEA). DEAs demonstrate excellent properties as artificial muscles. The main obstacle for the remote operation of DEA is the need for a high voltage source. The required driving voltage is in terms of few kilovolts TENG has a unique advantage as its output voltage is quite high even its size is rather small.<sup>318</sup> Some



applications are presented based on the TENG-DEA system. For example, Chen et al in 2017 introduced a tunable optical gratings system (TOGs) based on TENG (Figure 12F).<sup>316</sup> TOGs are usually constructed by silicon-based micro-fabrication technology, so they relied on rigid elements that give them a limited tuning range<sup>319</sup> as well as slow response and high power loss.<sup>320</sup> Another alternative approach for efficient TOGs based on soft elements and DEA are also introduced. In fact, they cannot give the same precision as hard elements, however large and continuous tuning range, as well as low fabrication cost and fast response, could be obtained. Chen et al. utilized a single electrode TENG based on contact-separation motion to drive a DEA element. Single electrode TENG is usually utilized for TENG-DEA system, since its internal capacitance is relatively small, and it will not change with different motion position. This large amount of TENG charge output is occupied by DEA. Hence, the efficient operation of the DEA could be guaranteed. A Kapton layer (negative) and Al foil (positive) are used as triboelectric layers. Contact-separation of the TENG applied a strong electric field on the DEA and has the dual function as a power supply and a control signal for the DEA. Tunable smart optical modulation (SOM) can be another application based on TENG-DEA. Chen et al also presented a tribo-SOM which can be used for privacy protection purposes (Figure 12G).<sup>255</sup> A single electrode TENG based on contact-separation is also utilized to power the SOM system. Kapton film and Al foil are used as contact triboelectric layers, where the Kapton film is covered with a series of nanopatterned structure using inductively coupled plasma (ICP) reactive-ion etching to improve the surface charge density and consequently the output performance of the TENG. DEA device is fabricated by applying a nanowire electrode on both the top and bottom sides of an elastomer film. Under the activation of TENG, the nanowire electrode can control the optical transmittance through the elastomer and hence change the observation image through the film, which can be considered as a privacy protection device.

## 5.4 | New materials for novel functionalities

Except for the adoption of dielectric materials, the introduction of other novel materials in TENG to enable new functionalities is another new and promising research direction. In this section, several interesting functionalities of TENG will be introduced, including shape memory capability, self-healing capability, shape adaptive capability, and stretchability.<sup>139,233,321-341</sup> In 2015, Lee et al proposed the first shape memory TENG, where the shape

memory polymer, PU serves as the triboelectric layer (Figure 13A).<sup>323</sup> PU film is patterned with a pyramid structure to enhance the output of TENG, while the pyramid pattern would be flattened under a higher applied force or long-time contact and separation process, resulting in a decrease of the output of TENG. Taking the advantages of shape memory capability of PU, the pyramid pattern of PU film as well as the output of TENG can quickly recover after healing. Xiong et al. reported a shape memory TENG based on PU as well.<sup>322</sup> The electrospun technique is applied in their work to fabricate PU film with microarchitectures including mats of microfibers, microspheres, and microspheres-nanofibers to increase the roughness of triboelectric materials so as to enhance the output performance of TENG. In the work of Liu et al, another shape memory polymer is introduced by incorporating a semicrystalline thermoplastic polymer in a chemically cross-linked elastomer.<sup>321</sup> Besides shape memory capability, self-healing ability is also a useful property to ensure the output and lifetime of the TENG device. Deng et al. developed a self-healing TENG based on the self-healing capability of vitrimer elastomer as the triboelectric layer due to the dynamic disulfide bonds (Figure 13B).<sup>329</sup> The damaged device can be cured via heat treatment. Also, two independent TENG devices can be healed together if they are put near each other and treated with heat. Guan et al. also reported a self-healing TENG based on the vitrimer elastomer as a triboelectric layer and a mixture of vitrimer elastomer and carbon nanotube as electrode material.<sup>233</sup> As shown in Figure 13C, Kaushik Parida et al proposed an extremely stretchable and fully self-healing TENG based on PUA as a triboelectric layer.<sup>107</sup> And the electrode layer is fabricated by embedding the conductive liquid metal and silver flakes into the PUA. The fluidity of liquid metal can ensure the conductivity of the electrode when stretched. Moreover, Chen et al proposed a stretchable, self-healing, and shape-adaptive TENG based on the viscoelastic supramolecular polymer, silly Putty (Figure 13D).<sup>324</sup> Putty is utilized as the triboelectric materials and the electrode materials are a conductive composite with multi-walled carbon nanotube filling in the putty matrix. Such a device can be healed at room temperature for 3 minutes if damaged. It can be adapted to various curvy surfaces and even the fingerprint can be recorded when touching the device with a finger. Reconstruction of a 2D device into a 3D cubic can be achieved by adapting the 2D device onto a PMMA cubic and healing the edges. Also, the Putty is turned to be more triboelectric negative than PTFE, thus the output of such TENG is enhanced.

Besides Putty, many other materials are reported to help enhance the output performance by improving the

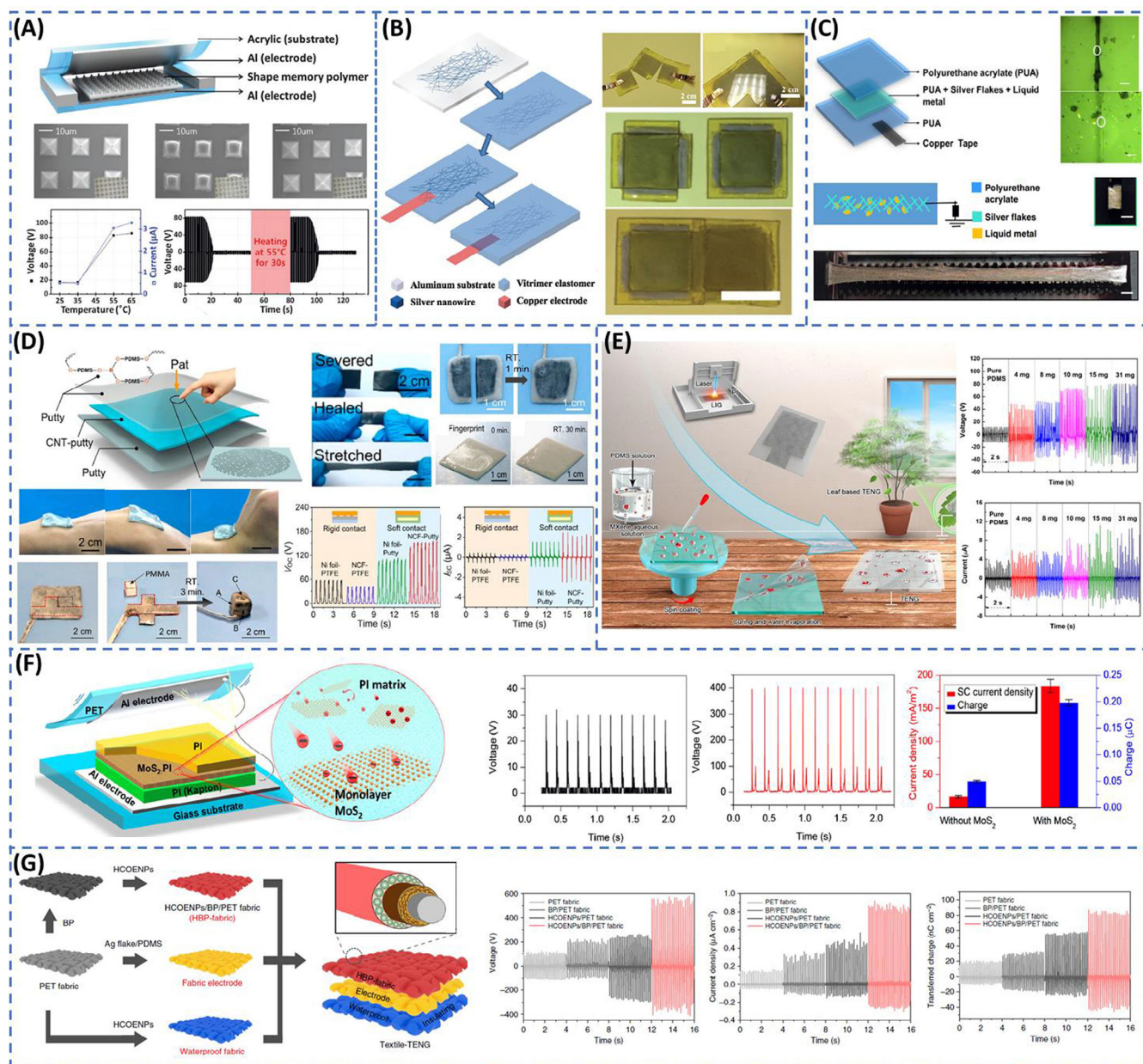


**FIGURE 13** New research direction: materials induced new functionalities and performance enhancement for TENG. A, Shape memory TENG. Reproduced with permission. Copyright 2015, The Royal Society of Chemistry.<sup>323</sup> B, Self-healing TENG. Reproduced with permission. Copyright 2018, Wiley.<sup>329</sup> C, A super-stretchable and self-healing TENG. Reproduced with permission. Copyright 2019, Nature.<sup>107</sup> D, Self-healing and shape-adaptive TENG. Reproduced with permission. Copyright 2019, American Chemical Society.<sup>324</sup> E, MXene based TENG for higher triboelectric negativity. Copyright 2019, Elsevier.<sup>342</sup> F, Monolayer MoS<sub>2</sub> based TENG for 120 times as large output energy density. Reproduced with permission. Copyright 2017, American Chemical Society.<sup>343</sup> G, Black phosphorous based TENG textile for waterproof fabric. Reproduced with permission. Copyright 2019, Springer<sup>344</sup>

surface charge density of triboelectric materials. Several strategies are reported including improvement of the active surface contact area,<sup>345,346</sup> improvements of the relative permittivity,<sup>347,348</sup> enhancement of triboelectric polarity<sup>342,349,350</sup> as well as applying electron trapping materials to prevent the leakage of charges.<sup>343,351</sup> Chen et al mixed dielectric powders with high relative permittivities, such as SiO<sub>2</sub>, TiO<sub>2</sub>, BaTiO<sub>3</sub>, SrTiO<sub>3</sub>, with the

PDMS, and the output of such TENG are enhanced compared with the pure PDMS-based TENG.<sup>348</sup> The recently investigated two-dimensional (2D) materials also play an important role in the research of performance enhancement of TENG. MXene, a novel 2D nanomaterial with a highly electronegative surface, is a great candidate for triboelectric materials of TENG.<sup>342,349,350</sup> As shown in Figure 13E, Jiang et al introduced MXene into PDMS by

mixing MXene aqueous solution with PDMS solution.<sup>349</sup> A flexible film can be obtained after spin-coating the mixed solution and curing on a glass, possessing higher triboelectric negativity. As a result, the output of TENG is significantly increased with increasing MXene concentrations, reaching 7-fold greater than the pure PDMS-based TENG when 31 mg MXene is added. Another 2D material, monolayer MoS<sub>2</sub> is introduced to enhance the output of TENG in the work of Wu et al, which can be attributed to its large specific area and quantum confinement effect enabled electron trapping capability (Figure 13F).<sup>343</sup> The monolayer MoS<sub>2</sub> sheet is embedded into the PI layer as an electron trapping layer under the triboelectric layer PI film. The power density of such TENG is dramatically increased by 120 times as large as that of the TENG without monolayer MoS<sub>2</sub>. Black phosphorus (BP) which also has a large specific area and quantum confinement can be another choice for enhancing the output performance of TENG as an electron-trapping layer. As illustrated in Figure 13G, Xiong et al. reported a textile-based TENG with BP protected by cellulose-derived hydrophobic nanoparticles (HCOENPs) as an electron trapping layer.<sup>344</sup> The triboelectric layer is realized by successive dip-coating BP and HCOENPs on PET fabric, with electrode fabric and waterproof fabric underneath. The output of such a device is greatly enhanced compared with other TENG textiles.

## 5.5 | Self-sustained NENS and/or IoT

The concept of IoT has experienced prosperous development with the innovation of various functional sensor nodes and communication technology. The energy supply for widely distributed IoT sensor nodes is a critical challenge. As a promising energy harvesting technology, TENG shows superior advantages of simple and diverse configurations, remarkable flexibility, high output performance, no material limitation, cost-effectiveness, and good scalability when compared with other energy harvesting technologies. Thus combining TENG with IoT sensor nodes is a promising solution to achieve self-sustained NENS. The following are typical applications to explain how it works.

As shown in Figure 14A, Luo et al. have proposed a smart sport monitoring table for ping-pong.<sup>352</sup> A kind of flexible wood is introduced into the TENG by removal of lignin/hemicellulose from natural wood followed by hot-pressing. Then, the TENG array is installed on the surface and edge of the table. This smart sport monitoring table possesses two capabilities: one is falling point distribution statistics for athletic big data analysis, where TENG array will accurately identify the impact point of

the ping-pong ball; the other is disputed edge ball judgment with signals collected from two single-electrode mode TENGs setting on the top edge and side edge of the table respectively. Wearable electronics with underwater sensing is another example of IoT TENG illustrated in Figure 14B. Zou et al reported an underwater wireless multi-site human motion monitoring system based on a bionic stretchable nanogenerator (BSNG).<sup>353</sup> Multiple channels in the BSNG can open and close simultaneously under the control of a simple mechanical force, thus generating electricity in an external circuit. By integrating the BSNG and a packaged multi-channel wireless signal transmission module, the motion signals of four articulation can be acquired in real-time through assorted software installed on a laptop. Environment monitoring in the seashore area is one more typical application shown in Figure 14C. Liu et al introduced a thin-film typed TENG to detect wave motions around the seashore.<sup>354</sup> The device is designed based on liquid-solid contact mode which directly collects signals from dynamic waves. A wave warning system has been built by using the exposed electrode in TENG as a safety switch. Moreover, a wireless transmitter can be powered with a prepared device as an IoT node, which can then wirelessly provide useful environment information to a mobile phone. Healthcare monitoring is also an edge application. As shown in Figure 14D, Fan et al prepared a machine-knitted washable sensor array textile for precise epidermal physiological signal monitoring.<sup>355</sup> This triboelectric all-textile sensor arrays (TATSAs) exhibit advantages of the pressure sensitivity, fast response time, stability, wide working frequency bandwidth, and machine washability. It can be integrated into a shirt for the monitoring of pulse and respiratory signals in real-time. Furthermore, a health monitoring system has been developed for long-term and noninvasive assessment of cardiovascular disease and sleep apnea syndrome (SAS), where significantly different data have been obtained from a healthy participant and a SAS participant. Endowing sensor nodes with wireless transmission capability is significant for the development of IoT.

As shown in Figure 14E, a battery-free wireless sensor network is achieved using TENG based direct sensory transmission. By novel integration of switch and coil, the resonance signal can be directly transmitted to the receiver ends within 1 m distance range, which has been envisioned for a long time but has not been realized until recently due to the low-frequency characteristic of the TENGs. Through varying series/parallel connection of stack layers and external capacitor adjustment, the control of multiple degrees of freedom is realized in 2D and 3D zoom base on the resonance frequency shift.<sup>108</sup> In addition to the wireless control integration, human



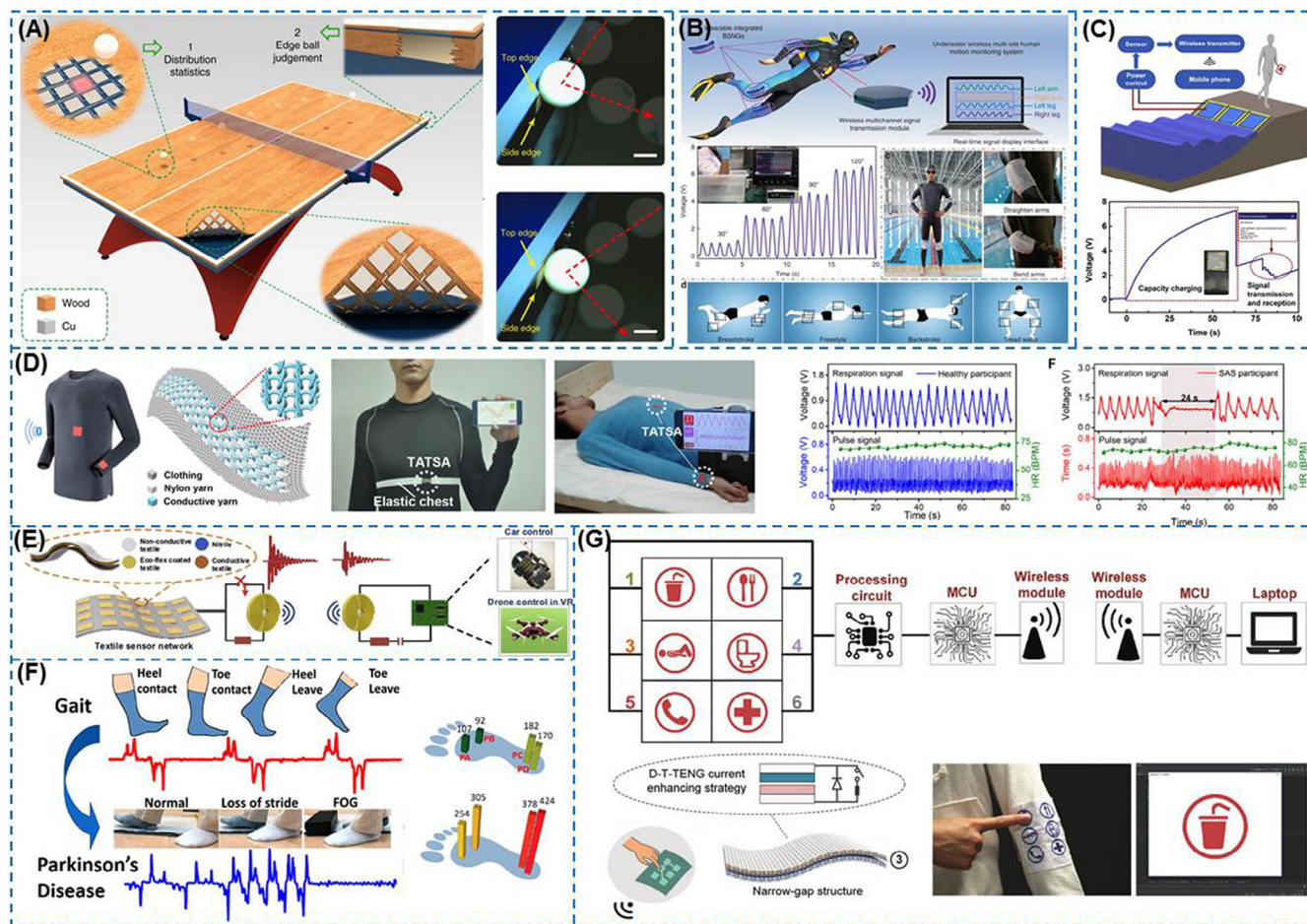


**FIGURE 14** New research direction: self-sustained NENS and/or IoT sensor nodes. A, A smart sport monitoring table. Reproduced with permission. Copyright 2019, Nature.<sup>352</sup> B, Underwater wireless multi-site human motion monitoring system. Reproduced with permission. Copyright 2019, Nature.<sup>353</sup> C, Smart environment monitoring around the seashore. Reproduced with permission. Copyright 2019, Elsevier.<sup>354</sup> D, Human healthcare monitoring. Reproduced with permission. Copyright 2020, American Association for the Advancement of Science.<sup>355</sup> E, Wireless triboelectric sensor network as a control interface. Reproduced with Permission. Copyright 2020, Elsevier.<sup>108</sup> F, Gait analysis using smart triboelectric socks. Reproduced with Permission. Copyright 2019, American Chemistry Society.<sup>127</sup> G, Communication pad based on narrow-gap textile TENG for healthcare applications. Reproduced with Permission. Copyright 2019, Wiley-VCH<sup>90</sup>

motion monitoring is crucial in IoT for smart home applications. Zhu et al demonstrated a smart PEDOT: PSS sock for gait analysis, aiming at motion tracking, personnel identification, and the diagnosis of Parkinson's disease (Figure 14F). With smart PZT involved, the deterioration of the triboelectric output resulting from human perspiration can be calibrated by the stable signals of the piezoelectric sensor as mentioned previously. Hence, by integrating into the sensory network of IoT, the real-time monitoring of this self-powered system can conveniently track the daily activity and assist the healthcare through wireless communication.<sup>127</sup> Except for the control interface and sensor unit development in IoT, the communication panel is equivalently important as the interaction of adjacent nodes has a heavy reliance on such functionality. As shown in Figure 14G, He et al

developed a textile-based narrow gap communication panel with the aid of diode and switch that accumulate charges and release in a short period. Thus, in spite of not using spacers benefiting from a large distance between the two triboelectric layers, the output of the panel is nevertheless sufficient for wireless communication via interfacing with Bluetooth, which possesses the potential for clinical applications.<sup>90</sup>

## 6 | OUTLOOKS AND CONCLUSIONS

With the prosperous development of the promising energy harvesting in the intelligent/smart systems, we reviewed the roadmap of TENG technology from the

viewpoint of advancement from energy harvesting to NENS. To boost the efficiency of energy harvesting, the surface micro/nanostructures is not the only solution to increase the effective contact surface area, the other possible solutions, such as the use of composite materials, the external electrical circuit system, and even the mechanical structure design with a proper time sequence operation.<sup>356-361</sup> Due to characteristics like simple and innovative design, easy working mechanism, lightweight, and compact in size, TENG has the potential to be used in conjunction with every electronic device, from small to large scale, which specifically suits the needs of the coming 5G and IoT regarding the aspect of self-powered sensors.<sup>362-367</sup> To increase the efficiency of energy harvesting from TENG, plenty of approaches (the materials composite, the external “charge pump”, and the electrical circuit system) have been investigated.<sup>368-373</sup> Furthermore, the novel mechanism for DC output generation has been investigated to directly power electronic devices. Meanwhile, a large quantity of self-powered physical sensors has been developed including pressure/force sensors, tactile sensors, strain, and bending sensors, acceleration and rotation sensors, and so on, for the applications in tactile, sensory robotics, HMI, and healthcare monitoring. To achieve multi-functionalities, with the aid of triboelectric materials and structural designs, advanced electrode designs can also be incorporated into conventional TENGs, resulting in application-oriented TENG configurations, that is, operating independently in the form of real-time and situ sensing.<sup>105,226,243,374-392</sup>

Toward NENS, blue energy is one of the most important application directions, which is mainly in forms of wave energy, tidal energy, and osmotic energy harvesting. To the aspect of the wearable electronics and HMI, TENG shows the potential abilities in realizing the advanced manipulation with the digital world. Meanwhile, the neural interface/implantable device with TENG technology opens the door to self-sustainable neuromodulation, muscle stimulation, sensing, therapy, and powering other medical devices, which reduces the reliance on battery and prolongs the device’ lifetime. Moreover, the TENG has also augmented a wide range of optical functions including light emission, photodetection, and optical modulation for the realization of applications including self-powered luminescence, smart display, wireless communication, personal privacy protection, and motion monitoring. Except for their function as energy harvester and self-powered sensors, more than TENG technologies have promoted the research directions on the hybrid energy harvesting technologies, such as integration with EM and/or piezoelectric mechanisms, which provides a promising energy

solution with high transduction efficiency, cost-efficiency, and compatibility for IoT sensor nodes in 5G. Another new research direction is to endow TENGs with new functionalities by exploring novel materials holding shape memory capability, self-healing capability, shape adaptive capability, and stretchability. With the aid of those functional materials, TENG shows superior advantages of simple and diverse configurations, remarkable flexibility/stretchability, shape-memory capability, self-healing ability, shape adaptive capability, high output performance, no material limitation, cost-effectiveness, and good scalability. Last but not least, the prosperous development of TENG technology has facilitated the emergence of various TENG-based and TENG-integrated brand-new research areas, that is, energy harvesting, self-powered sensing/actuation, and intelligent/smart NENS (energy harvesting module, power management module, signal processing module, display, and interactive module) with multi-functionality and self-sustainability, for the applications of personalized healthcare monitoring and treatment, identity recognition, smart home/building, and intelligent interactions in VR/AR scenarios, and so on.

## ACKNOWLEDGMENTS

Jianxiong Zhu, Minglu Zhu, and Qiongfeng Shi contributed equally to this work. This work was supported by the research grant of HIFES Seed Funding: “Hybrid Integration of Flexible Power Source and Pressure Sensors” (R-263-501-012-133) at the National University of Singapore (NUS), Singapore; the A\*STAR-NCBR research grant of “Chip-Scale MEMS Micro-Spectrometer for Monitoring Harsh Industrial Gases” (R-263-000-C91-305) at the NUS, Singapore; and the research grant of RIE Advanced Manufacturing and Engineering (AME) programmatic grant A18A4b0055 “Nanosystems at the Edge” at NUS, Singapore; National Key Research and Development Program of China (Grant No. 2019YFB2004800, Project No. R-2020-S-002) at NUSRI, Suzhou, China; NUS iHealthtech Joint Research Grant “Intelligent monitoring system based on smart wearable sensors and artificial technology for the treatment of adolescent idiopathic scoliosis” at NUS, Singapore.

## CONFLICT OF INTEREST

The authors declare that they have no known competing financial interests or personal relationships that could have appeared to influence the work reported in this article.

## ORCID

Chengkuo Lee  <https://orcid.org/0000-0002-8886-3649>

## REFERENCES

1. Fan FR, Tian ZQ, Lin Wang Z. Flexible triboelectric generator. *Nano Energy*. 2012;1(2):328-334. <https://doi.org/10.1016/j.nanoen.2012.01.004>.
2. Wang S, Lin ZH, Niu S, et al. Motion charged battery as sustainable flexible-power-unit. *ACS Nano*. 2013;7(12):11263-11271. <https://doi.org/10.1021/nn4050408>.
3. Wang S, Lin L, Wang ZL. Triboelectric nanogenerators as self-powered active sensors. *Nano Energy*. 2015;11:436-462. <https://doi.org/10.1016/j.nanoen.2014.10.034>.
4. Wu Y, Zhong X, Wang X, Yang Y, Wang ZL. Hybrid energy cell for simultaneously harvesting wind, solar, and chemical energies. *Nano Res*. 2014;7(11):1631-1639. <https://doi.org/10.1007/s12274-014-0523-y>.
5. Wang X, Dong L, Zhang H, Yu R, Pan C, Wang ZL. Recent progress in electronic skin. *Adv Sci*. 2015;2(10):1-21. <https://doi.org/10.1002/advs.201500169>.
6. Askari H, Khajepour A, Khamesee MB, Saadatnia Z, Wang ZL. Piezoelectric and triboelectric nanogenerators: trends and impacts. *Nano Today*. 2018;22:10-13. <https://doi.org/10.1016/j.nantod.2018.08.001>.
7. Yang B, Lee C, Kotlanka RK, Xie J, Lim SP. A MEMS rotary comb mechanism for harvesting the kinetic energy of planar vibrations. *J Micromech Microeng*. 2010;20(6):065017. <https://doi.org/10.1088/0960-1317/20/6/065017>.
8. Liu H, Zhang S, Kathiresan R, Kobayashi T, Lee C. Development of piezoelectric microcantilever flow sensor with wind-driven energy harvesting capability. *Appl Phys Lett*. 2012;100(22):1-4. <https://doi.org/10.1063/1.4723846>.
9. Yang B, Lee C, Ho GW, Ong WL, Liu J, Yang C. Modeling and experimental study of a low-frequency-vibration-based power generator using ZnO nanowire arrays. *J Microelectromech Syst*. 2012;21(4):776-778. <https://doi.org/10.1109/JMEMS.2012.2190716>.
10. Arab Hassani F, Mogan RP, Gammad GGL, et al. Toward self-control systems for neurogenic underactive bladder: a triboelectric nanogenerator sensor integrated with a bistable micro-actuator. *ACS Nano*. 2018;12(4):3487-3501. <https://doi.org/10.1021/acsnano.8b00303>.
11. Chen C, Chen L, Wu Z, et al. 3D double-faced interlock fabric triboelectric nanogenerator for bio-motion energy harvesting and as self-powered stretching and 3D tactile sensors. *Mater Today*. 2020;32:84-93. <https://doi.org/10.1016/j.mattod.2019.10.025>.
12. Fan FR, Lin L, Zhu G, Wu W, Zhang R, Wang ZL. Transparent triboelectric nanogenerators and self-powered pressure sensors based on micropatterned plastic films. *Nano Lett*. 2012;12(6):3109-3114. <https://doi.org/10.1021/nl300988z>.
13. Yang Y, Zhang H, Chen J, et al. Single-electrode-based sliding triboelectric nanogenerator for self-powered displacement vector sensor system. *ACS Nano*. 2013;7(8):7342-7351. <https://doi.org/10.1021/nn403021m>.
14. Chen J, Guo H, Hu C, Wang ZL. Robust triboelectric nanogenerator achieved by centrifugal force induced automatic working mode transition. 2020;2000886:1-8. <https://doi.org/10.1002/aenm.202000886>.
15. Ding W, Wu C, Zi Y, et al. Self-powered wireless optical transmission of mechanical agitation signals. *Nano Energy*. 2018;47:566-572. <https://doi.org/10.1016/j.nanoen.2018.03.044>.
16. Liu H, How Koh K, Lee C. Ultra-wide frequency broadening mechanism for micro-scale electromagnetic energy harvester. *Appl Phys Lett*. 2014;104(5):053901. <https://doi.org/10.1063/1.4863565>.
17. Shi Q, Wang T, Kobayashi T, Lee C. Investigation of geometric design in piezoelectric microelectromechanical systems diaphragms for ultrasonic energy harvesting. *Appl Phys Lett*. 2016;108(19):193902. <https://doi.org/10.1063/1.4948973>.
18. Liu H, Hou C, Lin J, et al. A non-resonant rotational electromagnetic energy harvester for low-frequency and irregular human motion. *Appl Phys Lett*. 2018;113(20):203901. <https://doi.org/10.1063/1.5053945>.
19. Liu H, Zhong J, Lee C, Lee SW, Lin L. A comprehensive review on piezoelectric energy harvesting technology: Materials, mechanisms, and applications. *Appl Phys Rev*. 2018;5(4):1-35. <https://doi.org/10.1063/1.5074184>.
20. Puttaswamy SV, Fishlock SJ, Steele D, Shi Q, Lee C, McLaughlin J. Versatile microfluidic platform embedded with sidewall three-dimensional electrodes for cell manipulation. *Biomed Phys Eng Express*. 2019;5(5):055003. <https://doi.org/10.1088/2057-1976/ab268e>.
21. Lee S, Lee C. Toward advanced neural interfaces for the peripheral nervous system (PNS) and their future applications. *Curr Opin Biomed Eng*. 2018;6:130-137. <https://doi.org/10.1016/j.cobme.2018.05.004>.
22. Yao G, Xu L, Cheng X, et al. Bioinspired triboelectric nanogenerators as self-powered electronic skin for robotic tactile sensing. *Adv Funct Mater*. 2020;30(6):1-9. <https://doi.org/10.1002/adfm.201907312>.
23. Zhou L, Liu D, Li S, et al. Rationally designed dual-mode triboelectric nanogenerator for harvesting mechanical energy by both electrostatic induction and dielectric breakdown effects. *Adv Energy Mater*. 2020;2000965:1-8. <https://doi.org/10.1002/aenm.202000965>.
24. Zhu M, Sun Z, Zhang Z, et al. Haptic-feedback smart glove as a creative human-machine interface (HMI) for virtual / augmented reality applications. *Sci Adv*. 2020;6:1-15. <https://doi.org/10.1126/sciadv.aaz8693>.
25. Chen T, Shi Q, Li K, et al. Investigation of position sensing and energy harvesting of a flexible triboelectric touch pad. *Nanomaterials*. 2018;8(8):1-15. <https://doi.org/10.3390/nano8080613>.
26. Wang ZL. Triboelectric nanogenerator (TENG)—sparking an energy and sensor revolution. *Adv Energy Mater*. 2020;10(17):1-6. <https://doi.org/10.1002/aenm.202000137>.
27. Liu H, Soon BW, Wang N, Tay CJ, Quan C, Lee C. Feasibility study of a 3D vibration-driven electromagnetic MEMS energy harvester with multiple vibration modes. *J Micromech Microeng*. 2012;22(12):125020. <https://doi.org/10.1088/0960-1317/22/12/125020>.
28. Dhakar L, Tay FEH, Lee C. Investigation of contact electrification based broadband energy harvesting mechanism using elastic PDMS microstructures. *J Micromech Microeng*. 2014;24(10):104002. <https://doi.org/10.1088/0960-1317/24/10/104002>.
29. Liu H, Zhang S, Kobayashi T, Chen T, Lee C. Flow sensing and energy harvesting characteristics of a wind-driven piezoelectric Pb(Zr0.52, Ti0.48)O<sub>3</sub> microcantilever. *Micro Nano Lett*. 2014;9(4):286-289. <https://doi.org/10.1049/mnl.2013.0750>.



30. Liu H, Zhang J, Shi Q, et al. Development of a thermoelectric and electromagnetic hybrid energy harvester from water flow in an irrigation system. *Micromachines*. 2018;9(8):1-10. <https://doi.org/10.3390/mi9080395>.
31. Wang ZL, Wang AC. On the origin of contact-electrification. *Mater Today*. 2019;30(November):34-51. <https://doi.org/10.1016/j.mattod.2019.05.016>.
32. Liu H, Qian Y, Lee C. A multi-frequency vibration-based MEMS electromagnetic energy harvesting device. *Sens Actuators A Phys*. 2013;204:37-43. <https://doi.org/10.1016/j.sna.2013.09.015>.
33. Wu Y, Hu Y, Huang Z, Lee C, Wang F. Electret-material enhanced triboelectric energy harvesting from air flow for self-powered wireless temperature sensor network. *Sens Actuators A Phys*. 2018;271:364-372. <https://doi.org/10.1016/j.sna.2017.12.067>.
34. Liu H, Ji Z, Chen T, Sun L, Menon SC, Lee C. An intermittent self-powered energy harvesting system from low-frequency hand shaking. *IEEE Sens J*. 2015;15(9):4782-4790. <https://doi.org/10.1109/JSEN.2015.2411313>.
35. Wang ZL. On the first principle theory of nanogenerators from Maxwell's equations. *Nano Energy*. 2020;68(October 2019):104272. <https://doi.org/10.1016/j.nanoen.2019.104272>.
36. Yang ZW, Pang Y, Zhang L, et al. Tribotronic transistor array as an active tactile sensing system. *ACS Nano*. 2016;10(12):10912-10920. <https://doi.org/10.1021/acsnano.6b05507>.
37. Yang B, Lee C, Xiang W, et al. Electromagnetic energy harvesting from vibrations of multiple frequencies. *J Micromech Microeng*. 2009;19(3):035001. <https://doi.org/10.1088/0960-1317/19/3/035001>.
38. Yang B, Lee C. A wideband electromagnetic energy harvester for random vibration sources. *Adv Mat Res*. 2009;74:165-168. <https://doi.org/10.4028/www.scientific.net/AMR.74.165>.
39. Liu H, Tay CJ, Quan C, Kobayashi T, Lee C. Piezoelectric MEMS energy harvester for low-frequency vibrations with wideband operation range and steadily increased output power. *J Microelectromech Syst*. 2011;20(5):1131-1142. <https://doi.org/10.1109/JMEMS.2011.2162488>.
40. Liu H, Lee C, Kobayashi T, Tay CJ, Quan C. Investigation of a MEMS piezoelectric energy harvester system with a frequency-widened-bandwidth mechanism introduced by mechanical stoppers. *Smart Mater Struct*. 2012;21(3):035005. <https://doi.org/10.1088/0964-1726/21/3/035005>.
41. Liu H, Lee C, Kobayashi T, Tay CJ, Quan C. A new S-shaped MEMS PZT cantilever for energy harvesting from low frequency vibrations below 30 Hz. *Microsyst Technol*. 2012;18(4):497-506. <https://doi.org/10.1007/s00542-012-1424-1>.
42. Shi Q, Wang T, Lee C. MEMS based broadband piezoelectric ultrasonic energy harvester (PUEH) for enabling self-powered implantable biomedical devices. *Sci Rep*. 2016;6:1-10. <https://doi.org/10.1038/srep24946>.
43. Gu L, Cui N, Cheng L, et al. Flexible fiber nanogenerator with 209 V output voltage directly powers a light-emitting diode. *Nano Lett*. 2013;13(1):91-94. <https://doi.org/10.1021/nl303539c>.
44. Yang Y, Lin ZH, Hou T, Zhang F, Wang ZL. Nanowire-composite based flexible thermoelectric nanogenerators and self-powered temperature sensors. *Nano Res*. 2012;5(12):888-895. <https://doi.org/10.1007/s12274-012-0272-8>.
45. Yang Y, Zhang H, Lin ZH, et al. A hybrid energy cell for self-powered water splitting. *Energ Environ Sci*. 2013;6(8):2429-2434. <https://doi.org/10.1039/c3ee41485j>.
46. Hu Y, Yang J, Jing Q, Niu S, Wu W, Wang ZL. Triboelectric nanogenerator built on suspended 3d spiral structure as vibration and positioning sensor and wave energy harvester. *ACS Nano*. 2013;7(11):10424-10432. <https://doi.org/10.1021/nn405209u>.
47. Yi F, Lin L, Niu S, et al. Self-powered trajectory, velocity, and acceleration tracking of a moving object/body using a triboelectric sensor. *Adv Funct Mater*. 2014;24(47):7488-7494. <https://doi.org/10.1002/adfm.201402703>.
48. Tang W, Han Y, Han CB, Gao CZ, Cao X, Wang ZL. Self-powered water splitting using flowing kinetic energy. *Adv Mater*. 2015;27(2):272-276. <https://doi.org/10.1002/adma.201404071>.
49. Su Y, Yang Y, Zhong X, et al. Fully enclosed cylindrical single-electrode-based triboelectric nanogenerator. *ACS Appl Mater Interfaces*. 2014;6(1):553-559. <https://doi.org/10.1021/am404611h>.
50. Quan Z, Han CB, Jiang T, Wang ZL. Robust thin films-based triboelectric nanogenerator arrays for harvesting bidirectional wind energy. *Adv Energy Mater*. 2016;6(5):1-11. <https://doi.org/10.1002/aenm.201501799>.
51. He C, Zhu W, Chen B, et al. Smart floor with integrated triboelectric nanogenerator as energy harvester and motion sensor. *ACS Appl Mater Interfaces*. 2017;9(31):26126-26133. <https://doi.org/10.1021/acsami.7b08526>.
52. Xi Y, Wang J, Zi Y, et al. High efficient harvesting of underwater ultrasonic wave energy by triboelectric nanogenerator. *Nano Energy*. 2017;38:101-108. <https://doi.org/10.1016/j.nanoen.2017.04.053>.
53. Xiao TX, Liang X, Jiang T, et al. Spherical triboelectric nanogenerators based on spring-assisted multilayered structure for efficient water wave energy harvesting. *Adv Funct Mater*. 2018;28(35):1-8. <https://doi.org/10.1002/adfm.201802634>.
54. Bai Y, Xu L, Lin S, et al. Charge pumping strategy for rotation and sliding type triboelectric nanogenerators. *Adv Energy Mater*. 2020;2000605:1-9. <https://doi.org/10.1002/aenm.202000605>.
55. Leung S-F, Fu H-C, Zhang M, et al. Blue energy fuels: converting ocean wave energy to carbon-based liquid fuels via CO<sub>2</sub> reduction. *Energ Environ Sci*. 2020;13:1300-1308. <https://doi.org/10.1039/c9ee03566d>.
56. Dhakar L, Pitchappa P, Tay FEH, Lee C. An intelligent skin based self-powered finger motion sensor integrated with triboelectric nanogenerator. *Nano Energy*. 2016;19:532-540. <https://doi.org/10.1016/j.nanoen.2015.04.020>.
57. Wang J, Wang H, Thakor NV, Lee C. Self-powered direct muscle stimulation using a triboelectric nanogenerator (TENG) integrated with a flexible multiple-channel intramuscular electrode. *ACS Nano*. 2019;13(3):3589-3599. <https://doi.org/10.1021/acsnano.9b00140>.
58. Shi Q, Wu H, Wang H, Wu H, Lee C. Self-powered gyroscope ball using a triboelectric mechanism. *Adv Energy Mater*. 2017;7(22):1-11. <https://doi.org/10.1002/aenm.201701300>.
59. Hassani FA, Peh WYX, Gammad GGL, et al. A 3D printed implantable device for voiding the bladder using shape memory alloy (SMA) actuators. *Adv Sci*. 2017;4(11):1-10. <https://doi.org/10.1002/advs.201700143>.

60. Lee S, Peh WYX, Wang J, et al. Toward bioelectronic medicine—neuromodulation of small peripheral nerves using flexible neural clip. *Adv Sci*. 2017;4(11):1-10. <https://doi.org/10.1002/advs.201700149>.
61. Wang J, Thow XY, Wang H, et al. A highly selective 3D spiked ultraflexible neural (SUN) interface for decoding peripheral nerve sensory information. *Adv Healthc Mater*. 2018;7(5):1-8. <https://doi.org/10.1002/adhm.201700987>.
62. Xiang Z, Yen SC, Sheshadri S, et al. Progress of flexible electronics in neural interfacing - a self-adaptive non-invasive neural ribbon electrode for small nerves recording. *Adv Mater*. 2016;28(22):4472-4479. <https://doi.org/10.1002/adma.201503423>.
63. Hassani FA, Gammad GGL, Mogan RP, et al. Design and anchorage dependence of shape memory alloy actuators on enhanced voiding of a bladder. *Adv Mater Technol*. 2018;3(1):1-12. <https://doi.org/10.1002/admt.201700184>.
64. Xiang Z, Sheshadri S, Lee SH, et al. Mapping of small nerve trunks and branches using adaptive flexible electrodes. *Adv Sci*. 2016;3(9):1-8. <https://doi.org/10.1002/advs.201500386>.
65. Wang H, Pastorin G, Lee C. Toward self-powered wearable adhesive skin patch with bendable microneedle array for transdermal drug delivery. *Adv Sci*. 2016;3(9):1-10. <https://doi.org/10.1002/advs.201500441>.
66. Wang J, Wang H, He T, He B, Thakor NV, Lee C. Investigation of low-current direct stimulation for rehabilitation treatment related to muscle function loss using self-powered TENG system. *Adv Sci*. 2019;6(14):1900149. <https://doi.org/10.1002/advs.201900149>.
67. Hassani FA, Lee C. A triboelectric energy harvester using low-cost, flexible, and biocompatible ethylene vinyl acetate (EVA). *J Microelectromech Syst*. 2015;24(5):1338-1345. <https://doi.org/10.1109/JMEMS.2015.2403256>.
68. Dhakar L, Tay FEH, Lee C. Development of a broadband triboelectric energy harvester with SU-8 micropillars. *J Microelectromech Syst*. 2015;24(1):91-99. <https://doi.org/10.1109/JMEMS.2014.2317718>.
69. Lee S, Wang H, Shi Q, et al. Development of battery-free neural interface and modulated control of tibialis anterior muscle via common peroneal nerve based on triboelectric nanogenerators (TENGs). *Nano Energy*. 2017;33:1-11. <https://doi.org/10.1016/j.nanoen.2016.12.038>.
70. Sun C, Shi Q, Hasan D, et al. Self-powered multifunctional monitoring system using hybrid integrated triboelectric nanogenerators and piezoelectric microsensors. *Nano Energy*. 2019;58:612-623. <https://doi.org/10.1016/j.nanoen.2019.01.096>.
71. Chen T, Shi Q, Zhu M, et al. Intuitive-augmented human-machine multidimensional nano-manipulation terminal using triboelectric stretchable strip sensors based on minimalist design. *Nano Energy*. 2019;60:440-448. <https://doi.org/10.1016/j.nanoen.2019.03.071>.
72. Wang J, He T, Lee C. Development of neural interfaces and energy harvesters towards self-powered implantable systems for healthcare monitoring and rehabilitation purposes. *Nano Energy*. 2019;65:104039. <https://doi.org/10.1016/j.nanoen.2019.104039>.
73. Zheng Q, Zhang H, Shi B, et al. In vivo self-powered wireless cardiac monitoring via implantable triboelectric nanogenerator. *ACS Nano*. 2016;10(7):6510-6518. <https://doi.org/10.1021/acsnano.6b02693>.
74. Wei XY, Wang X, Kuang SY, et al. Dynamic Triboelectrification-induced electroluminescence and its use in visualized sensing. *Adv Mater*. 2016;28(31):6656-6664. <https://doi.org/10.1002/adma.201600604>.
75. Zheng Q, Jin Y, Liu Z, et al. Robust multilayered encapsulation for high-performance triboelectric nanogenerator in harsh environment. *ACS Appl Mater Interfaces*. 2016;8(40):26697-26703. <https://doi.org/10.1021/acsaami.6b06866>.
76. Zhao Z, Pu X, Du C, et al. Freestanding flag-type triboelectric nanogenerator for harvesting high-altitude wind energy from arbitrary directions. *ACS Nano*. 2016;10(2):1780-1787. <https://doi.org/10.1021/acsnano.5b07157>.
77. Zhu G, Yang WQ, Zhang T, et al. Self-powered, ultrasensitive, flexible tactile sensors based on contact electrification. *Nano Lett*. 2014;14(6):3208-3213. <https://doi.org/10.1021/nl5005652>.
78. Liu S, Wang H, He T, Dong S, Lee C. Switchable textile-triboelectric nanogenerators (S-TENGs) for continuous profile sensing application without environmental interferences. *Nano Energy*. 2020;69:104462. <https://doi.org/10.1016/j.nanoen.2020.104462>.
79. Chen T, Shi Q, Yang Z, et al. A self-powered six-axis tactile sensor by using triboelectric mechanism. *Nanomaterials*. 2018;8(7):1-14. <https://doi.org/10.3390/nano8070503>.
80. Yin X, Liu D, Zhou L, et al. Structure and dimension effects on the performance of layered triboelectric nanogenerators in contact-separation mode. *ACS Nano*. 2019;13(1):698-705. <https://doi.org/10.1021/acsnano.8b07935>.
81. Wu C, Kim TW, Park JH, et al. Self-powered tactile sensor with learning and memory. *ACS Nano*. 2020;14(2):1390-1398. <https://doi.org/10.1021/acsnano.9b07165>.
82. Xu L, Wu H, Yao G, et al. Giant voltage enhancement via triboelectric charge supplement channel for self-powered electroadhesion. *ACS Nano*. 2018;12(10):10262-10271. <https://doi.org/10.1021/acsnano.8b05359>.
83. Wang J, Wu C, Dai Y, et al. Achieving ultrahigh triboelectric charge density for efficient energy harvesting. *Nat Commun*. 2017;8(1):1-7. <https://doi.org/10.1038/s41467-017-00131-4>.
84. Harmon W, Bamgboje D, Guo H, Hu T, Wang ZL. Self-driven power management system for triboelectric nanogenerators. *Nano Energy*. 2020;71:104642. <https://doi.org/10.1016/j.nanoen.2020.104642>.
85. Niu S, Wang ZL. Theoretical systems of triboelectric nanogenerators. *Nano Energy*. 2014;14:161-192. <https://doi.org/10.1016/j.nanoen.2014.11.034>.
86. Niu S, Liu Y, Wang S, et al. Theory of sliding-mode triboelectric nanogenerators. *Adv Mater*. 2013;25(43):6184-6193. <https://doi.org/10.1002/adma.201302808>.
87. Xu C, Zi Y, Wang AC, et al. On the electron-transfer mechanism in the contact-electrification effect. *Adv Mater*. 2018;30(15):1-9. <https://doi.org/10.1002/adma.201706790>.
88. Liu W, Wang Z, Wang G, et al. Integrated charge excitation triboelectric nanogenerator. *Nat Commun*. 2019;10(1):1-9. <https://doi.org/10.1038/s41467-019-09464-8>.
89. Liu W, Wang Z, Wang G, et al. Switched-capacitor-convertors based on fractal design for output power management of triboelectric nanogenerator. *Nat Commun*. 2020;11(1):1-10. <https://doi.org/10.1038/s41467-020-15373-y>.
90. He T, Wang H, Wang J, et al. Self-sustainable wearable textile nano-energy nano-system (NENS) for next-generation

- healthcare applications. *Adv Sci*. 2019;6(24):1901437. <https://doi.org/10.1002/advs.201901437>.
91. Zhang Y, Mei Z, Wang T, et al. Full paper flexible transparent high-voltage diodes for energy management in wearable electronics. *Nano Energy*. 2017;40:289-299. <https://doi.org/10.1016/j.nanoen.2017.08.025>.
  92. Wang H, Wang J, He T, Li Z, Lee C. Direct muscle stimulation using diode-amplified triboelectric nanogenerators (TENGs). *Nano Energy*. 2019;63:103844. <https://doi.org/10.1016/j.nanoen.2019.06.040>.
  93. Ghaffarinejad A, Hasani JY, Hinchet R, et al. A conditioning circuit with exponential enhancement of output energy for triboelectric nanogenerator. *Nano Energy*. 2018;51:173-184. <https://doi.org/10.1016/j.nanoen.2018.06.034>.
  94. Liu D, Yin X, Guo H, et al. A constant current triboelectric nanogenerator arising from electrostatic breakdown. *Sci Adv*. 2019;5(4):1-7. <https://doi.org/10.1126/sciadv.aav6437>.
  95. Shi Q, Wang H, Wang T, Lee C. Self-powered liquid triboelectric microfluidic sensor for pressure sensing and finger motion monitoring applications. *Nano Energy*. 2016;30:450-459. <https://doi.org/10.1016/j.nanoen.2016.10.046>.
  96. Shi Q, Lee C. Self-powered bio-inspired spider-net-coding interface using single-electrode triboelectric nanogenerator. *Adv Sci*. 2019;6(15):1900617. <https://doi.org/10.1002/advs.201900617>.
  97. Cui S, Zheng Y, Zhang T, Wang D, Zhou F, Liu W. Self-powered ammonia nanosensor based on the integration of the gas sensor and triboelectric nanogenerator. *Nano Energy*. 2018;49:31-39. <https://doi.org/10.1016/j.nanoen.2018.04.033>.
  98. Zheng Q, Zou Y, Zhang Y, et al. Biodegradable triboelectric nanogenerator as a life-time designed implantable power source. *Sci Adv*. 2016;2(3):1-10. <https://doi.org/10.1126/sciadv.1501478>.
  99. Chen B, Tang W, He C, et al. Water wave energy harvesting and self-powered liquid-surface fluctuation sensing based on bionic-jellyfish triboelectric nanogenerator. *Mater Today*. 2018;21:88-97. <https://doi.org/10.1016/j.mattod.2017.10.006>.
  100. Ahmed A, Saadatnia Z, Hassan I, et al. Self-powered wireless sensor node enabled by a duck-shaped triboelectric nanogenerator for harvesting water wave energy. *Adv Energy Mater*. 2017;7(7):1601705. <https://doi.org/10.1002/aenm.201601705>.
  101. Pan L, Wang J, Wang P, et al. Liquid-FEP-based U-tube triboelectric nanogenerator for harvesting water-wave energy. *Nano Res*. 2018;11(8):4062-4073. <https://doi.org/10.1007/s12274-018-1989-9>.
  102. Ma Y, Zheng Q, Liu Y, et al. Self-powered, one-stop, and multifunctional implantable triboelectric active sensor for real-time biomedical monitoring. *Nano Lett*. 2016;16(10):6042-6051. <https://doi.org/10.1021/acs.nanolett.6b01968>.
  103. Shi Q, Zhang Z, Chen T, Lee C. Minimalist and multifunctional human machine interface (HMI) using a flexible wearable triboelectric patch. *Nano Energy*. 2019;62:355-366. <https://doi.org/10.1016/j.nanoen.2019.05.033>.
  104. Zhang C, Wang H, Guan S, et al. Self-powered optical switch based on triboelectrification-triggered liquid crystal alignment for wireless sensing. *Adv Funct Mater*. 2019;29(13):1-8. <https://doi.org/10.1002/adfm.201808633>.
  105. Yang H, Pang Y, Bu T, et al. Triboelectric micromotors actuated by ultralow frequency mechanical stimuli. *Nat Commun*. 2019;10:2309. <https://doi.org/10.1038/s41467-019-10298-7>.
  106. Li S, Wang J, Peng W, et al. Sustainable energy source for wearable electronics based on multilayer elastomeric triboelectric nanogenerators. *Adv Energy Mater*. 2017;7(13):1-9. <https://doi.org/10.1002/aenm.201602832>.
  107. Parida K, Thangavel G, Cai G, et al. Extremely stretchable and self-healing conductor based on thermoplastic elastomer for all-three-dimensional printed triboelectric nanogenerator. *Nat Commun*. 2019;10(1):1-9. <https://doi.org/10.1038/s41467-019-10061-y>.
  108. Wen F, Wang H, He T, et al. Battery-free short-range self-powered wireless sensor network (SS-WSN) using TENG based direct sensory transmission (TDST) mechanism. *Nano Energy*. 2020;67:104266. <https://doi.org/10.1016/j.nanoen.2019.104266>.
  109. Qin H, Cheng G, Zi Y, et al. High energy storage efficiency triboelectric nanogenerators with unidirectional switches and passive power management circuits. *Adv Funct Mater*. 2018;28(51):1-10. <https://doi.org/10.1002/adfm.201805216>.
  110. Zhu J, Wang H, Zhang Z, et al. Continuous direct current by charge transportation for next-generation IoT and real-time virtual reality applications. *Nano Energy*. 2020;73:104760. <https://doi.org/10.1016/j.nanoen.2020.104760>.
  111. Tao J, Bao R, Wang X, et al. Self-powered tactile sensor array systems based on the triboelectric effect. *Adv Funct Mater*. 2019;29(41):1-23. <https://doi.org/10.1002/adfm.201806379>.
  112. Yi F, Zhang Z, Kang Z, Liao Q, Zhang Y. Recent advances in triboelectric nanogenerator-based health monitoring. *Adv Funct Mater*. 2019;29(41):1-16. <https://doi.org/10.1002/adfm.201808849>.
  113. Shi Q, He T, Lee C. More than energy harvesting—combining triboelectric nanogenerator and flexible electronics technology for enabling novel micro-/nano-systems. *Nano Energy*. 2019;57:851-871. <https://doi.org/10.1016/j.nanoen.2019.01.002>.
  114. Wang ZL, Chen J, Lin L. Progress in triboelectric nanogenerators as a new energy technology and self-powered sensors. *Energy Environ Sci*. 2015;8(8):2250-2282. <https://doi.org/10.1039/c5ee01532d>.
  115. Chen J, Wang ZL. Reviving vibration energy harvesting and self-powered sensing by a triboelectric nanogenerator. *Joule*. 2017;1(3):480-521. <https://doi.org/10.1016/j.joule.2017.09.004>.
  116. Dong K, Peng X, Wang ZL. Fiber/fabric-based piezoelectric and triboelectric nanogenerators for flexible/stretchable and wearable electronics and artificial intelligence. *Adv Mater*. 2020;32(5):1-43. <https://doi.org/10.1002/adma.201902549>.
  117. Wang ZL. Triboelectric nanogenerators as new energy technology and self-powered sensors—principles, problems and perspectives. *Faraday Discuss*. 2014;176:447-458. <https://doi.org/10.1039/c4fd00159a>.
  118. Ha M, Park J, Lee Y, Ko H. Triboelectric generators and sensors for self-powered wearable electronics. *ACS Nano*. 2015;9(4):3421-3427. <https://doi.org/10.1021/acs.nano.5b01478>.
  119. Chen L, Shi Q, Sun Y, Nguyen T, Lee C, Soh S. Controlling surface charge generated by contact electrification: strategies and applications. *Adv Mater*. 2018;30(47):1-15. <https://doi.org/10.1002/adma.201802405>.



120. Wang X, Que M, Chen M, et al. Full dynamic-range pressure sensor matrix based on optical and electrical dual-mode sensing. *Adv Mater.* 2017;29(15):1-7. <https://doi.org/10.1002/adma.201605817>.
121. Liu M, Pu X, Jiang C, et al. Large-area all-textile pressure sensors for monitoring human motion and physiological signals. *Adv Mater.* 2017;29(41):1-9. <https://doi.org/10.1002/adma.201703700>.
122. Dhakar L, Gudla S, Shan X, et al. Large scale triboelectric nanogenerator and self-powered pressure sensor array using low cost roll-to-roll UV embossing. *Sci Rep.* 2016;6:1-10. <https://doi.org/10.1038/srep22253>.
123. Lee KY, Yoon HJ, Jiang T, et al. Fully packaged self-powered triboelectric pressure sensor using hemispheres-array. *Adv Energy Mater.* 2016;6(11):1-5. <https://doi.org/10.1002/aenm.201502566>.
124. Pu X, Guo H, Chen J, et al. Eye motion triggered self-powered mechnosensational communication system using triboelectric nanogenerator. *Sci Adv.* 2017;3(7):e1700694. <https://doi.org/10.1126/sciadv.1700694>.
125. Chen SW, Cao X, Wang N, et al. An ultrathin flexible single-electrode triboelectric-nanogenerator for mechanical energy harvesting and instantaneous force sensing. *Adv Energy Mater.* 2017;7(1):1-9. <https://doi.org/10.1002/aenm.201601255>.
126. Lai YC, Deng J, Liu R, et al. Actively perceiving and responsive soft robots enabled by self-powered, highly extensible, and highly sensitive triboelectric proximity- and pressure-sensing skins. *Adv Mater.* 2018;30(28):1-12. <https://doi.org/10.1002/adma.201801114>.
127. Zhu M, Shi Q, He T, et al. Self-powered and self-functional cotton sock using piezoelectric and triboelectric hybrid mechanism for healthcare and sports monitoring. *ACS Nano.* 2019;13:acs.nano.8b08329. <https://doi.org/10.1021/acs.nano.8b08329>.
128. Lin Z, Wu Z, Zhang B, et al. A triboelectric nanogenerator-based smart insole for multifunctional gait monitoring. *Adv Mater Technol.* 2019;4(2):1-7. <https://doi.org/10.1002/admt.201800360>.
129. Meng K, Chen J, Li X, et al. Flexible weaving constructed self-powered pressure sensor enabling continuous diagnosis of cardiovascular disease and measurement of cuffless blood pressure. *Adv Funct Mater.* 2019;29(5):1-10. <https://doi.org/10.1002/adfm.201806388>.
130. Wang X, Zhang H, Dong L, et al. Self-powered high-resolution and pressure-sensitive triboelectric sensor matrix for real-time tactile mapping. *Adv Mater.* 2016;28(15):2896-2903. <https://doi.org/10.1002/adma.201503407>.
131. He X, Zi Y, Guo H, et al. A highly stretchable fiber-based triboelectric nanogenerator for self-powered wearable electronics. *Adv Funct Mater.* 2017;27(4):1-8. <https://doi.org/10.1002/adfm.201604378>.
132. Zhang B, Zhang L, Deng W, et al. Self-powered acceleration sensor based on liquid metal triboelectric nanogenerator for vibration monitoring. *ACS Nano.* 2017;11(7):7440-7446. <https://doi.org/10.1021/acs.nano.7b03818>.
133. Wang J, Ding W, Pan L, et al. Self-powered wind sensor system for detecting wind speed and direction based on a triboelectric nanogenerator. *ACS Nano.* 2018;12(4):3954-3963. <https://doi.org/10.1021/acs.nano.8b01532>.
134. Cheng J, Ding W, Zi Y, et al. Triboelectric microplasma powered by mechanical stimuli. *Nat Commun.* 2018;9(1):1-11. <https://doi.org/10.1038/s41467-018-06198-x>.
135. Zhu XX, Bin LZ, Li XS, et al. Triboelectrification-enabled thin-film tactile matrix for self-powered high-resolution imaging. *Nano Energy.* 2018;50:497-503. <https://doi.org/10.1016/j.nanoen.2018.05.061>.
136. Zhu XX, Meng XS, Kuang SY, et al. Triboelectrification-enabled touch sensing for self-powered position mapping and dynamic tracking by a flexible and area-scalable sensor array. *Nano Energy.* 2017;41:387-393. <https://doi.org/10.1016/j.nanoen.2017.09.025>.
137. Cao R, Pu X, Du X, et al. Screen-printed washable electronic textiles as self-powered touch/gesture tribo-sensors for intelligent human-machine interaction. *ACS Nano.* 2018;12:5190-5196. <https://doi.org/10.1021/acs.nano.8b02477>.
138. Ren Z, Nie J, Xu L, et al. Directly visualizing tactile perception and ultrasensitive tactile sensors by utilizing body-enhanced induction of ambient electromagnetic waves. *Adv Funct Mater.* 2018;28(47):1-9. <https://doi.org/10.1002/adfm.201805277>.
139. Pu X, Liu M, Chen X, et al. Ultrastretchable, transparent triboelectric nanogenerator as electronic skin for biomechanical energy harvesting and tactile sensing. *Sci Adv.* 2017;3(5):1-11. <https://doi.org/10.1126/sciadv.1700015>.
140. Wu H, Shi Q, Wang F, Thean AV-Y, Lee C. Self-powered cursor using a triboelectric mechanism. *Small Methods.* 2018;2(7):1800078. <https://doi.org/10.1002/smt.201800078>.
141. Zhang SL, Lai YC, He X, Liu R, Zi Y, Wang ZL. Auxetic foam-based contact-mode triboelectric nanogenerator with highly sensitive self-powered strain sensing capabilities to monitor human body movement. *Adv Funct Mater.* 2017;27(25):1-7. <https://doi.org/10.1002/adfm.201606695>.
142. Huang H, Wu ZS. Static and dynamic measurement of low-level strains with carbon fibers. *Sens Actuators A Phys.* 2012;183:140-147. <https://doi.org/10.1016/j.sna.2012.06.006>.
143. Song JK, Son D, Kim J, et al. Wearable force touch sensor array using a flexible and transparent electrode. *Adv Funct Mater.* 2017;27(6):1-9. <https://doi.org/10.1002/adfm.201605286>.
144. Pang YK, Li XH, Chen MX, Han CB, Zhang C, Wang ZL. Triboelectric nanogenerators as a self-powered 3D acceleration sensor. *ACS Appl Mater Interfaces.* 2015;7(34):19076-19082. <https://doi.org/10.1021/acsami.5b04516>.
145. Zhang H, Yang Y, Su Y, et al. Triboelectric nanogenerator for harvesting vibration energy in full space and as self-powered acceleration sensor. *Adv Funct Mater.* 2014;24(10):1401-1407. <https://doi.org/10.1002/adfm.201302453>.
146. Liu C, Wang Y, Zhang N, et al. A self-powered and high sensitivity acceleration sensor with V-Q-a model based on triboelectric nanogenerators (TENGs). *Nano Energy.* 2020;67:104228. <https://doi.org/10.1016/j.nanoen.2019.104228>.
147. Xiang C, Liu C, Hao C, Wang Z, Che L, Zhou X. A self-powered acceleration sensor with flexible materials based on triboelectric effect. *Nano Energy.* 2017;31:469-477. <https://doi.org/10.1016/j.nanoen.2016.11.056>.
148. Gupta RK, Shi Q, Dhakar L, Wang T, Heng CH, Lee C. Broad-band energy harvester using non-linear polymer spring and electromagnetic/triboelectric hybrid mechanism. *Sci Rep.* 2017;7:1-13. <https://doi.org/10.1038/srep41396>.

149. Yu H, He X, Ding W, et al. A self-powered dynamic displacement monitoring system based on triboelectric accelerometer. *Adv Energy Mater.* 2017;7(19):1-8. <https://doi.org/10.1002/aenm.201700565>.
150. Chen H, Miao L, Su Z, et al. Fingertip-inspired electronic skin based on triboelectric sliding sensing and porous piezo-resistive pressure detection. *Nano Energy.* 2017;40:65-72. <https://doi.org/10.1016/j.nanoen.2017.08.001>.
151. Wu W, Cao X, Zou J, et al. Triboelectric nanogenerator boosts smart green tires. *Adv Funct Mater.* 2019;29(41):1-9. <https://doi.org/10.1002/adfm.201806331>.
152. Guo H, Pu X, Chen J, et al. A highly sensitive, self-powered triboelectric auditory sensor for social robotics and hearing aids. *Sci Robot.* 2018;3(20):eaat2516. <https://doi.org/10.1126/scirobotics.aat2516>.
153. Koh KH, Shi Q, Cao S, et al. A self-powered 3D activity inertial sensor using hybrid sensing mechanisms. *Nano Energy.* 2019; 56:651-661. <https://doi.org/10.1016/j.nanoen.2018.11.075>.
154. Vera Anaya D, He T, Lee C, Yuce MR. Self-powered eye motion sensor based on triboelectric interaction and near-field electrostatic induction for wearable assistive technologies. *Nano Energy.* 2020;72:104675. <https://doi.org/10.1016/j.nanoen.2020.104675>.
155. Qiu C, Wu F, Shi Q, Lee C, Yuce MR. Sensors and control interface methods based on triboelectric nanogenerator in IoT applications. *IEEE Access.* 2019;7:92745-92757. <https://doi.org/10.1109/ACCESS.2019.2927394>.
156. Lee HE, Park JH, Kim TJ, et al. Novel electronics for flexible and neuromorphic computing. *Adv Funct Mater.* 2018;28(32): 1-18. <https://doi.org/10.1002/adfm.201801690>.
157. Yuan Z, Du X, Li N, et al. Triboelectric-based transparent secret code. *Adv Sci.* 2018;5(4):1-7. <https://doi.org/10.1002/advs.201700881>.
158. Chen T, Shi Q, Zhu M, et al. Triboelectric self-powered wearable flexible patch as 3D motion control interface for robotic manipulator. *ACS Nano.* 2018;12(11):11561-11571. <https://doi.org/10.1021/acsnano.8b06747>.
159. Li T, Zou J, Xing F, et al. From dual-mode triboelectric nanogenerator to smart tactile sensor: a multiplexing design. *ACS Nano.* 2017;11(4):3950-3956. <https://doi.org/10.1021/acsnano.7b00396>.
160. Bui VT, Zhou Q, Kim JN, et al. Treefrog toe pad-inspired micropatterning for high-power triboelectric nanogenerator. *Adv Funct Mater.* 2019;29(28):1-10. <https://doi.org/10.1002/adfm.201901638>.
161. Qiu C, Wu F, Lee C, Yuce MR. Self-powered control interface based on gray code with hybrid triboelectric and photovoltaics energy harvesting for IoT smart home and access control applications. *Nano Energy.* 2020;70:104456. <https://doi.org/10.1016/j.nanoen.2020.104456>.
162. Pu X, Guo H, Tang Q, et al. Rotation sensing and gesture control of a robot joint via triboelectric quantization sensor. *Nano Energy.* 2018;54:453-460. <https://doi.org/10.1016/j.nanoen.2018.10.044>.
163. Chen J, Pu X, Guo H, et al. A self-powered 2D barcode recognition system based on sliding mode triboelectric nanogenerator for personal identification. *Nano Energy.* 2018;43: 253-258. <https://doi.org/10.1016/j.nanoen.2017.11.028>.
164. Kuang SY, Zhu G, Wang ZL. Triboelectrification-enabled self-powered data storage. *Adv Sci.* 2018;5(2):1-8. <https://doi.org/10.1002/advs.201700658>.
165. Shi M, Zhang J, Chen H, et al. Self-powered analogue smart skin. *ACS Nano.* 2016;10(4):4083-4091. <https://doi.org/10.1021/acsnano.5b07074>.
166. Zi Y, Guo H, Wang J, et al. An inductor-free auto-power-management design built-in triboelectric nanogenerators. *Nano Energy.* 2017;31:302-310. <https://doi.org/10.1016/j.nanoen.2016.11.025>.
167. Uddin ASMI, Chung GS. A self-powered active hydrogen gas sensor with fast response at room temperature based on triboelectric effect. *Sens Actuators B.* 2016;231:601-608. <https://doi.org/10.1016/j.snb.2016.03.063>.
168. Wang H, Wu H, Hasan D, He T, Shi Q, Lee C. Self-powered dual-mode amenity sensor based on the water-air triboelectric nanogenerator. *ACS Nano.* 2017;11(10):10337-10346. <https://doi.org/10.1021/acsnano.7b05213>.
169. He T, Shi Q, Wang H, et al. Beyond energy harvesting - multifunctional triboelectric nanosensors on a textile. *Nano Energy.* 2019;57:338-352. <https://doi.org/10.1016/j.nanoen.2018.12.032>.
170. Wang S, Tai H, Liu B, et al. A facile respiration-driven triboelectric nanogenerator for multifunctional respiratory monitoring. *Nano Energy.* 2019;58:312-321. <https://doi.org/10.1016/j.nanoen.2019.01.042>.
171. Su Y, Xie G, Tai H, et al. Self-powered room temperature NO<sub>2</sub> detection driven by triboelectric nanogenerator under UV illumination. *Nano Energy.* 2018;47:316-324. <https://doi.org/10.1016/j.nanoen.2018.02.031>.
172. Lee JW, Jung S, Lee TW, et al. High-output triboelectric nanogenerator based on dual inductive and resonance effects-controlled highly transparent polyimide for self-powered sensor network systems. *Adv Energy Mater.* 2019;9(36):1-11. <https://doi.org/10.1002/aenm.201901987>.
173. Chen CH, Lee PW, Tsao YH, Lin ZH. Utilization of self-powered electrochemical systems: metallic nanoparticle synthesis and lactate detection. *Nano Energy.* 2017;42:241-248. <https://doi.org/10.1016/j.nanoen.2017.10.064>.
174. Khandelwal G, Chandrasekhar A, Maria Joseph Raj NP, Kim SJ. Metal-organic framework: a novel material for triboelectric nanogenerator-based self-powered sensors and systems. *Adv Energy Mater.* 2019;9(14):1-8. <https://doi.org/10.1002/aenm.201803581>.
175. Wan P, Wen X, Sun C, et al. Flexible transparent films based on nanocomposite networks of polyaniline and carbon nanotubes for high-performance gas sensing. *Small.* 2015;11(40): 5409-5415. <https://doi.org/10.1002/smll.201501772>.
176. Heo JS, Eom J, Kim YH, Park SK. Recent progress of textile-based wearable electronics: a comprehensive review of materials, devices, and applications. *Small.* 2018;14(3):1-16. <https://doi.org/10.1002/smll.201703034>.
177. Furui A, Eto S, Nakagaki K, et al. A myoelectric prosthetic hand with muscle synergy-based motion determination and impedance model-based biomimetic control. *Sci Robot.* 2019;4 (31):eaaw6339. <https://doi.org/10.1126/scirobotics.aaw6339>.
178. Lee WW, Tan YJ, Yao H, et al. A neuro-inspired artificial peripheral nervous system for scalable electronic skins. *Sci*

- Robot.* 2019;4(32):eaax2198. <https://doi.org/10.1126/scirobotics.aax2198>.
179. Boutry CM, Negre M, Jorda M, et al. A hierarchically patterned, bioinspired e-skin able to detect the direction of applied pressure for robotics. *Sci Robot.* 2018;3(24):eaau6914. <https://doi.org/10.1126/scirobotics.aau6914>.
180. Chung HU, Kim BH, Lee JY, et al. Binodal, wireless epidermal electronic systems with in-sensor analytics for neonatal intensive care. *Science.* 2019;363(6430):eaau0780. <https://doi.org/10.1126/science.aau0780>.
181. Wang C, Li X, Hu H, et al. Monitoring of the central blood pressure waveform via a conformal ultrasonic device. *Nat Biomed Eng.* 2018;2(9):687-695. <https://doi.org/10.1038/s41551-018-0287-x>.
182. Li W, Chen R, Qi W, et al. Reduced graphene oxide/mesoporous ZnO NSs hybrid fibers for flexible, stretchable, twisted, and wearable NO<sub>2</sub> e-textile gas sensor. *ACS Sensors.* 2019;4(10):2809-2818. <https://doi.org/10.1021/acssensors.9b01509>.
183. Sundaram S, Kellnhofer P, Li Y, Zhu J-Y, Torralba A, Matusik W. Learning the signatures of the human grasp using a scalable tactile glove. *Nature.* 2019;569(7758):698-702. <https://doi.org/10.1038/s41586-019-1234-z>.
184. Liu H, Dong W, Li Y, et al. An epidermal sEMG tattoo-like patch as a new human-machine interface for patients with loss of voice. *Microsyst Nanoeng.* 2020;6:1-13. <https://doi.org/10.1038/s41378-019-0127-5>.
185. Tollefson J. Power from the oceans: blue energy. *Nature.* 2014;508(7496):302-304. <https://doi.org/10.1038/508302a>.
186. Cho A. To catch a wave. *Science.* 2015;347(6226):1084-1088. <https://doi.org/10.1126/science.347.6226.1084>.
187. Chen H, Xing C, Li Y, Wang J, Xu Y. Triboelectric nanogenerators for a macro-scale blue energy harvesting and self-powered marine environmental monitoring system. *Sustain Energy Fuels.* 2020;4(3):1063-1077. <https://doi.org/10.1039/c9se01184f>.
188. Wang ZL. Catch wave power in floating nets. *Nature.* 2017;542(7640):159-160. <https://doi.org/10.1038/542159a>.
189. Wang ZL, Jiang T, Xu L. Toward the blue energy dream by triboelectric nanogenerator networks. *Nano Energy.* 2017;39:9-23. <https://doi.org/10.1016/j.nanoen.2017.06.035>.
190. Tian J, Chen X, Wang Z. Environmental energy harvesting based on triboelectric nanogenerator. *Nanotechnology.* 2020;31(24):242001. <https://doi.org/10.1088/1361-6528/ab793e>.
191. Wang Y, Gao S, Xu W, Wang Z. Nanogenerators with super-wetting surfaces for harvesting water/liquid energy. *Adv Funct Mater.* 2020;30:1908252. <https://doi.org/10.1002/adfm.201908252>.
192. Tang W, Chen BD, Wang ZL. Recent progress in power generation from water/liquid droplet interaction with solid surfaces. *Adv Funct Mater.* 2019;29(41):1901069. <https://doi.org/10.1002/adfm.201901069>.
193. Xi F, Pang Y, Liu G, et al. Self-powered intelligent buoy system by water wave energy for sustainable and autonomous wireless sensing and data transmission. *Nano Energy.* 2019;61:1-9. <https://doi.org/10.1016/j.nanoen.2019.04.026>.
194. Wang H, Zhu Q, Ding Z, et al. A fully-packaged ship-shaped hybrid nanogenerator for blue energy harvesting toward seawater self-desalination and self-powered positioning. *Nano Energy.* 2019;57:616-624. <https://doi.org/10.1016/j.nanoen.2018.12.078>.
195. Liang X, Jiang T, Liu G, et al. Triboelectric nanogenerator networks integrated with power management module for water wave energy harvesting. *Adv Funct Mater.* 2019;29(41):1807241. <https://doi.org/10.1002/adfm.201807241>.
196. Cheng P, Guo H, Wen Z, et al. Largely enhanced triboelectric nanogenerator for efficient harvesting of water wave energy by soft contacted structure. *Nano Energy.* 2019;57:432-439. <https://doi.org/10.1016/j.nanoen.2018.12.054>.
197. Jiang T, Zhang LM, Chen X, et al. Structural optimization of triboelectric nanogenerator for harvesting water wave energy. *ACS Nano.* 2015;9(12):12562-12572. <https://doi.org/10.1021/acsnano.5b06372>.
198. Zhang SL, Xu M, Zhang C, et al. Rationally designed sea snake structure based triboelectric nanogenerators for effectively and efficiently harvesting ocean wave energy with minimized water screening effect. *Nano Energy.* 2018;48:421-429. <https://doi.org/10.1016/j.nanoen.2018.03.062>.
199. Tan J, Duan J, Zhao Y, He B, Tang Q. Generators to harvest ocean wave energy through electrokinetic principle. *Nano Energy.* 2018;48:128-133. <https://doi.org/10.1016/j.nanoen.2018.03.032>.
200. Zhao XJ, Kuang SY, Wang ZL, Zhu G. Highly adaptive solid-liquid interfacing triboelectric nanogenerator for harvesting diverse water wave energy. *ACS Nano.* 2018;12(5):4280-4285. <https://doi.org/10.1021/acsnano.7b08716>.
201. Zhu G, Su Y, Bai P, et al. Harvesting water wave energy by asymmetric screening of electrostatic charges on a nanostructured hydrophobic thin-film surface. *ACS Nano.* 2014;8(6):6031-6037. <https://doi.org/10.1021/nn5012732>.
202. Lin Z-H, Cheng G, Wu W, Pradel KC, Wang ZL. Dual-mode triboelectric nanogenerator for harvesting water energy and as a self-powered ethanol nanosensor. *ACS Nano.* 2014;8(6):6440-6448. <https://doi.org/10.1021/nn501983s>.
203. Liu W, Xu L, Bu T, et al. Torus structured triboelectric nanogenerator array for water wave energy harvesting. *Nano Energy.* 2019;58:499-507. <https://doi.org/10.1016/j.nanoen.2019.01.088>.
204. Yang X, Xu L, Lin P, et al. Macroscopic self-assembly network of encapsulated high-performance triboelectric nanogenerators for water wave energy harvesting. *Nano Energy.* 2019;60:404-412. <https://doi.org/10.1016/j.nanoen.2019.03.054>.
205. Liu G, Guo H, Xu S, Hu C, Wang ZL. Oblate spheroidal triboelectric nanogenerator for all-weather blue energy harvesting. *Adv Energy Mater.* 2019;9(26):1900801. <https://doi.org/10.1002/aenm.201900801>.
206. Xu M, Wang S, Zhang SL, et al. A highly-sensitive wave sensor based on liquid-solid interfacing triboelectric nanogenerator for smart marine equipment. *Nano Energy.* 2019;57:574-580. <https://doi.org/10.1016/j.nanoen.2018.12.041>.
207. Li X, Tao J, Wang X, Zhu J, Pan C, Wang ZL. Networks of high performance triboelectric nanogenerators based on liquid-solid interface contact electrification for harvesting low-frequency blue energy. *Adv Energy Mater.* 2018;8(21):1800705. <https://doi.org/10.1002/aenm.201800705>.
208. Shi Q, Wang H, Wu H, Lee C. Self-powered triboelectric nanogenerator buoy ball for applications ranging from



- environment monitoring to water wave energy farm. *Nano Energy*. 2017;40:203-213. <https://doi.org/10.1016/j.nanoen.2017.08.018>.
209. Liang X, Jiang T, Liu G, Feng Y, Zhang C, Wang ZL. Spherical triboelectric nanogenerator integrated with power management module for harvesting multidirectional water wave energy. *Energ Environ Sci*. 2020;13(1):277-285. <https://doi.org/10.1039/C9EE03258D>.
  210. Cheng P, Sun M, Zhang C, et al. Self-powered active spherical triboelectric sensor for fluid velocity detection. *IEEE Trans Nanotechnol*. 2020;19:230-235. <https://doi.org/10.1109/TNANO.2020.2976154>.
  211. Yang J, Chen J, Su Y, et al. Eardrum-inspired active sensors for self-powered cardiovascular system characterization and throat-attached anti-interference voice recognition. *Adv Mater*. 2015;27(8):1316-1326. <https://doi.org/10.1002/adma.201404794>.
  212. Ma L, Zhou M, Wu R, et al. Continuous and scalable manufacture of hybridized nano-micro triboelectric yarns for energy harvesting and signal sensing. 2020;14(4):4716-4726. doi: <https://doi.org/10.1021/acsnano.0c00524>
  213. Bu C, Li F, Yin K, Pang J, Wang L, Wang K. Research progress and prospect of triboelectric nanogenerators as self-powered human body sensors. *ACS Appl Electron Mater*. 2020;2(4):863-878. <https://doi.org/10.1021/acsaelm.0c00022>.
  214. Tang Y, Zhou H, Sun X, et al. Triboelectric touch-free screen sensor for noncontact gesture recognizing. *Adv Funct Mater*. 2020;30(5):1-9. <https://doi.org/10.1002/adfm.201907893>.
  215. Zhong J, Zhong Q, Hu Q, et al. Stretchable self-powered fiber-based strain sensor. *Adv Funct Mater*. 2015;25(12):1798-1803. <https://doi.org/10.1002/adfm.201404087>.
  216. He Q, Wu Y, Feng Z, et al. Triboelectric vibration sensor for a human-machine interface built on ubiquitous surfaces. *Nano Energy*. 2019;59:689-696. <https://doi.org/10.1016/j.nanoen.2019.03.005>.
  217. Wu F, Rüdiger C, Yuce MR. Real-time performance of a self-powered environmental IoT sensor network system. *Sensors (Switzerland)*. 2017;17(2):282. <https://doi.org/10.3390/s17020282>.
  218. Su Z, Wu H, Chen H, et al. Digitalized self-powered strain gauge for static and dynamic measurement. *Nano Energy*. 2017;42:129-137. <https://doi.org/10.1016/j.nanoen.2017.10.004>.
  219. Wang X, Zhang Y, Zhang X, et al. A highly stretchable transparent self-powered triboelectric tactile sensor with metallized nanofibers for wearable electronics. *Adv Mater*. 2018;30(12):1706738. <https://doi.org/10.1002/adma.201706738>.
  220. Jeon SB, Kim WG, Park SJ, et al. Self-powered wearable touchpad composed of all commercial fabrics utilizing a crossline array of triboelectric generators. *Nano Energy*. 2019;65:103994. <https://doi.org/10.1016/j.nanoen.2019.103994>.
  221. Lee Y, Kim J, Jang B, et al. Nano energy graphene-based stretchable/wearable self-powered touch sensor. *Nano Energy*. 2019;62:259-267. <https://doi.org/10.1016/j.nanoen.2019.05.039>.
  222. Shi Q, Qiu C, He T, et al. Triboelectric single-electrode-output control interface using patterned grid electrode. *Nano Energy*. 2019;60:545-556. <https://doi.org/10.1016/j.nanoen.2019.03.090>.
  223. Chen T, Zhao M, Shi Q, et al. Novel augmented reality interface using a self-powered triboelectric based virtual reality 3D-control sensor. *Nano Energy*. 2018;51:162-172. <https://doi.org/10.1016/j.nanoen.2018.06.022>.
  224. Pu X, Guo H, Chen J, et al. Eye motion triggered self-powered mechnosensational communication system using triboelectric nanogenerator. *Sci Adv*. 2017;3(7):1-8. <https://doi.org/10.1126/sciadv.1700694>.
  225. He T, Sun Z, Shi Q, et al. Self-powered glove-based intuitive interface for diversified control applications in real/cyber space. *Nano Energy*. 2019;58:641-651. <https://doi.org/10.1016/j.nanoen.2019.01.091>.
  226. Wen F, Sun Z, He T, et al. Machine learning glove using self-powered conductive superhydrophobic triboelectric textile for gesture recognition in VR/AR applications. *Adv Sci*. 2020;7(14):1-15. <https://doi.org/10.1002/advs.202000261>.
  227. Lee Y, Cha SH, Kim YW, Choi D, Sun JY. Transparent and attachable ionic communicators based on self-cleanable triboelectric nanogenerators. *Nat Commun*. 2018;9(1):1-8. <https://doi.org/10.1038/s41467-018-03954-x>.
  228. Xu Z, Wu C, Li F, Chen W, Guo T, Kim TW. Triboelectric electronic-skin based on graphene quantum dots for application in self-powered, smart, artificial fingers. *Nano Energy*. 2018;49:274-282. <https://doi.org/10.1016/j.nanoen.2018.04.059>.
  229. Ding W, Wang AC, Wu C, Guo H, Wang ZL. Human-machine interfacing enabled by triboelectric nanogenerators and tribotronics. *Adv Mater Technol*. 2019;4(1):1-16. <https://doi.org/10.1002/admt.201800487>.
  230. Yao G, Kang L, Li J, et al. Effective weight control via an implanted self-powered vagus nerve stimulation device. *Nat Commun*. 2018;9(1):1-10. <https://doi.org/10.1038/s41467-018-07764-z>.
  231. Lee S, Wang H, Xian Peh WY, et al. Mechano-neuromodulation of autonomic pelvic nerve for underactive bladder: a triboelectric neurostimulator integrated with flexible neural clip interface. *Nano Energy*. 2019;60:449-456. <https://doi.org/10.1016/j.nanoen.2019.03.082>.
  232. Zhao C, Feng H, Zhang L, et al. Highly efficient in vivo cancer therapy by an implantable magnet triboelectric nanogenerator. *Adv Funct Mater*. 2019;29(41):1-11. <https://doi.org/10.1002/adfm.201808640>.
  233. Guan Q, Dai Y, Yang Y, Bi X, Wen Z, Pan Y. Near-infrared irradiation induced remote and efficient self-healable triboelectric nanogenerator for potential implantable electronics. *Nano Energy*. 2018;51:333-339. <https://doi.org/10.1016/j.nanoen.2018.06.060>.
  234. Zheng Q, Shi B, Fan F, et al. In vivo powering of pacemaker by breathing-driven implanted triboelectric nanogenerator. *Adv Mater*. 2014;26(33):5851-5856. <https://doi.org/10.1002/adma.201402064>.
  235. Lee S, Wang H, Wang J, et al. Battery-free neuromodulator for peripheral nerve direct stimulation. *Nano Energy*. 2018;50:148-158. <https://doi.org/10.1016/j.nanoen.2018.04.004>.
  236. Wang J, Wang H, Lee C. Mechanism and applications of electrical stimulation disturbance on motoneuron excitability studied using flexible intramuscular electrode. *Adv Biosyst*. 2019;3(7):1-11. <https://doi.org/10.1002/adbi.201800281>.
  237. Zhong J, Zhong Q, Fan F, et al. Finger typing driven triboelectric nanogenerator and its use for instantaneously lighting up

- LEDs. *Nano Energy*. 2013;2(4):491-497. <https://doi.org/10.1016/j.nanoen.2012.11.015>.
238. Bian Y, Jiang T, Xiao T, et al. Triboelectric nanogenerator tree for harvesting wind energy and illuminating in subway tunnel. *Adv Mater Technol*. 2018;3(3):1-7. <https://doi.org/10.1002/admt.201700317>.
239. Zhang C, Li J, Han CB, et al. Organic tribotronic transistor for contact-electrification-gated light-emitting diode. *Adv Funct Mater*. 2015;25(35):5625-5632. <https://doi.org/10.1002/adfm.201502450>.
240. Yang Y, Zhang H, Zhong X, et al. Electret film-enhanced triboelectric nanogenerator matrix for self-powered instantaneous tactile imaging. *ACS Appl Mater Interfaces*. 2014;6(5):3680-3688. <https://doi.org/10.1021/am406018h>.
241. Zhang Y, Peng M, Liu Y, et al. Flexible self-powered real-time ultraviolet photodetector by coupling triboelectric and photoelectric effects. *ACS Appl Mater Interfaces*. 2020;12(17):19384-19392. <https://doi.org/10.1021/acsami.9b22572>.
242. Pang Y, Xue F, Wang L, et al. Tribotronic enhanced photoresponsivity of a MOS<sub>2</sub> phototransistor. *Adv Sci*. 2015;3(6):1-7. <https://doi.org/10.1002/advs.201500419>.
243. Dong B, Shi Q, He T, et al. Wearable triboelectric/aluminum nitride nano-energy-nano-system with self-sustainable photonic modulation and continuous force sensing. *Adv Sci*. 2020;7:1903636. <https://doi.org/10.1002/advs.201903636>.
244. Wei XY, Kuang SY, Li HY, Pan C, Zhu G, Wang ZL. Interface-free area-scalable self-powered electroluminescent system driven by triboelectric generator. *Sci Rep*. 2015;5:1-7. <https://doi.org/10.1038/srep13658>.
245. Wei XY, Wang HL, Wang Y, et al. Fully-integrated motion-driven electroluminescence enabled by triboelectrification for customized flexible display. *Nano Energy*. 2019;61:158-164. <https://doi.org/10.1016/j.nanoen.2019.04.005>.
246. Fang H, Tian H, Li J, et al. Self-powered flat panel displays enabled by motion-driven alternating current electroluminescence. *Nano Energy*. 2016;20:48-56. <https://doi.org/10.1016/j.nanoen.2015.12.001>.
247. Wei XY, Liu L, Wang HL, et al. High-intensity triboelectrification-induced electroluminescence by micro-sized contacts for self-powered display and illumination. *Adv Mater Interfaces*. 2018;5(4):1701063. <https://doi.org/10.1002/admi.201701063>.
248. Wang Y, Wang HL, Li HY, Wei XY, Wang ZL, Zhu G. Enhanced high-resolution triboelectrification-induced electroluminescence for self-powered visualized interactive sensing. *ACS Appl Mater Interfaces*. 2019;11(14):13796-13802. <https://doi.org/10.1021/acsami.9b02313>.
249. Park HJ, Kim S, Lee JH, et al. Self-powered motion-driven triboelectric electroluminescence textile system. *ACS Appl Mater Interfaces*. 2019;11(5):5200-5207. <https://doi.org/10.1021/acsami.8b16023>.
250. Yu A, Chen X, Wang R, et al. Triboelectric nanogenerator as a self-powered communication unit for processing and transmitting information. *ACS Nano*. 2016;10(4):3944-3950. <https://doi.org/10.1021/acsnano.5b07407>.
251. Huang J, Yang X, Yu J, et al. A universal and arbitrary tactile interactive system based on self-powered optical communication. *Nano Energy*. 2020;69:104419. <https://doi.org/10.1016/j.nanoen.2019.104419>.
252. Su L, Wang H, Tian Z, Wang H, Cheng Q, Yu W. Low detection limit and high sensitivity wind speed sensor based on triboelectrification-induced electroluminescence. *Adv Sci*. 2019;6(23):1901980. <https://doi.org/10.1002/advs.201901980>.
253. Wen Z, Fu J, Han L, et al. Toward self-powered photo-detection enabled by triboelectric nanogenerators. *J Mater Chem C*. 2018;6(44):11893-11902. <https://doi.org/10.1039/c8tc02964d>.
254. Zhang C, Tang W, Pang Y, Han C, Wang ZL. Active micro-actuators for optical modulation based on a planar sliding triboelectric nanogenerator. *Adv Mater*. 2015;27(4):719-726. <https://doi.org/10.1002/adma.201404291>.
255. Chen X, Pu X, Jiang T, Yu A, Xu L, Wang ZL. Tunable optical modulator by coupling a triboelectric nanogenerator and a dielectric elastomer. *Adv Funct Mater*. 2017;27(1):1-9. <https://doi.org/10.1002/adfm.201603788>.
256. Zhang C, Guo Z, Zheng X, et al. A contact-sliding-triboelectrification-driven dynamic optical transmittance modulator for self-powered information covering and selective visualization. *Adv Mater*. 2020;32(1):1-8. <https://doi.org/10.1002/adma.201904988>.
257. Yan C, Gao Y, Zhao S, et al. A linear-to-rotary hybrid nanogenerator for high-performance wearable biomechanical energy harvesting. *Nano Energy*. 2020;67:1-5. <https://doi.org/10.1016/j.nanoen.2019.104235>.
258. He C, Chen BD, Jiang T, et al. Radial-grating pendulum-structured triboelectric nanogenerator for energy harvesting and tilting-angle sensing. *Adv Mater Technol*. 2018;3(4):1-7. <https://doi.org/10.1002/admt.201700251>.
259. Gao L, Chen X, Lu S, et al. Enhancing the output performance of triboelectric nanogenerator via grating-electrode-enabled surface plasmon excitation. *Adv Energy Mater*. 2019;9(44):1-11. <https://doi.org/10.1002/aenm.201902725>.
260. Zi Y, Lin L, Wang J, et al. Triboelectric-pyroelectric-piezoelectric hybrid cell for high-efficiency energy-harvesting and self-powered sensing. *Adv Mater*. 2015;27(14):2340-2347. <https://doi.org/10.1002/adma.201500121>.
261. Song W, Yin X, Liu D, et al. A highly elastic self-charging power system for simultaneously harvesting solar and mechanical energy. *Nano Energy*. 2019;65:103997. <https://doi.org/10.1016/j.nanoen.2019.103997>.
262. Hou C, Chen T, Li Y, et al. A rotational pendulum based electromagnetic/triboelectric hybrid-generator for ultra-low-frequency vibrations aiming at human motion and blue energy applications. *Nano Energy*. 2019;63:103871. <https://doi.org/10.1016/j.nanoen.2019.103871>.
263. Ryu H, Yoon HJ, Kim SW. Hybrid energy harvesters: toward sustainable energy harvesting. *Adv Mater*. 2019;31(34):1-19. <https://doi.org/10.1002/adma.201802898>.
264. Zhong Y, Zhao H, Guo Y, et al. An easily assembled electromagnetic-triboelectric hybrid nanogenerator driven by magnetic coupling for fluid energy harvesting and self-powered flow monitoring in a smart home/city. *Adv Mater Technol*. 2019;4(12):1900741. <https://doi.org/10.1002/admt.201900741>.
265. Zhang B, Chen J, Jin L, et al. Rotating-disk-based hybridized electromagnetic-triboelectric nanogenerator for sustainably powering wireless traffic volume sensors. *ACS Nano*. 2016;10(6):6241-6247. <https://doi.org/10.1021/acsnano.6b02384>.

266. Wang X, Wang S, Yang Y, Wang ZL. Hybridized electromagnetic-triboelectric nanogenerator for scavenging air-flow energy to sustainably power temperature sensors. *ACS Nano*. 2015;9(4):4553-4562. <https://doi.org/10.1021/acsnano.5b01187>.
267. Cao R, Zhou T, Wang B, et al. Rotating-sleeve triboelectric-electromagnetic hybrid nanogenerator for high efficiency of harvesting mechanical energy. *ACS Nano*. 2017;11(8):8370-8378. <https://doi.org/10.1021/acsnano.7b03683>.
268. Guo H, Wen Z, Zi Y, et al. A water-proof triboelectric-electromagnetic hybrid generator for energy harvesting in harsh environments. *Adv Energy Mater*. 2016;6(6):1-7. <https://doi.org/10.1002/aenm.201501593>.
269. Wang J, Pan L, Guo H, et al. Rational structure optimized hybrid nanogenerator for highly efficient water wave energy harvesting. *Adv Energy Mater*. 2019;9(8):1-12. <https://doi.org/10.1002/aenm.201802892>.
270. Rahman MT, Rana SS, Salauddin M, Maharjan P, Bhatta T, Park JY. Biomechanical energy-driven hybridized generator as a universal portable power source for smart/wearable electronics. *Adv Energy Mater*. 2020;10(12):1-14. <https://doi.org/10.1002/aenm.201903663>.
271. Fu J, Xia X, Xu G, Li X, Zi Y. On the maximal output energy density of nanogenerators. *ACS Nano*. 2019;13(11):13257-13263. <https://doi.org/10.1021/acsnano.9b06272>.
272. Diaz AF, Felix-Navarro RM. A semi-quantitative tribo-electric series for polymeric materials: the influence of chemical structure and properties. *J Electrostat*. 2004;62(4):277-290. <https://doi.org/10.1016/j.elstat.2004.05.005>.
273. Wang ZL. Triboelectric nanogenerators as new energy technology for self-powered systems and as active mechanical and chemical sensors. *ACS Nano*. 2013;7(11):9533-9557. <https://doi.org/10.1021/nn404614z>.
274. Chen T, Xia Y, Liu W, Liu H, Sun L, Lee C. A hybrid flapping-blade wind energy harvester based on vortex shedding effect. *J Microelectromech Syst*. 2016;25(5):845-847. <https://doi.org/10.1109/JMEMS.2016.2588529>.
275. Zhu J, Zhu Y, Wang X. A hybrid piezoelectric and triboelectric nanogenerator with PVDF nanoparticles and leaf-shaped microstructure PTFE film for scavenging mechanical energy. *Adv Mater Interfaces*. 2018;5(2):1700750. <https://doi.org/10.1002/admi.201700750>.
276. Qin S, Zhang Q, Yang X, Liu M, Sun Q, Wang ZL. Hybrid piezo/triboelectric-driven self-charging electrochromic supercapacitor power package. *Adv Energy Mater*. 2018;8(23):1800069. <https://doi.org/10.1002/aenm.201800069>.
277. Zhang K, Wang S, Yang Y. A one-structure-based piezo-tribo-pyro-photoelectric effects coupled nanogenerator for simultaneously scavenging mechanical, thermal, and solar energies. *Adv Energy Mater*. 2017;7(6):1601852. <https://doi.org/10.1002/aenm.201601852>.
278. Zhao C, Zhang Q, Zhang W, et al. Hybrid piezo/triboelectric nanogenerator for highly efficient and stable rotation energy harvesting. *Nano Energy*. 2019;57:440-449. <https://doi.org/10.1016/j.nanoen.2018.12.062>.
279. He X, Wen Q, Sun Y, Wen Z. A low-frequency piezoelectric-electromagnetic-triboelectric hybrid broadband vibration energy harvester. *Nano Energy*. 2017;40:300-307. <https://doi.org/10.1016/j.nanoen.2017.08.024>.
280. Bu L, Chen Z, Chen Z, et al. Impact induced compound method for triboelectric-piezoelectric hybrid nanogenerators to achieve watt level average power in low frequency rotations. *Nano Energy*. 2020;70:104500. <https://doi.org/10.1016/j.nanoen.2020.104500>.
281. Zheng H, Zi Y, He X, et al. Concurrent harvesting of ambient energy by hybrid nanogenerators for wearable self-powered systems and active remote sensing. *ACS Appl Mater Interfaces*. 2018;10(17):14708-14715. <https://doi.org/10.1021/acsami.8b01635>.
282. Rodrigues C, Gomes A, Ghosh A, Pereira A, Ventura J. Power-generating footwear based on a triboelectric-electromagnetic-piezoelectric hybrid nanogenerator. *Nano Energy*. 2019;62:660-666. <https://doi.org/10.1016/j.nanoen.2019.05.063>.
283. Li Z, Saadatnia Z, Yang Z, Naguib H. A hybrid piezoelectric-triboelectric generator for low-frequency and broad-bandwidth energy harvesting. *Energ Conver Manage*. 2018;174:188-197. <https://doi.org/10.1016/j.enconman.2018.08.018>.
284. Han M, Zhang X, Liu W, Sun X, Peng X, Zhang H. Low-frequency wide-band hybrid energy harvester based on piezoelectric and triboelectric mechanism. *Sci China Technol Sci*. 2013;56(8):1835-1841. <https://doi.org/10.1007/s11431-013-5270-x>.
285. He J, Wen T, Qian S, et al. Triboelectric-piezoelectric-electromagnetic hybrid nanogenerator for high-efficient vibration energy harvesting and self-powered wireless monitoring system. *Nano Energy*. 2018;43:326-339. <https://doi.org/10.1016/j.nanoen.2017.11.039>.
286. Lou Z, Li L, Wang L, Shen G. Recent progress of self-powered sensing systems for wearable electronics. *Small*. 2017;13(45):1-27. <https://doi.org/10.1002/sml.201701791>.
287. Yang X, Daoud WA. Triboelectric and piezoelectric effects in a combined tribo-piezoelectric nanogenerator based on an interfacial ZnO nanostructure. *Adv Funct Mater*. 2016;26(45):8194-8201. <https://doi.org/10.1002/adfm.201602529>.
288. Lapčinskis L, Mačlnieks K, Linarts A, et al. Hybrid tribo-piezo-electric nanogenerator with unprecedented performance based on ferroelectric composite contacting layers. *ACS Appl Energy Mater*. 2019;2(6):4027-4032. <https://doi.org/10.1021/acsaem.9b00836>.
289. Shu Fang L, Tsai CY, Xu MH, et al. Hybrid nano-textured nanogenerator and self-powered sensor for on-skin triggered biomechanical motions. *Nanotechnology*. 2020;31(15):155502. <https://doi.org/10.1088/1361-6528/ab6677>.
290. Guo Y, Zhang XS, Wang Y, et al. All-fiber hybrid piezoelectric-enhanced triboelectric nanogenerator for wearable gesture monitoring. *Nano Energy*. 2018;48:152-160. <https://doi.org/10.1016/j.nanoen.2018.03.033>.
291. Zhu Y, Yang B, Liu J, Wang X, Chen X, Yang C. An integrated flexible harvester coupled triboelectric and piezoelectric mechanisms using PDMS/MWCNT and PVDF. *J Microelectromech Syst*. 2015;24(3):513-515. <https://doi.org/10.1109/JMEMS.2015.2404037>.
292. Jung W-S, Kang M-G, Moon HG, et al. High output piezo/triboelectric hybrid generator. *Sci Rep*. 2015;5(1):9309. <https://doi.org/10.1038/srep09309>.
293. Zhu J, Hou X, Niu X, et al. The d-arched piezoelectric-triboelectric hybrid nanogenerator as a self-powered vibration



- sensor. *Sens Actuators A Phys.* 2017;263:317-325. <https://doi.org/10.1016/j.sna.2017.06.012>.
294. Chen X, Han M, Chen H, et al. A wave-shaped hybrid piezoelectric and triboelectric nanogenerator based on P(VDF-TrFE) nanofibers. *Nanoscale.* 2017;9(3):1263-1270. <https://doi.org/10.1039/C6NR07781A>.
  295. Chen S, Tao X, Zeng W, Yang B, Shang S. Quantifying energy harvested from contact-mode hybrid nanogenerators with cascaded piezoelectric and triboelectric units. *Adv Energy Mater.* 2017;7(5):1-9. <https://doi.org/10.1002/aenm.201601569>.
  296. Wang X, Yang B, Liu J, Zhu Y, Yang C, He Q. A flexible triboelectric-piezoelectric hybrid nanogenerator based on P(VDF-TrFE) nanofibers and PDMS/MWCNT for wearable devices. *Sci Rep.* 2016;6(1):36409. <https://doi.org/10.1038/srep36409>.
  297. Kim DH, Dudem B, Yu JS. High-performance flexible piezoelectric-assisted triboelectric hybrid nanogenerator via polydimethylsiloxane-encapsulated nanoflower-like ZnO composite films for scavenging energy from daily human activities. *ACS Sustain Chem Eng.* 2018;6(7):8525-8535. <https://doi.org/10.1021/acssuschemeng.8b00834>.
  298. Li H, Su L, Kuang S, et al. Multilayered flexible nanocomposite for hybrid nanogenerator enabled by conjunction of piezoelectricity and triboelectricity. *Nano Res.* 2017;10(3):785-793. <https://doi.org/10.1007/s12274-016-1331-3>.
  299. Yu J, Hou X, Cui M, et al. Highly skin-conformal wearable tactile sensor based on piezoelectric-enhanced triboelectric nanogenerator. *Nano Energy.* 2019;64:103923. <https://doi.org/10.1016/j.nanoen.2019.103923>.
  300. Seung W, Yoon HJ, Kim TY, et al. Boosting power-generating performance of triboelectric nanogenerators via artificial control of ferroelectric polarization and dielectric properties. *Adv Energy Mater.* 2017;7(2):1-8. <https://doi.org/10.1002/aenm.201600988>.
  301. Suo G, Yu Y, Zhang Z, et al. Piezoelectric and triboelectric dual effects in mechanical-energy harvesting using BaTiO<sub>3</sub>/polydimethylsiloxane composite film. *ACS Appl Mater Interfaces.* 2016;8(50):34335-34341. <https://doi.org/10.1021/acsami.6b11108>.
  302. Xue C, Li J, Zhang Q, et al. A novel arch-shape nanogenerator based on piezoelectric and triboelectric mechanism for mechanical energy harvesting. *Nanomaterials.* 2014;5(1):36-46. <https://doi.org/10.3390/nano5010036>.
  303. Patnam H, Dudem B, Alluri NR, et al. Piezo/triboelectric hybrid nanogenerators based on Ca-doped barium zirconate titanate embedded composite polymers for wearable electronics. *Compos Sci Technol.* 2020;188:107963. <https://doi.org/10.1016/j.compscitech.2019.107963>.
  304. Wang W, Zhang J, Zhang Y, et al. Remarkably enhanced hybrid piezo/triboelectric nanogenerator via rational modulation of piezoelectric and dielectric properties for self-powered electronics. *Appl Phys Lett.* 2020;116(2):023901. <https://doi.org/10.1063/1.5134100>.
  305. Wu Y, Qu J, Daoud WA, Wang L, Qi T. Flexible composite-nanofiber based piezo-triboelectric nanogenerators for wearable electronics. *J Mater Chem A.* 2019;7(21):13347-13355. <https://doi.org/10.1039/c9ta02345c>.
  306. Wang G, Xi Y, Xuan H, Liu R, Chen X, Cheng L. Hybrid nanogenerators based on triboelectrification of a dielectric composite made of lead-free ZnSnO<sub>3</sub> nanocubes. *Nano Energy.* 2015;18:28-36. <https://doi.org/10.1016/j.nanoen.2015.09.012>.
  307. Jirayupat C, Wongwiriyan W, Kasamechongchun P, et al. Piezoelectric-induced triboelectric hybrid nanogenerators based on the ZnO nanowire layer decorated on the au/polydimethylsiloxane-Al structure for enhanced triboelectric performance. *ACS Appl Mater Interfaces.* 2018;10(7):6433-6440. <https://doi.org/10.1021/acsami.7b17314>.
  308. He W, Qian Y, Lee BS, et al. Ultrahigh output piezoelectric and triboelectric hybrid nanogenerators based on ZnO nanoflakes/polydimethylsiloxane composite films. *ACS Appl Mater Interfaces.* 2018;10(51):44415-44420. <https://doi.org/10.1021/acsami.8b15410>.
  309. Qian Y, Kang DJ. Poly(dimethylsiloxane)/ZnO nanoflakes/three-dimensional graphene heterostructures for high-performance flexible energy harvesters with simultaneous piezoelectric and triboelectric generation. *ACS Appl Mater Interfaces.* 2018;10(38):32281-32288. <https://doi.org/10.1021/acsami.8b05636>.
  310. Chowdhury AR, Abdullah AM, Hussain I, et al. Lithium doped zinc oxide based flexible piezoelectric-triboelectric hybrid nanogenerator. *Nano Energy.* 2019;61:327-336. <https://doi.org/10.1016/j.nanoen.2019.04.085>.
  311. He J, Qian S, Niu X, et al. Piezoelectric-enhanced triboelectric nanogenerator fabric for biomechanical energy harvesting. *Nano Energy.* 2019;64:103933. <https://doi.org/10.1016/j.nanoen.2019.103933>.
  312. Wang S, Wang ZL, Yang Y. A one-structure-based hybridized nanogenerator for scavenging mechanical and thermal energies by triboelectric-piezoelectric-pyroelectric effects. *Adv Mater.* 2016;28(15):2881-2887. <https://doi.org/10.1002/adma.201505684>.
  313. Li X, Jiang C, Zhao F, et al. Fully stretchable triboelectric nanogenerator for energy harvesting and self-powered sensing. *Nano Energy.* 2019;61:78-85. <https://doi.org/10.1016/j.nanoen.2019.04.025>.
  314. Nayak S, Li Y, Tay W, et al. Liquid-metal-elastomer foam for moldable multi-functional triboelectric energy harvesting and force sensing. *Nano Energy.* 2019;64:103912. <https://doi.org/10.1016/j.nanoen.2019.103912>.
  315. Wang H, Shi M, Zhu K, et al. High performance triboelectric nanogenerators with aligned carbon nanotubes. *Nanoscale.* 2016;8(43):18489-18494. <https://doi.org/10.1039/c6nr06319e>.
  316. Chen X, Wu Y, Yu A, et al. Self-powered modulation of elastomeric optical grating by using triboelectric nanogenerator. *Nano Energy.* 2017;38:91-100. <https://doi.org/10.1016/j.nanoen.2017.05.039>.
  317. Fan FR, Luo J, Tang W, et al. Highly transparent and flexible triboelectric nanogenerators: performance improvements and fundamental mechanisms. *J Mater Chem A.* 2014;2(33):13219-13225. <https://doi.org/10.1039/c4ta02747g>.
  318. Tugui C, Bele A, Tiron V, et al. Dielectric elastomers with dual piezo-electrostatic response optimized through chemical design for electromechanical transducers. *J Mater Chem C.* 2017;5:824-834. <https://doi.org/10.1039/C6TC05193F>.
  319. Kollosche M, Döring S, Stumpe J, Kofod G. Voltage-controlled compression for period tuning of optical surface relief gratings. *Opt Lett.* 2011;36(8):1389. <https://doi.org/10.1364/ol.36.001389>.

320. Ji X, Rosset S, Shea HR. Soft tunable diffractive optics with multifunctional transparent electrodes enabling integrated actuation. *Appl Phys Lett*. 2016;109(19):191901. <https://doi.org/10.1063/1.4967001>.
321. Liu R, Kuang X, Deng J, et al. Shape memory polymers for body motion energy harvesting and self-powered mechanosensing. *Adv Mater*. 2018;30(8):1-8. <https://doi.org/10.1002/adma.201705195>.
322. Xiong J, Luo H, Gao D, et al. Self-restoring, waterproof, tunable microstructural shape memory triboelectric nanogenerator for self-powered water temperature sensor. *Nano Energy*. 2019;61:584-593. <https://doi.org/10.1016/j.nanoen.2019.04.089>.
323. Lee JH, Hinchet R, Kim SK, Kim S, Kim SW. Shape memory polymer-based self-healing triboelectric nanogenerator. *Energ Environ Sci*. 2015;8(12):3605-3613. <https://doi.org/10.1039/c5ee02711j>.
324. Chen Y, Pu X, Liu M, et al. Shape-adaptive, self-healable triboelectric nanogenerator with enhanced performances by soft solid-solid contact electrification. *ACS Nano*. 2019;13(8):8936-8945. <https://doi.org/10.1021/acsnano.9b02690>.
325. Kee S, Haque MA, Corzo D, Alshareef HN, Baran D. Self-healing and stretchable 3D-printed organic thermoelectrics. *Adv Funct Mater*. 2019;29(51):1905426. <https://doi.org/10.1002/adfm.201905426>.
326. Parida K, Kumar V, Jiangxin W, Bhavanasi V, Bendi R, Lee PS. Highly transparent, stretchable, and self-healing ionic-skin triboelectric nanogenerators for energy harvesting and touch applications. *Adv Mater*. 2017;29(37):1702181. <https://doi.org/10.1002/adma.201702181>.
327. Yao S, Ren P, Song R, et al. Nanomaterial-enabled flexible and stretchable sensing systems: processing, integration, and applications. *Adv Mater*. 2020;32(15):1-31. <https://doi.org/10.1002/adma.201902343>.
328. Sun J, Pu X, Liu M, et al. Self-healable, stretchable, transparent triboelectric nanogenerators as soft power sources. *ACS Nano*. 2018;12(6):6147-6155. <https://doi.org/10.1021/acsnano.8b02479>.
329. Deng J, Kuang X, Liu R, et al. Vitrimers elastomer-based jigsaw puzzle-like healable triboelectric nanogenerator for self-powered wearable electronics. *Adv Mater*. 2018;30(14):1-10. <https://doi.org/10.1002/adma.201705918>.
330. Guan Q, Lin G, Gong Y, et al. Highly efficient self-healable and dual responsive hydrogel-based deformable triboelectric nanogenerators for wearable electronics. *J Mater Chem A*. 2019;7(23):13948-13955. <https://doi.org/10.1039/c9ta02711d>.
331. Xu W, Huang LB, Hao J. Fully self-healing and shape-tailorable triboelectric nanogenerators based on healable polymer and magnetic-assisted electrode. *Nano Energy*. 2017;40(June):399-407. <https://doi.org/10.1016/j.nanoen.2017.08.045>.
332. Yi F, Wang X, Niu S, et al. A highly shape-adaptive, stretchable design based on conductive liquid for energy harvesting and self-powered biomechanical monitoring. *Sci Adv*. 2016;2(6):1-11. <https://doi.org/10.1126/sciadv.1501624>.
333. Guo H, Yeh MH, Lai YC, et al. All-in-one shape-adaptive self-charging power package for wearable electronics. *ACS Nano*. 2016;10(11):10580-10588. <https://doi.org/10.1021/acsnano.6b06621>.
334. Lai YC, Deng J, Niu S, et al. Electric eel-skin-inspired mechanically durable and super-stretchable nanogenerator for deformable power source and fully autonomous conformable electronic-skin applications. *Adv Mater*. 2016;28(45):10024-10032. <https://doi.org/10.1002/adma.201603527>.
335. Wen Z, Yang Y, Sun N, et al. A wrinkled PEDOT:PSS film based stretchable and transparent triboelectric nanogenerator for wearable energy harvesters and active motion sensors. *Adv Funct Mater*. 2018;28(37):1-8. <https://doi.org/10.1002/adfm.201803684>.
336. Shi J, Chen X, Li G, et al. A liquid PEDOT:PSS electrode-based stretchable triboelectric nanogenerator for a portable self-charging power source. *Nanoscale*. 2019;11(15):7513-7519. <https://doi.org/10.1039/c9nr01271k>.
337. Dong K, Wang YC, Deng J, et al. A highly stretchable and washable all-yarn-based self-charging knitting power textile composed of fiber triboelectric nanogenerators and supercapacitors. *ACS Nano*. 2017;11(9):9490-9499. <https://doi.org/10.1021/acsnano.7b05317>.
338. Yang Y, Sun N, Wen Z, et al. Liquid-metal-based super-stretchable and structure-designable triboelectric nanogenerator for wearable electronics. *ACS Nano*. 2018;12(2):2027-2034. <https://doi.org/10.1021/acsnano.8b00147>.
339. Dong K, Wu Z, Deng J, et al. A stretchable yarn embedded triboelectric nanogenerator as electronic skin for biomechanical energy harvesting and multifunctional pressure sensing. *Adv Mater*. 2018;30(43):1-12. <https://doi.org/10.1002/adma.201804944>.
340. Yi F, Wang J, Wang X, et al. Stretchable and waterproof self-charging power system for harvesting energy from diverse deformation and powering wearable electronics. *ACS Nano*. 2016;10(7):6519-6525. <https://doi.org/10.1021/acsnano.6b03007>.
341. Zhou C, Yang Y, Sun N, et al. Flexible self-charging power units for portable electronics based on folded carbon paper. *Nano Res*. 2018;11(8):4313-4322. <https://doi.org/10.1007/s12274-018-2018-8>.
342. Jiang C, Li X, Yao Y, et al. A multifunctional and highly flexible triboelectric nanogenerator based on MXene-enabled porous film integrated with laser-induced graphene electrode. *Nano Energy*. 2019;66:104121. <https://doi.org/10.1016/j.nanoen.2019.104121>.
343. Wu C, Kim TW, Park JH, et al. Enhanced triboelectric nanogenerators based on MoS<sub>2</sub> monolayer nanocomposites acting as electron-acceptor layers. *ACS Nano*. 2017;11(8):8356-8363. <https://doi.org/10.1021/acsnano.7b03657>.
344. Xiong J, Cui P, Chen X, et al. Skin-touch-actuated textile-based triboelectric nanogenerator with black phosphorus for durable biomechanical energy harvesting. *Nat Commun*. 2018;9(1):1-9. <https://doi.org/10.1038/s41467-018-06759-0>.
345. Zhao L, Zheng Q, Ouyang H, et al. A size-unlimited surface microstructure modification method for achieving high performance triboelectric nanogenerator. *Nano Energy*. 2016;28:172-178. <https://doi.org/10.1016/j.nanoen.2016.08.024>.
346. Wang HS, Jeong CK, Seo MH, et al. Performance-enhanced triboelectric nanogenerator enabled by wafer-scale nanogates of multistep pattern downscaling. *Nano Energy*. 2017;35:415-423. <https://doi.org/10.1016/j.nanoen.2017.04.012>.

347. Chun J, Kim JW, Jung WS, et al. Mesoporous pores impregnated with au nanoparticles as effective dielectrics for enhancing triboelectric nanogenerator performance in harsh environments. *Energ Environ Sci*. 2015;8(10):3006-3012. <https://doi.org/10.1039/c5ee01705j>.
348. Chen J, Guo H, He X, et al. Enhancing performance of triboelectric nanogenerator by filling high dielectric nanoparticles into sponge PDMS film. *ACS Appl Mater Interfaces*. 2016;8(1):736-744. <https://doi.org/10.1021/acsami.5b09907>.
349. Jiang C, Wu C, Li X, et al. All-electrospun flexible triboelectric nanogenerator based on metallic MXene nanosheets. *Nano Energy*. 2019;59:268-276. <https://doi.org/10.1016/j.nanoen.2019.02.052>.
350. Dong Y, Mallineni SSK, Maleski K, et al. Metallic MXenes: a new family of materials for flexible triboelectric nanogenerators. *Nano Energy*. 2018;44:103-110. <https://doi.org/10.1016/j.nanoen.2017.11.044>.
351. Wu C, Kim TW, Choi HY. Reduced graphene-oxide acting as electron-trapping sites in the friction layer for giant triboelectric enhancement. *Nano Energy*. 2017;32:542-550. <https://doi.org/10.1016/j.nanoen.2016.12.035>.
352. Luo J, Wang Z, Xu L, et al. Flexible and durable wood-based triboelectric nanogenerators for self-powered sensing in athletic big data analytics. *Nat Commun*. 2019;10(1):5147. <https://doi.org/10.1038/s41467-019-13166-6>.
353. Zou Y, Tan P, Shi B, et al. A bionic stretchable nanogenerator for underwater sensing and energy harvesting. *Nat Commun*. 2019;10(1):2695. <https://doi.org/10.1038/s41467-019-10433-4>.
354. Liu L, Shi Q, Ho JS, Lee C. Study of thin film blue energy harvester based on triboelectric nanogenerator and seashore IoT applications. *Nano Energy*. 2019;66:104167. <https://doi.org/10.1016/j.nanoen.2019.104167>.
355. Fan W, He Q, Meng K, et al. Machine-knitted washable sensor array textile for precise epidermal physiological signal monitoring. *Sci Adv*. 2020;6(11):eaay2840. <https://doi.org/10.1126/sciadv.aay2840>.
356. Zhu J, Song W, Ma F, Wang H. A flexible multi-layer electret nanogenerator for bending deformation energy harvesting and strain sensing. *Mater Res Bull*. 2018;102:130-136. <https://doi.org/10.1016/j.materresbull.2018.02.020>.
357. Liu L, Tang W, Chen B, et al. A self-powered portable power bank based on a hybridized nanogenerator. *Adv Mater Technol*. 2018;3(3):1-7. <https://doi.org/10.1002/admt.201700209>.
358. Liu L, Tang W, Deng C, et al. Self-powered versatile shoes based on hybrid nanogenerators. *Nano Res*. 2018;11(8):3972-3978. <https://doi.org/10.1007/s12274-018-1978-z>.
359. Zhu J, Ma F, Zhu H. Single-electrode, nylon-fiber-enhanced polytetrafluoroethylene electret film with hollow cylinder structure for mechanical energy harvesting. *Energ Technol*. 2018;6(6):1112-1118. <https://doi.org/10.1002/ente.201700779>.
360. Xia K, Zhu Z, Zhang H, Xu Z. A triboelectric nanogenerator as self-powered temperature sensor based on PVDF and PTFE. *Appl Phys A Mater Sci Process*. 2018;124(8):1-7. <https://doi.org/10.1007/s00339-018-1942-5>.
361. Zhu J, Wang A, Hu H, Zhu H. Hybrid electromagnetic and triboelectric nanogenerators with multi-impact for wideband frequency energy harvesting. *Energies*. 2017;10(12):1-11. <https://doi.org/10.3390/en10122024>.
362. Zhu J, Chen C, Guo X. Suspended polytetrafluoroethylene nanostructure electret film in dual variable cavities for self-powered micro-shock sensing. *Mater Res Express*. 2018;5(4):046305. <https://doi.org/10.1088/2053-1591/aabd22>.
363. Zhu J, Guo X, Meng D, et al. A flexible comb electrode triboelectric-electret nanogenerator with separated microfibers for a self-powered position, motion direction and acceleration tracking sensor. *J Mater Chem A*. 2018;6(34):16548-16555. <https://doi.org/10.1039/c8ta04443k>.
364. Zhu J, Jia L, Huang R. Electrospinning poly(l-lactic acid) piezoelectric ordered porous nanofibers for strain sensing and energy harvesting. *J Mater Sci Mater Electron*. 2017;28(16):12080-12085. <https://doi.org/10.1007/s10854-017-7020-5>.
365. Liu L, Tang W, Wang ZL. Inductively-coupled-plasma-induced electret enhancement for triboelectric nanogenerators. *Nanotechnology*. 2017;28(3):035405. <https://doi.org/10.1088/1361-6528/28/3/035405>.
366. Zhu J, Huang R, Zhu H. Proximity sensing of electrostatic induction electret nanoparticles device using separation electrode. *AIP Adv*. 2017;7(4):3-7. <https://doi.org/10.1063/1.4980050>.
367. Song W, Wang C, Gan B, et al. High performance lithium-sulfur batteries for storing pulsed energy generated by triboelectric nanogenerators. *Sci Rep*. 2017;7(1):1-7. <https://doi.org/10.1038/s41598-017-00545-6>.
368. Su Y, Chen J, Wu Z, Jiang Y. Low temperature dependence of triboelectric effect for energy harvesting and self-powered active sensing. *Appl Phys Lett*. 2015;106(1):013114. <https://doi.org/10.1063/1.4905553>.
369. Sun L, Chen S, Guo Y, et al. Ionogel-based, highly stretchable, transparent, durable triboelectric nanogenerators for energy harvesting and motion sensing over a wide temperature range. *Nano Energy*. 2019;63:103847. <https://doi.org/10.1016/j.nanoen.2019.06.043>.
370. Wen X, Su Y, Yang Y, Zhang H, Wang ZL. Applicability of triboelectric generator over a wide range of temperature. *Nano Energy*. 2014;4:150-156. <https://doi.org/10.1016/j.nanoen.2014.01.001>.
371. Wang S, Xie Y, Niu S, et al. Maximum surface charge density for triboelectric nanogenerators achieved by ionized-air injection: methodology and theoretical understanding. *Adv Mater*. 2014;26(39):6720-6728. <https://doi.org/10.1002/adma.201402491>.
372. Zhang C, Zhou T, Tang W, Han C, Zhang L, Wang ZL. Rotating-disk-based direct-current triboelectric nanogenerator. *Adv Energy Mater*. 2014;4(9):1-7. <https://doi.org/10.1002/aenm.201301798>.
373. Cheng G, Lin ZH, Lin L, Du ZL, Wang ZL. Pulsed nanogenerator with huge instantaneous output power density. *ACS Nano*. 2013;7(8):7383-7391. <https://doi.org/10.1021/nn403151t>.
374. Dong B, Yang Y, Shi Q, et al. Wearable triboelectric-human-machine-interface (THMI) using robust nanophotonic read-out. *ACS Nano*. 2020;14(7):8915-8930. <https://doi.org/10.1021/acsnano.0c03728>.
375. Zhang P, Chen Y, Guo ZH, Guo W, Pu X, Wang ZL. Stretchable, transparent, and thermally stable triboelectric nanogenerators based on solvent-free ion-conducting elastomer electrodes. *Adv Funct Mater*. 2020;30(15):1-9. <https://doi.org/10.1002/adfm.201909252>.



376. Luo J, Tang W, Fan FR, et al. Transparent and flexible self-charging power film and its application in a sliding unlock system in touchpad technology. *ACS Nano*. 2016;10(8):8078-8086. <https://doi.org/10.1021/acsnano.6b04201>.
377. Luo J, Xu L, Tang W, et al. Direct-current triboelectric nanogenerator realized by air breakdown induced ionized air channel. *Adv Energy Mater*. 2018;8(27):1-8. <https://doi.org/10.1002/aenm.201800889>.
378. Luo J, Fan FR, Jiang T, et al. Integration of micro-supercapacitors with triboelectric nanogenerators for a flexible self-charging power unit. *Nano Res*. 2015;8(12):3934-3943. <https://doi.org/10.1007/s12274-015-0894-8>.
379. Wang ZL. On Maxwell's displacement current for energy and sensors: the origin of nanogenerators. *Mater Today*. 2017;20(2):74-82. <https://doi.org/10.1016/j.mattod.2016.12.001>.
380. Yang JH, Kim YK, Lee JY. Simplified process for manufacturing macroscale patterns to enhance voltage generation by a triboelectric generator. *Energies*. 2015;8(11):12729-12740. <https://doi.org/10.3390/en81112340>.
381. Lee S, Shi Q, Lee C. From flexible electronics technology in the era of IoT and artificial intelligence toward future implanted body sensor networks. *APL Mater*. 2019;7(3):1-13. <https://doi.org/10.1063/1.5063498>.
382. Todaro MT, Guido F, Algieri L, et al. Biocompatible, flexible, and compliant energy harvesters based on piezoelectric thin films. *IEEE Trans Nanotechnol*. 2018;17(2):220-230. <https://doi.org/10.1109/TNANO.2017.2789300>.
383. Wang DF, Zhu Y, Yang X, Xia C, Fu Y, Song J. A ball-impact piezoelectric converter wrapped by copper coils. *IEEE Trans Nanotechnol*. 2018;17(4):723-726. <https://doi.org/10.1109/TNANO.2018.2823342>.
384. Bahoumina P, Hallil-Abbas H, Lachaud J, et al. VOCs monitoring using differential microwave capacitive resonant transducer and conductive PEDOT:PSS-MWCNTs nanocomposite film for environmental applications. *IEEE Transactions on Nanotechnology*. 2018;1-1. <https://doi.org/10.1109/tnano.2018.2828302>.
385. Xia K, Zhu Z, Zhang H, Du C, Wang R, Xu Z. High output compound triboelectric nanogenerator based on paper for self-powered height sensing system. *IEEE Trans Nanotechnol*. 2018;17(6):1217-1223. <https://doi.org/10.1109/TNANO.2018.2869934>.
386. Khan AA, Mahmud A, Ban D. Evolution from single to hybrid nanogenerator: a contemporary review on multimode energy harvesting for self-powered electronics. *IEEE Trans Nanotechnol*. 2019;18:21-36. <https://doi.org/10.1109/TNANO.2018.2876824>.
387. Chou JC, Wu CY, Kuo PY, et al. The flexible urea biosensor using magnetic nanoparticles. *IEEE Trans Nanotechnol*. 2019;18:484-490. <https://doi.org/10.1109/TNANO.2019.2895137>.
388. Wen F, He T, Liu H, Chen HY, Zhang T, Lee C. Advances in chemical sensing technology for enabling the next-generation self-sustainable integrated wearable system in the IoT era. *Nano Energy*. 2020;78(July):105155. <https://doi.org/10.1016/j.nanoen.2020.105155>.
389. Wang H, Zhu J, He T, Zhang Z, Lee C. Programmed-triboelectric nanogenerators—a multi-switch regulation methodology for energy manipulation. *Nano Energy*. 2020;78(July):105241. <https://doi.org/10.1016/j.nanoen.2020.105241>.
390. Hassani FA, Shi Q, Wen F, et al. Smart materials for smart healthcare—moving from sensors and actuators to self-sustained nanoenergy nanosystems. *Smart Mater Med*. 2020;1(July):92-124. <https://doi.org/10.1016/j.smaim.2020.07.005>.
391. Shi Q, Zhang Z, He T, et al. Deep learning enabled smart mats as a scalable floor monitoring system. *Nat Commun*. 2020;11(1):1-11. <https://doi.org/10.1038/s41467-020-18471-z>.
392. Zhu M, He T, Lee C. Technologies toward next generation human machine interfaces: from machine learning enhanced tactile sensing to neuromorphic sensory systems. *Appl Phys Rev*. 2020;7:31305. <https://doi.org/10.1063/5.0016485>.

**How to cite this article:** Zhu J, Zhu M, Shi Q, et al. Progress in TENG technology—A journey from energy harvesting to nanoenergy and nanosystem. *EcoMat*. 2020;2:e12058. <https://doi.org/10.1002/eom2.12058>